UC Santa Cruz
UC Santa Cruz Electronic Theses and Dissertations

Title

Evolutionary consequences of Cenozoic climate change on African lacertid lizards (Squamata: Lacertidae)

Permalink

https://escholarship.org/uc/item/23p1k768

Author

Hipsley, Christy Anna

Publication Date

2012-01-01

Peer reviewed|Thesis/dissertation

UNIVERSITY OF CALIFORNIA

SANTA CRUZ

**EVOLUTIONARY CONSEQUENCES OF CENOZOIC CLIMATE CHANGE ON
AFRICAN LACERTID LIZARDS (SQUAMATA: LACERTIDAE)**

A dissertation submitted in partial satisfaction
of the requirements for the degree of

DOCTOR OF PHILOSOPHY

in

ECOLOGY AND EVOLUTIONARY BIOLOGY

by

Christy A. Hipsley

September 2012

The Dissertation of Christy Hipsley
is approved:

_____
Professor Barry Sinervo, Chair

_____
Professor Giacomo Bernardi

_____
Professor Johannes Müller

_____
Tyrus Miller
Vice Provost and Dean of Graduate Studies

TABLE OF CONTENTS

LIST OF TABLES AND FIGURES

CHAPTER 3:

ABSTRACT

EVOLUTIONARY CONSEQUENCES OF CENOZOIC CLIMATE CHANGE ON AFRICAN LACERTID LIZARDS (SQUAMATA: LACERTIDAE)

CHRISTY A. HIPSLEY

The evolutionary diversification of many terrestrial vertebrate groups is strongly linked to climatic events in the Cenozoic, the period from 65 Million years ago to today when modern animals first appeared. I investigated the effects of Cenozoic climate change on the taxonomic and morphological diversification of the Old World lizard family Lacertidae, with particular emphasis on the African radiation. African lacertids exhibit an unusual pattern of diversification, in which their highest species richness occurs in deserts north and south of the equator, despite being spread throughout the continent. This disparity is particularly surprising given that desert lacertids are thought to be evolutionarily younger than their mesic-dwelling relatives, suggesting increased diversification rates in arid habitats. To identify the evolutionary factors underlying this pattern, I use a combination of phylogenetic, morphological and ecological techniques. In Chapter 1, I apply Bayesian methods and fossil-based calibrations to molecular sequence data to construct a time-calibrated phylogeny for Lacertidae. I estimate that the family arose in the early Cenozoic, with the majority of their African radiation occurring in the Eocene and Oligocene. In Chapter 2, I describe changes in lacertid body shape across biomes and substrates, and find widespread morphological convergence in similar habitat types. I suggest that in addition to foraging demands, fluctuating and extreme climatic conditions, largely driven by precipitation and temperature, contribute to morphological convergence across independent arid-dwelling clades. Finally, I test if ancestral transitions in ecology, morphology, and rates of diversification temporally coincide with paleoclimatic events in the Cenozoic. I use High Resolution X-ray Computed Tomography to characterize changes in the skull related to life in arid habitats, and apply

maximum likelihood methods to test if the origins of those traits temporally coincide with significant shifts in habitat, diversification rates and climatic changes. My results show that African lacertids experienced three major peaks in diversification, accompanied by the evolution of suites of arid-adapted morphological traits. These changes coincide with climatic shifts in Africa, including the transition from closed forests to open grasslands and savanna in the late Oligocene, prior to the peak temperatures of the mid-Miocene Climatic Optimum, and following the formation of the Benguela current leading to hyper-aridity in southern Africa. I conclude that deserts are important centers for reptile evolution, but that expected changes in climate due to global warming may outpace the ability of arid-dwelling species to adapt and persist in the future.

ACKNOWLEDGEMENTS

The two people who undoubtedly deserve the most credit for getting me this far are my parents, Bruce and Shelly Hipsley. They never once said no to my unending pleas for support (financial and emotional), and I am both sorry and comforted to think that that will never change. I only hope that I have given something back through my achievements to make it all worth it. I am likewise indebted to my grandparents, Steve and Helen Saradin, for supporting me throughout my undergraduate years and for letting me know that there was a world outside of Bel Air.

I also want to thank and acknowledge the people who have directly participated in this dissertation. The text of this dissertation includes a reprint of the following previously published material:

CHAPTER 1.

Hipsley, C. A., Himmelmann, L., Metzler, D. and J. Müller. 2009. Integration of Bayesian molecular clock methods and fossil-based soft bounds reveals early Cenozoic colonization of African lacertid lizards. BMC Evolutionary Biology 9:151.

The co-authors listed in this publication directed and supervised the research which forms the basis for the chapter. The contributions of the co-authors are as follows: Christy Hipsley designed the study, collected genetic sequence data, performed the sequence alignment and wrote the manuscript. The original idea was conceived by Johannes Müller, who also participated in data interpretation. Lin Himmelmann and Dirk Metzler designed the bioinformatics program used and Lin Himmelmann carried out the molecular clock analyses. All authors reviewed and approved the final manuscript.

Although I'll never be able to noose as many lizards in a day, I hope that I can at least endure as many field seasons in my career.

My fellow labmates at Santa Cruz, especially Lesley Lancaster, Mitchel Mulks, Ammon Corl, and Alison Davis, are also partially responsible for my scientific achievements. Lesley has been the ideal academic big sister, by showing me how to train undergraduates, teach, do research and still have fun at the same time. It's been great to see our research interests intersect over the past few years and I hope that I have contributed to her academic growth as much as she has influenced mine. I also enjoyed many conversations with Ammon about evolution and research, and I'm glad and grateful that he helped me collect data in Namibia. Mitch and Alison were also great companions in the lab, and a fun distraction outside of it.

Finally, I have to thank the person who has been with me since the beginning and has supported me in every way possible, Staffan Persson. His influence as a scientist and a person has been overwhelmingly positive and has played a role in everything I have done. Det är omöjligt att beskriva hur tacksam och lycklig jag är att ha dig. Tack!

INTRODUCTION

Understanding the factors underlying patterns of biological diversity has remained an active endeavor for over a century (e.g., Wallace 1876, Currie 1991, Gaston 2000, Currie et al. 2004), but has recently gained particular attention as a result of global climate change. Biotic responses to global warming have been observed at increasing rates over the past century, including shifts in species ranges, migration routes and reproductive timing (for a review, see Parmesan 2006). The overwhelming consensus is that climate change has already impacted natural systems and will continue to do so in the future (Parmesan and Galbraith 2004). Much less understood, however, are the long-term impacts of climate change on the evolutionary processes underlying biodiversity (i.e. speciation and extinction). Since the majority of climate impact studies are limited to small temporal and spatial scales, extrapolating their results to a macroevolutionary level has been difficult (Walther et al. 2002). Therefore, in order to predict the long-term consequences of current and future climate change on diversification, an understanding of their interactions in the past is required.

Global patterns of biodiversity have been shown to vary significantly with nearly every climatic factor studied, including temperature, precipitation, and evapotranspiration (Currie 1991). Some of the best known examples come from terrestrial vertebrates, whose species richness increases from high to low latitudes in nearly every taxonomic group studied (Hillebrand 2004). While most efforts to explain this pattern have focused on identifying contemporary environmental correlates, few studies have examined historical variation in the evolutionary processes that directly affect species richness: speciation (or cladogenesis) and extinction. Fortunately, recent advances in the statistical modeling of evolution based on molecular phylogenies now allow the estimation of diversification

1

rates over time. This is commonly done using molecular clock models to derive clade ages from phylogenetic data and, in conjunction with clade size, modeling speciation and extinction of those lineages based on a stochastic birth-death process (e.g., Rabosky 2006, Ricklefs 2007). By comparing variation in diversification rates to paleoclimatic records, recent studies have shown that historical climatic events have shaped diversification patterns of groups as widespread as cetaceans (Steeman et al. 2009), xenarthrans (Delsuc et al. 2004), boreal birds (Weir and Schluter 2004), leaf-nosed bats (Stevens 2006), and rodents (Mercer and Roth 2003).

In contrast to the many investigations of evolutionary diversification in birds and mammals, only a handful of studies have examined diversity-climate relationships in squamate reptiles, the clade including snakes, lizards, and amphisbaenians (e.g., Harmon et al. 2003, Rabosky et al. 2007, Ricklefs et al. 2007, Tolley et al. 2008). This is particularly surprising given that squamates are among the largest groups of terrestrial vertebrates, with an evolutionary history extending back to the Triassic and significant variation in clade size, ecology and morphology. Part of this bias is due to the unresolved nature of squamate relationships (Townsend et al. 2004, Ricklefs et al. 2007). Convergent morphologies among independent clades (e.g., limblessness in snakes, some lizards and amphisbaenians) have long confounded phylogenetic analyses, and the availability of molecular data is relatively low due to the inherent difficulties of sampling in some groups (e.g., fossorial taxa). Squamate reptiles also have a remarkably poor fossil record for the Cenozoic from which molecular clock calibrations can be derived (Evans 2003). This lack of paleontological material has seriously hampered our ability to date the origins of specific clades, which is necessary for testing hypotheses on their evolutionary radiations.

In addition to the taxonomic bias in climate impact studies, there is also a large geographical gap in the literature. Most records of biological responses to climate change come from North America and Europe, while very few have focused on climate impacts on African taxa (Parmesan 2006). This is unfortunate as it precludes the opportunity to explore diversification patterns across a broader range of habitats, including desert, tropical rainforest, montane grassland, and moist and arid savannas. African fauna are also well suited for molecular-based studies of evolution, since most of the continent was not affected by episodes of severe glaciation that can erase genetic signatures through population bottlenecks (Tolley et al. 2008). In this regard, the investigation of paleoclimatic effects on the diversification of a widely spread clade of African squamates would be highly desirable, both for comparisons with other terrestrial vertebrates and for filling gaps in our knowledge of general biodiversity patterns.

Here I to use lizards from the Old World family Lacertidae as a model system to study the evolutionary effects of climate change on squamate reptiles in Africa. Lacertids are excellent candidates for climate-driven diversification as they are widespread, evolutionarily old, and show considerable variation in species richness, morphology and ecology. They are also appropriate for comparative studies, since at least three lineages show independent colonization of arid habitats (Mayer and Pavlicev 2007, Hipsley et al. 2009), providing a unique case for ecological, functional, and morphological comparisons. I use a combination of statistical and phylogenetically based approaches to test if geographic patterns of species richness are explained by variation in diversification rates, and if shifts in those rates are associated with historical climatic events. Specifically, I test if changes in rates of speciation and extinction coincide with paleoclimatic shifts during the Cenozoic, and if radiations into arid environments promote ecological and morphological diversification in the African clades.

Applying these methods to Lacertidae first requires a robust, time-calibrated phylogeny from which to derive patterns of taxonomic and morphological evolution. So far this has been challenging due to widespread morphological convergence, variability in molecular markers, and lack of an adequate fossil record from which to derive molecular clock calibrations (Arnold 1989a, Harris et al. 1998a, Fu 2000, Pavlicev and Mayer 2009). My first step was therefore to perform a phylogenetic analysis of Lacertidae using recent advances in evolutionary modeling and divergence dating methods.

In Chapter 1, I construct a phylogenetic tree for the family using a combination of mitochondrial and nuclear genes, and apply several evolutionary models and fossil-based calibrations within a Bayesian framework. Based on the best-fit relaxed molecular clock model, I estimate the crown clade of Lacertidae arose shortly after the Cretaceous–Paleogene (K–Pg) boundary, approximately 60 Mya. The subclade Eremiadini is estimated to have split from its palearctic sister group (and potentially invaded Africa concurrently) in the mid-Eocene, and continued to diversify into the Oligocene and mid-Miocene, some 10 Mya.

Although the main clade ages are significantly greater than previous estimates (e.g., Carranza et al. 2004, Arnold et al. 2007), older dates for the African radiation are supported by independent evidence from paleontological, geological and climatic records. In contrast to suggestions that lacertids entered Africa in the Miocene via a land bridge from the Middle East (e.g., Mayer and Benyr 1994, Arnold et al. 2007), my results corroborate a primarily western migration across what was then the southern European archipelago (Popov et al. 2004). Generally longer branch lengths in the African clades compared to their palearctic sister taxa also suggest that they experienced accelerated

rates of evolution after entering Africa, possibly due to selective pressures of extreme environments. I hypothesize that 'r-selected' strategies (e.g., reproducing and dying quickly) were favored in arid habitats such as aeolian deserts, leading to shortened generation times and thus faster evolutionary rates for arid-dwelling taxa (also, see Arnold et al. 2007). Indeed, many desert lacertids appear to be short-lived compared to their mesic-dwelling relatives (Branch 1998), indicating that adaptations to arid environments may underlie their rapid diversification.

To investigate if specific characteristics of arid environments are associated with increased diversification, I looked for patterns of morphological adaptation that are expected to accompany rapid radiations (Simpson 1953, Foote 1997, Schluter 2000). In Chapter 2, I collected external measurements from ethanol-preserved museum specimens and live animals in the field to compare body shapes across biomes and substrates. Across the family, I found morphological convergence within arid and mesic biomes, indicating that similarities in habitat drive covariation in head and limb proportions. In general, arid-dwelling forms tended to have longer hindlimbs than forelimbs and relatively wide and deep heads. Mesic-dwelling forms in temperate, tropical and subtropical forests were slightly longer bodied, with longer forelimbs than hindlimbs and flatter, narrower heads. These patterns persisted even after adjusting for phylogenetic relationships, and are in line with expectations related to foraging mode and diet of species inhabiting different environments.

Within arid-dwelling clades in Africa, morphological variation was also found to covary with site-specific climatic variables. Factors related to climatic fluctuations and extremes, including precipitation seasonality and mean temperature of the wettest quarter, accounted for a quarter of the morphological variation observed. The most extreme

climatic values occurred across multiple substrate types, suggesting that climate itself, particularly related to moisture and the interaction between extreme temperatures and precipitation, has direct effects on lacertid body shape. Widespread convergence across arid-dwelling clades was also supported by morphological overlap between distantly related species in similar habitats in northern and southern Africa. Results of Pagel's lambda test for phylogenetic signal support this view, since nearly every trait measured failed to show phylogenetic structure. Overall, these patterns suggest that arid environments exert a strong selective pressure overriding the effects of shared ancestry, and that independent colonizations of similar arid regions in Africa underlie convergent morphological evolution in African lacertids.

The final chapter of the thesis attempts to temporally link shifts to arid habitat and the origins of adaptive traits with changes in diversification rates and paleoclimatic events. In African lacertids, adaptations to arid environments have often been used to establish a scenario for the rapid diversification of desert lineages (Arnold 1989a, Arnold et al. 2007). However, this has never been tested within a phylogenetic framework, as rigorous methods for estimating increases in speciation rates have only recently become available (e.g., Rabosky 2006). In Chapter 3, I use maximum likelihood approaches to reconstruct the temporal origins of habitat transitions and adaptive cranial traits in Lacertidae, and test if they temporally coincide with shifts in diversification rates and climatic events in the Cenozoic. I focus on features of the skull, since a large number of derived traits (>10) related to arid habitats are found there (e.g., Arnold 1983, 1989a, 1991, Arnold et al. 2007). I use qualitative rather than quantitative traits (such as head/limb length proportions reported in Chapter 2), as the statistical properties of ratios can be misleading regarding relative changes in body parts (Atchley et al. 1976).

For cranial examinations, I used High Resolution X-ray Computed Tomography (CT), a nondestructive technique for visualizing bone. This approach circumvents the need to disarticulate (and thus destroy) museum specimens, and prevents fragile structures such as osteoderms and processes from being lost. Based on the CT images of ethanol-preserved museum specimens, I characterized 46 species of Lacertidae for 19 morphological traits. Species were also scored for habitat type as mesic or arid, based on described distributions. Habitat optimization onto the phylogenetic tree revealed up to 6 independent shifts to arid environments in the African radiation, supported by both parsimony and maximum likelihood. In tests for correlated evolution among traits, shifts to arid habitat were accompanied by evolutionary transitions in 11 of the 19 examined osteological characters. Among those, approximately two-thirds exhibited significant evolutionary correlations with each other, indicating functional and/or adaptive complexes. For example, narrow frontal bones were strongly associated with frontal fusion, which may act to strengthen the thin interorbital area. Likewise, some traits were typically lost together during reversals to mesic habitat, such as a complex septomaxilla and large, dorsally exposed nasal openings, both traits assumed to be adaptive for breathing hot, dusty air (e.g., Arnold 1989a).

Finally, I examined rates of speciation and extinction in Lacertidae using several different yet complementary approaches. First, I constructed lineage-through-time plots to visualize patterns of species accumulation over time. Second, net rates of diversification (speciation-extinction) were estimated for the family and its subclades by applying a pure-birth model to the ultrametric tree. Lastly, I tested for the effects of incomplete taxon sampling on observed patterns of diversification by computing the gamma statistic (γ), which describes the distribution of branching times across the tree assuming a constant rate of diversification (Pybus and Harvey 2000). The observed gamma was compared to a

simulated set of randomly pruned trees to test if it falls outside of the null distribution.

Results of all three tests showed a decrease in diversification rates towards the present, indicative of an early and rapid radiation (see McPeek 2008). Incomplete taxon sampling does not affect this pattern. Lacertids appear to have undergone three major peaks in diversification during their evolutionary history. The family as a whole experiences its greatest diversification at the end Oligocene (~27 Mya) as it diverged into its African clades. This coincides with a significant habitat transition in Africa from closed tropical forests to dry, open savanna and grassland (Lunt et al. 2007, Strömberg 2011). Eremiadini and the Ethiopian radiation experience their highest diversification rates just prior to the mid-Miocene Climatic Optimum (~18 Mya), when temperatures reached the highest levels of the Neogene (Flowers and Kennett 1994). The final major peak in diversification occurs in the late Miocene (~9-11 Mya), following the development of the Benguela current along the southwest coast of Africa (Siesser 1980). The expansion of the Benguela current is responsible for the extreme xeric conditions of the Namib Desert and has been linked to rapid evolutionary radiations of its many endemic taxa, including plants, arachnids, insects, amphibians and other reptiles (Simmons et al. 1998, Steckel et al. 2010). I conclude that historical climate change has played an important role in lacertid evolution, and that increasing aridity and the expansion of open habitat in Africa has led to the evolution of suites of adaptive traits and convergent morphologies among independent clades.

BMC Evolutionary Biology

Research article

Integration of Bayesian molecular clock methods and fossil-based soft bounds reveals early Cenozoic origin of African lacertid lizards

Christy A Hipsley[1,2], Lin Himmelmann[3], Dirk Metzler[4] and Johannes Müller*[1]

Address: [1]Museum für Naturkunde – Leibniz-Institut für Evolutions- und Biodiversitätsforschung an der Humboldt-Universität zu Berlin, Invalidenstr. 43, 10115 Berlin, Germany, [2]Department of Ecology and Evolutionary Biology, University of California, Santa Cruz, A316 Earth and Marine Sciences Building, CA 95064, USA, [3]Institut für Informatik, Goethe-Universität, Robert Mayer Str. 11-15, D-60325 Frankfurt am Main, Germany and [4]Department of Biology, University of Munich (LMU), Grosshaderner Str. 2, D-82152 Planegg-Martinsried, Germany

Email: Christy A Hipsley - Christy.Hipsley@mfn-berlin.de; Lin Himmelmann - lin@linhi.de; Dirk Metzler - metzler@bio.lmu.de; Johannes Müller* - Johannes.Mueller@mfn-berlin.de

* Corresponding author

Abstract

Background: Although current molecular clock methods offer greater flexibility in modelling evolutionary events, calibration of the clock with dates from the fossil record is still problematic for many groups. Here we implement several new approaches in molecular dating to estimate the evolutionary ages of Lacertidae, an Old World family of lizards with a poor fossil record and uncertain phylogeny. Four different models of rate variation are tested in a new program for Bayesian phylogenetic analysis called TreeTime, based on a combination of mitochondrial and nuclear gene sequences. We incorporate paleontological uncertainty into divergence estimates by expressing multiple calibration dates as a range of probabilistic distributions. We also test the reliability of our proposed calibrations by exploring effects of individual priors on posterior estimates.

Results: According to the most reliable model, as indicated by Bayes factor comparison, modern lacertids arose shortly after the K/T transition and entered Africa about 45 million years ago, with the majority of their African radiation occurring in the Eocene and Oligocene. Our findings indicate much earlier origins for these clades than previously reported, and we discuss our results in light of paleogeographic trends during the Cenozoic.

Conclusion: This study represents the first attempt to estimate evolutionary ages of a specific group of reptiles exhibiting uncertain phylogenetic relationships, molecular rate variation and a poor fossil record. Our results emphasize the sensitivity of molecular divergence dates to fossil calibrations, and support the use of combined molecular data sets and multiple, well-spaced dates from the fossil record as minimum node constraints. The bioinformatics program used here, TreeTime, is publicly available, and we recommend its use for molecular dating of taxa faced with similar challenges.

9

Background

The molecular clock [1] has become an increasingly common tool among biologists for dating the origins of species or lineages using genetic sequence data. This is commonly done by measuring the genetic distance between two species and, assuming mutations occur at a constant rate, applying an external calibration to convert those distances into geological time (for a review of molecular clock methods, see [2]). Despite its widespread application, calibration of the clock using independent evidence, typically derived from the fossil record, is still problematic for many groups. While proper calibration dates for major evolutionary events like the mammal-bird or fish-tetrapod split are under constant debate [3-6], less attention has been given to smaller, less inclusive clades, which often have poor fossil records. Such discussions would be particularly useful for evolutionary biologists since it is often these clades that are the subject of more detailed investigations, e.g. in the context of biogeography or diversification. In the present study, we investigate how molecular divergences can be estimated in the absence of a good fossil record, and how fossil calibrations should be applied in such a case.

Here we combine a number of new approaches in molecular dating to assign evolutionary ages to the Old World lizard family Lacertidae (Squamata). Lacertidae, with about 280 species [7], is the dominant reptile group in Europe and a substantial component of the squamate reptile diversity in Africa. The family is divided into two subfamilies, the Gallotiinae and Lacertinae, with the latter group composed of two monophyletic clades, the mainly Palearctic Lacertini and Eremiadini of Africa (see [7] for a review of lacertid systematics). Compared to their Eurasian sister taxa, the African radiation shows extraordinary taxic diversity in desert habitats, while mesic-adapted genera in Africa are relatively species-poor. This disparity in species richness is surprising given that desert lacertids are considered evolutionarily younger and therefore have had less time to speciate than their mesic sister taxa, suggesting increased speciation rates in xeric habitat. Testing this hypothesis, however, has been difficult due to our lack of knowledge on the relative antiquity of desert clades. Terrestrial squamate fossils from the Cenozoic of Africa are rare [8], and this lack of fossil material has seriously hampered our ability to date the main lacertid lineages – a key step towards uncovering the ecological and evolutionary factors shaping their unique biogeographic patterns.

Based on previous molecular clock estimates, lacertids may have entered Africa (and at the same time split from the Palearctic clade) after Eurasia contacted Africa in the Neogene, some 17–19 million years ago (Mya) [7]. Fluctuating climatic conditions and aridification during that time may have promoted speciation in African lacertids

through ecological displacement. According to Arnold [9], competitive interactions among species in mesic habitats forced subordinate taxa into drier, heterogeneous areas, resulting in niche divergence and diversification. However, a fundamental problem with this hypothesis is that other molecular divergence studies [e.g. [10,11]] have estimated a much older age for crown (and African) lacertids, pushing their origin far into the early Cenozoic. Furthermore, dates given by Arnold et al. [7] are largely based on Carranza et al. [12], which in contrast to other molecular clock studies relies on only a single calibration point for their estimates (the age of the Canary island El Hierro to calibrate the node between *Gallotia caesaris caesaris* and *G. c. gomerensis*). In addition, both of the above studies rely on the method of nonparametric rate smoothing [13] which may not properly account for rate variation as it has a tendency to overfit data, particularly for regions of the tree with short branches [14]. Therefore, thoroughly performed divergence estimates for Lacertidae, particularly for the African radiation, are still needed.

In this article, we estimate evolutionary relationships and divergence dates for the major lineages of Lacertidae with the goal of forming biogeographical hypotheses for their origin and subsequent spread throughout Africa. We construct a molecular phylogeny for the family using published nuclear and mitochondrial gene sequences, which for the first time are combined in a total evidence approach. We use multiple, well-spaced dates from fossil taxa within and outside of the family as independent calibrations. To account for uncertainty in paleontological dates we use flexible priors, meaning that calibrations are expressed as probabilistic distributions with minimum and maximum bounds [15,16]. The use of "soft" bounds is advantageous over simple point calibrations, as potential errors in fossil dating and identification, as well as the lag time between speciation and appearance of a fossil descendent, are statistically incorporated into the prior distribution [15-17]. Additionally, we test the reliability of our proposed calibrations by excluding individual priors and evaluating posterior estimates.

All molecular clock analyses are performed in a newly available software application for Bayesian analysis called TreeTime [18]. Like MrBayes [19] and BEAST [20], Tree-Time uses a Metropolis-Coupled Markov Chain Monte Carlo (MCMCMC) method for Bayesian phylogenetic sampling. TreeTime simultaneously estimates tree topology and diversification dates and therefore does not require a starting tree topology, making it particularly appropriate for groups with uncertain phylogenies. Prior information on tree topology can be input by specifying two taxa, A and B, so that only trees in which at least one branch separates A from B are permitted. The user can also specify differently distributed priors for the time of the

10

split between A and B. Within TreeTime, we implement four different models of rate variation and compare their performance using Bayes factor analysis. Phylogenetic relationships among the different genera are compared to previous studies, and age estimates from the different models are evaluated against available data from geology, climatology and the fossil record. Finally, we use our results as a platform for evaluating alternative hypotheses for the origins of Lacertidae and interpret our findings in light of paleogeographic trends in the Cenozoic.

Methods
Taxon sampling and alignment
Thirty-five species, representing 33 of 41 currently recognized genera, were used to construct a molecular phylogeny for the main lineages of Lacertidae. Partial DNA sequences of 3 mitochondrial genes (*12S, 16S* and *Cytb*) and 2 nuclear genes (*Rag-1* and *C-mos*) were retrieved from GenBank. Most lacertid genera are represented by a single species, with the exception of *Psammodromus* and *Mesalina*, which are each represented by two. All genes used in this study were not available for some of the species, so that six of the genera (*Acanthodactylus, Algyroides, Eremias, Nucras, Parvilacerta* and *Pedioplanis*) are represented by a combination of genes from two congeneric species. For example, the missing *Cytb* sequence of *Acanthodactylus boskianus* is substituted by that of *A. erythrurus*. Such substitutions at the genus level should have no effect on overall tree topology, since we are primarily interested in phylogenetic relationships of higher taxonomic units (i.e. above the generic level). The final data set for Lacertidae consists of 3 individuals from the subfamily Gallotinae (*Gallotia* + *Psammodromus*), 15 individuals from Eremiadini corresponding to 14 genera, and 17 individuals from Lacertini each representing a single genus. Three additional species were used as outgroups: the teiid *Cnemidophorus tigris*, the amphisbaenian *Rhineura floridana*, and one of two living members of Rhynchocephalia, *Sphenodon punctatus*, as outgroup to all squamates. GenBank accession numbers for sequence data are listed in Table 1. Lacertid taxonomy follows Arnold et al. [7].

Alignments were performed separately for each gene using ClustalW [21] and manually corrected in SEAVIEW [22]. A total of 15–20 base pairs (bp) of *16S* that could not be aligned unambiguously were excluded from the analysis. Final gene lengths are 254 bp *16S*, 327 bp *12S*, 281 bp *Cytb*, 1012 bp *Rag-1* and 375 bp *C-mos*. To test for incongruence among genes, a partition homogeneity test [23] was conducted in PAUP* 4.0b10 [24]. The test (100 replicates of random addition heuristic search option with tree-bisection-reconnection branch swapping) indicated significant heterogeneity among genes (p = 0.01). However, since a growing number of studies indicate that incongruence tests are not reliable indicators of data set

combinability [25] and no strongly supported nodes were in conflict with previous studies, genes were concatenated into a multigene data set of 2249 bp. Following a total evidence approach [26], the following analyses were conducted on the combined data to maximize the amount of characters and explanatory power of the available data. As a test of our combined approach, we also analyzed partitioned mitochondrial DNA (mtDNA) and nuclear DNA (nDNA) sequences for one of the relaxed clock models (Uncorrelated lognormal with 10% prior probability distributions, described below). These values were then compared to results from the concatenated data set to explore possible biases associated with the different genomes.

Phylogenetic and molecular clock analyses
Divergence dates for Lacertidae were estimated under four different Bayesian molecular clock models. Minimum constraints for five nodes were chosen based on evidence from the fossil record. In a conservative approach, the oldest age of the stratigraphic layer in which a fossil was found was used to represent the earliest occurrence of that lineage, and potential calibrations were limited to fossils that are reliably assigned to extant clades. Calibrated nodes are: (i) *Sphenodon punctatus – Cnemidophorus tigris*, 228.0 Mya, based on the earliest identified rhynchocephalian from the late Triassic [Carnian; [27]], and corroborated by the oldest-known fossil squamate, *Tikiguania*, from the Carnian of India [28], (ii) *Cnemidophorus tigris – Rhineura floridana*, 113.0 Mya, corresponding to the oldest known teiid, *Ptilotodon*, from the lower Cretaceous [Aptian-Albian; [29]], (iii) *Rhineura floridana – Gallotia galloti*, 64.2 Mya, based on the fossil rhineurid *Plesiorhineura* from the Paleocene [Torrejonian; [30]], and (iv) *Timon lepidus – Dalmatolacerta oxycephala*, 5.3 Mya based on the Pliocene "*Lacerta ruscinensis*" from Roussillon, France, whose fossil remains are indistinguishable from the modern *T. lepidus* presently living in the same area [31].

To incorporate uncertainty surrounding fossil calibrations, prior constraints are expressed as probability based distributions. We use a rigid, or "hard", minimum bound, meaning that the true divergence date cannot be younger than the earliest known fossil. The probability that the divergence event occurred above the minimum date declines according to an exponential distribution, such that 95% of the posterior density falls within the range [x - x + 10%] (Figure 1). For example, the minimum age constraint for the split between Rhynchocephalia and Squamata is 228 Mya, and the expected posterior estimate is between 228.0 and 239.4. To test the sensitivity of posterior estimates to prior distributions, we also allow expectancy values for calibrated nodes to fall within 20% of the minimum age, so that 95% of the posterior density is between [x - x + 20%]. This allows us to evaluate the influ-

Table 1: GenBank accession numbers for mitochondrial and nuclear gene sequences used in the phylogenetic analysis of Lacertidae.

Species	c-mos	rag1	12S	16S	cytb
Acanthodactylus boskianus	EF632251	EF632206	AY633417	AY633441	AF206536[a]
Adolfus jacksoni	EF632253	EF632208	AF206615	AF206615	AF206539
Algyroides fitzingeri	EF632254[b]	EF632209[b]	AF206598	AF111177	AF206529
Anatololacerta danfordi	DQ461743	EF632224	AJ238188	AF080324	AF080323
Apathya cappadocica	EF632268	EF632223	AF145444	AF149946	AF080329
Archaeolacerta bedriagae	EF632256	EF632211	AF206592	AF206592	AF080326
Cnemidophorus tigris	AF039481	AY662620	AF206585	AY046492	AF006270
Dalmatolacerta oxycephala	EF632271	EF632228	AF440601	AF440616	AY256651
Darevskia valentini	EF632257	EF632212	AF206597	AF206597	LVU88611
Dinarolacerta mosorensis	EF632270	EF632227	AF440600	AF440615	AY151902
Eremias arguta	EF632258	EF632213	AY035827	AY035837	AF206549[c]
Gallotia galloti	EF632260	EF632215	AF206587	AF206587	AY151840
Heliobolus spekii	EF632262	EF632217	AF206608	AF206608	AF206544
Hellenolacerta graeca	EF632269	EF632225	AF440602	AF440617	AF080272
Iberolacerta monticola	EF632265	EF632220	AF440589	AF440604	AY151872
Ichnotropis squamulosa	EF632266	EF632221	AF080365	AF080367	AF080366
Lacerta agilis	EF632267	EF632222	AF149947	DQ494823	AF080299
Latastia longicaudata	EF632272	EF632229	AF206609	AF206609	AF206545
Meroles suborbitalis	EF632273	EF632230	AF206611	AF206611	AF206540
Mesalina guttulata	EF632274	EF632231	AY218019	AY217969	AY217815
Mesalina rubropunctata	EF632275	EF632232	AY035830	AY035840	EF555274
Nucras tessellata	EF632276[d]	EF632233[d]	AF206612	AF206612	AF206550
Omanosaura jayakari	EF632277	EF632234	AF080350	AF080352	AF080351
Ophisops elegans	EF632278	EF632235	AF206605	AF206605	AF206532
Parvilacerta fraasii	EF632279[e]	EF632236[e]	AJ238187	AF080318	AF080317
Pedioplanis namaquensis	EF632280[f]	EF632237[f]	AF206613	AF206613	AF206546
Phoenicolacerta laevis	DQ461740	EF632226	AJ238183	AF080333	AF080332
Podarcis muralis	EF632282	EF632239	AF206600	AF206600	AY151912
Poramera fordii	EF632283	EF632240	AF080368	AF080370	AF080369
Psammodromus algirus	EF632284	EF632241	AY218020	DQ298734	AY217816
Psammodromus hispanicus	EF632285	EF632242	DQ298606	DQ298676	DQ298562
Rhineura floridana	AY444021	AY662618	AY881097	AY605473	AY605473
Sphenodon punctatus	AF039483	AY662576	AF534390	DQ267621	AF534390
Takydromus sexlineatus	EF632288	EF632245	AF206589	AF206589	AY248472
Tiera dugesii	EF632289	EF632246	AF543309	AF080315	AF080314
Timon lepidus	EF632290	EF632247	AF206595	AF206595	AY151899
Tropidosaura gularis	EF632291	EF632248	AF206616	AF206616	AF206541
Zootoca vivipara	EF632292	EF632249	AF206594	AF206594	AY151913

[a] Acanthodactylus erythrurus
[b] Algyroides moreoticus
[c] Eremias velox
[d] Nucras lalandii
[e] Parvilacerta parva
[f] Pedioplanis undata
Species substitutions for missing gene sequences are noted by superscripts.

ence of the range of soft bounds used for a given data set, irrespective of possible errors in fossil calibration dates.

In addition to estimating divergence dates, we evaluate the reliability of our proposed fossil calibrations by systematically removing individual priors and comparing posterior estimates. Specifically, we test the accuracy of the dates proposed for amphisbaenians (*Plesiorhineura*, 64.2 Mya) and teiids (*Ptilotodon*, 113.0 Mya) using three different treatments. In the first treatment, both the amphisbaenian and teiid are excluded so that only the oldest date (Rhynchocephalia, 228 Mya) and youngest date (*Lacerta ruscinensis*, 5.3 Mya) remain. In the second and third treatments, only the amphisbaenian or teiid is removed, respectively. If a calibration is accurate, provided the remaining calibrations are reliable and the data and model are appropriate, the posterior estimate should remain within the prior range even in the absence of the fossil constraint. If the calibration is poor, the posterior should move away from the prior [32]. This approach also

12
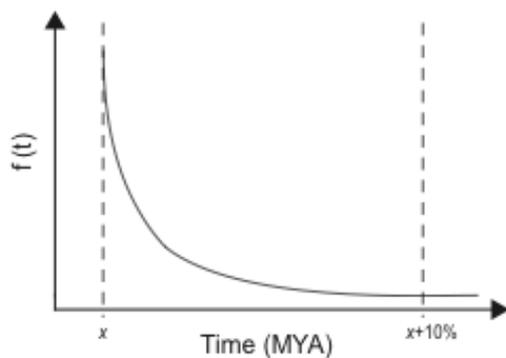
Figure 1
Exponential prior probability distribution with a minimum bound. The probability that the actual divergence date occurs earlier than the fossil calibration *x* declines according to an exponential distribution, with 95% of the posterior density within 10% of the fossil age.

allows us to compare our results with other studies using similar combinations of fossil calibrations to date the origins of squamate groups [see [10,11]].

For nucleotide data, all models are nested in the General Time Reversible model of sequence evolution with a proportion of invariant sites and gamma distributed rate heterogeneity (GTR+I+Γ), as determined by jModelTest 0.1.1 [33,34]. For each analysis, the MCMC was run for 50,500,000 steps each chain and sampled every 500,000 steps. The first 1,000,000 steps of each run were discarded as burnin. To couple the four parallel chains we used a heating coefficient of 0.3. This resulted in a sample of size of 100 from the posterior distribution, taken from the cold chain.

MCMC calculations were performed in the program Tree-Time, freely available at http://www.zi.biologie.uni-muenchen.de/evol/statgen/software/treetime[18]. Within that program, the following models were implemented:

MC: Strict molecular clock model [1], assumes a fixed rate of evolution along all branches of the tree.

CPP: Compound Poisson Process [35], in which points of rate change are interspersed along branches. Following each substitution event, the current rate is modified according to a Poisson process with an adaptive intensity, which determines the *a priori* distribution of the number of changes. Rate modulations are gamma distributed, such that the expectancy value of the product of multiple rate changes is equal to 1.

ULN: Uncorrelated lognormal distributed model of Drummond et al. [16], in which the evolutionary rate of each branch is independently drawn from a lognormal distribution. There is no autocorrelation of rates between neighbouring branches. Parameters within the model determine the expectancy value and variance of rates. A smaller variance indicates a smaller deviation from the strict molecular clock, since rates of change are similar across branches.

DM: Dirichlet model [36]. The *a priori* distribution of evolutionary rates at the branches follows a dirichlet distribution. Parameters within the model determine the variance of rates. The smaller the variance, the smaller the deviation from a strict molecular clock. The average evolutionary rate across branches is kept constant, so that only relative differences between rates are considered.

As an independent evaluation of our results, we also calculate divergence dates for Lacertidae under the ULN model in BEAST [20], an alternative program for Bayesian analysis. Identical model parameters were used in the two programs with the following exceptions: 1) In addition to priors for calibrated nodes, BEAST requires a prior for the distribution of divergence dates, for which we chose the Yule process. 2) BEAST estimates the equilibrium distribution of nucleotides only once at the beginning of the analysis, TreeTime samples these estimates continuously. 3) In BEAST the molecular clock is relaxed by varying molecular rates of the substitution model among branches, for which reason the rates are dependent on the time scale of the tree. TreeTime compresses or stretches the lengths of branches in the tree, given in molecular time units, by rate multipliers with a mean of one.

Finally, we test the performance of alternative clock relaxations on our data by computing Bayes factors, a Bayesian alternative to likelihood ratio tests. Bayes factors calculate the ratio of marginal likelihoods between two given models by integrating over all possible parameter values (as opposed to estimating the maximum likelihood for each parameter). In a comparison between models M_1 and M_2, a Bayes factor >10 on a logarithmic scale indicates that M_1 is more strongly supported by the data under consideration than M_2 [37]. A significant advantage of Bayes factors over likelihood ratio tests is that they automatically penalize models with increasing complexity, and thus guard against overfitting. Furthermore, by using the strict molecular clock as a reference, they allow for a general comparison among any number of independent models [38].

Results
Phylogenetic analysis of the combined genetic data recovers the major lineages of Lacertidae in accordance with previous studies [e.g. [7,39]]. The subfamily Gallotinae

appears most basal and is sister to Lacertinae, which contains the subclades Lacertini and Eremiadini. In all cases the amphisbaenian *Rhineura floridana* forms the sister taxon to Lacertidae, as suggested by previous studies [10,40]. The four independent Bayesian analyses differed only slightly in their tree topology, so that only the tree with the highest posterior probability is shown here (ULN 95% consensus tree, Figure 2).

In all phylogenetic analyses, relationships within Gallotinae were identical, however some differences in tree topology exist regarding the subfamily Lacertinae. The Eurasian subclade Lacertini is represented by a comb-like topology, where generic relationships are largely unresolved. In contrast, the African radiation is split into two monophyletic groups corresponding to Saharo-Eurasian and Ethiopian (Africa south of the Sahara Desert) distributions [e.g. [7,39]], with the latter divided into southern and east African subclades. Phylogenetic resolution is generally higher among African genera, with the only differences between trees limited to the placement of *Acanthodactylus boskianus* as sister taxon to *Mesalina* in all cases except for the CPP 20% model, and *Poromera* as outgroup to the inclusive *Nucras/Latastia/Heliobolus* in all cases except for the strict molecular clock (MC), where it instead branches from the base of the Ethiopian clade. These slight variations in topology have no affect on relationships among the major lineages, so they are not discussed further here. Overall, all trees are essentially in agreement and in the following discussion we refer to the single tree shown in Figure 2.

Divergence estimates

Divergence dates for Lacertidae estimated from each of the molecular clock analyses are listed in Additional file 1: **Lacertid clade ages**. For nearly all of the relaxed clock models, the origin of modern lacertids, as indicated by the split between Gallotinae and Lacertinae, is estimated to be in the Paleocene (56–58 Mya), with the initial radiation of the African clade occurring in the mid-Eocene (44–46 Mya). Within the Eremiadini, the separation of the Saharo-Eurasian and Ethiopian clades occurred after their split from the Lacertini, 40–43 Mya. The subfamily Gallotinae diverged into its component genera, *Gallotia* and *Psammodromus*, during the Oligocene, 29–32 Mya.

To assess the relative fitness of the alternative clock relaxations, we calculated Bayes factors between each model using the strict molecular clock as a reference. Results are shown in Table 2 on a logarithmic scale. In all comparisons, the strict molecular clock was strongly rejected in favour of relaxed clock models, with Bayes factors ranging from -170 to -101. Among the different clock relaxations, the CPP model performed most poorly and gave considerably younger ages for almost all nodes. The DM and

ULN model received comparable Bayes factors, though ULN performs slightly better (ln ULN_DM = 24). Taken together, the relative ordering of MC, CPP, DM, and ULN indicates that the Uncorrelated lognormal model is most appropriate for our data set.

In addition to our original divergences calculated with a 10% maximum soft bound, we expanded probability ranges to within 20% of the minimum date. Doubling prior bounds increased divergence estimates for all nodes, as well as widening confidence intervals (Additional file 1). For example, the original bounds for the Amphisbaenia-Lacertidae split were (64.2, 70.6) and the posterior estimate from to the ULN model was 68.5–83.3 Mya. When prior bounds were increased to 20%, the prior range became (64.2, 77) and the posterior estimate increased to 77.2–100.2 Mya (Additional file 1, node 3). The smallest changes resulting from this increase occurred at the *Sphenodon*-Squamata and Teiidae-Amphisbaenia nodes, which increased by an average of 3.2% and 7.5%, respectively. The largest change occurred at the *Timon/Dalmatolacerta* node, where the divergence date increased by an average of 43.6% across all models, more than double that of any other posterior expansion. Effects were most dramatic in the CPP model, which without exception produced the largest increase in divergence estimates and standard deviations when prior distributions were expanded to 20%. However, because the CPP model is unreliable for our data (see Bayes factors, Table 2), we ignore these dates in the final discussion.

The BEAST analysis of the combined data resulted in a tree topology identical to TreeTime, except for the loss of the *Archaeolacerta/Zootoca* sister group. Molecular dates were younger in BEAST for all but one node (Figure 3; Additional file 1, node 19), but still all fall within the 95% confidence intervals produced in TreeTime. The most significant differences occur at the major lacertid splits (Additional file 1, nodes 4, 5 and 6), where divergences occur approximately 10 My later. These changes are most likely attributed to differences in model parameters and not performance of the programs themselves. The prior distribution on branching times used in BEAST, the Yule Process, has a tendency to pull divergence dates towards the tips of the tree when basal internodes are short but terminal branches are long. This influence can be even stronger when rates vary inside the tree, as is most likely the case in Lacertidae. In TreeTime, prior information on branching times is applied only to calibrated nodes, and every allocation of branching times for remaining nodes in the tree is equally likely. Because of these differences in program settings, we refer only to the age estimates given by TreeTime for our discussion.

14
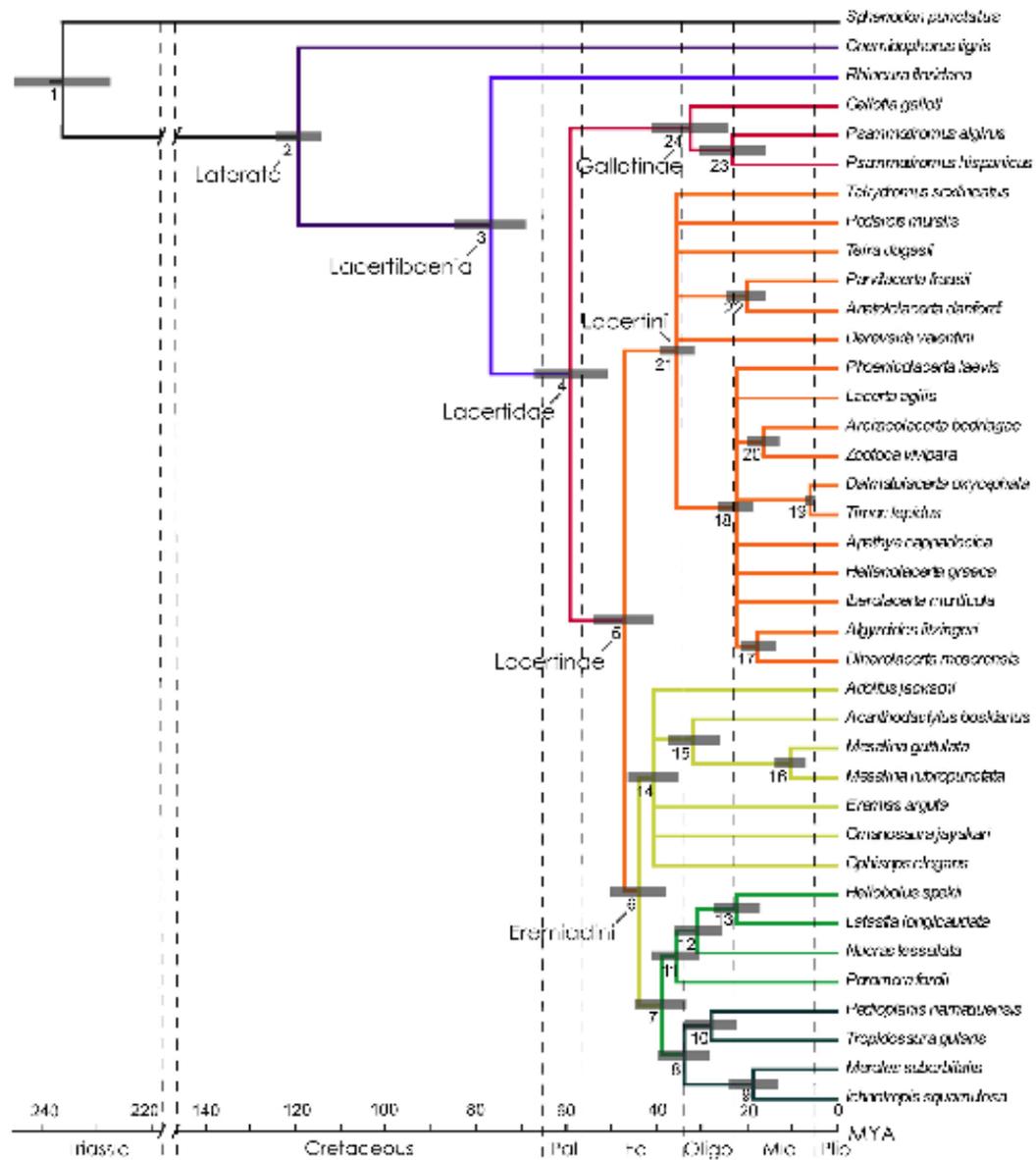
Figure 2
95% majority rule consensus tree for Lacertidae with divergences estimated under an Uncorrelated Lognormal relaxed molecular clock, based on a concatenated data set of 3 mitochondrial and 2 nuclear genes. Gray bars represent mean divergence dates ± 1 standard deviation. Nodes are numbered consecutively and correspond to node numbers in the Additional file 1. A geological time scale in millions of years is shown below.

15

Table 2: Natural logarithm of Bayes factors for the molecular clock models Compound Poisson Process (CPP), Dirichlet Model (DM), Uncorrelated lognormal (ULN), and the strict Molecular Clock (MC), based on the concatenated data set.

	CPP	DM	MC	ULN
CPP		31	-101	56
DM	-31		-133	24
MC	101	133		157
ULN	-56	-24	-157	

Partitioned data sets

Phylogenies based on the partitioned mtDNA and nDNA do not reach a resolution equivalent to the combined data set, leaving large parts of Eremiadini and Lacertini unresolved. Although we refrained from constraining nodes prior to the analysis since there is no current consensus on lacertid ingroup phylogeny, all major nodes were still recovered. Overall, mtDNA produced older dates when compared to the nDNA and combined data. Node ages based on nDNA alone were marginally younger than in the combined analysis (Figure 4; Additional file 1). Among the major nodes, dates among the partitioned and combined data vary little, with the largest difference being the Amphisbaenia-Lacertidae split. Mean dates for the major clades, including European and African lacertids, still remain within the 95% confidence intervals of the combined data.
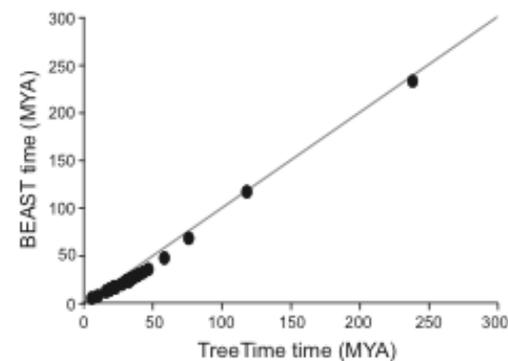
Figure 3
Comparison of divergence dates estimated in the Bayesian programs TreeTime and BEAST. Mean molecular divergence dates, in millions of years, estimated under the ULN relaxed molecular clock model with a 10% prior probability distribution in TreeTime plotted against dates estimated in BEAST for all nodes in the Additional file 1. The solid line indicates a 1:1 relationship between the two values.
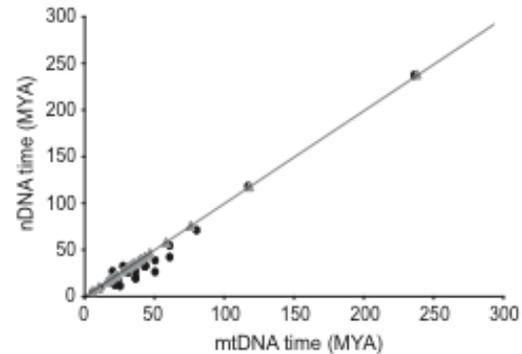
Figure 4
Comparison of mitochondrial DNA and nuclear DNA based estimates of divergence times. Mean molecular divergence dates, in millions of years, estimated from partitioned mtDNA and nDNA for selected nodes. Gray triangles show dates based on the combined data (mtDNA + nDNA), plotted against both axes. The solid line indicates a 1:1 relationship between mtDNA and nDNA estimates. All estimations were made under the ULN relaxed molecular clock model in the program TreeTime.

Selective deletion of calibration points

Three analyses were run under the ULN model each excluding one or more fossil priors. In almost all cases, estimated divergence dates were older and had larger standard deviations than when all calibrations were used (Figure 5). The largest changes occurred when both the amphisbaenian and teiid calibrations were removed. With the exception of the most recent split (*Mesalina guttulata/ Mesalina rubropunctata*), divergence estimates became significantly older and standard deviations expanded by 5–20 My. Excluding the amphisbaenian calibration caused posterior ranges to increase by up to 30 My. Age increases were most strongly evident at the origins of the major lineages. Removing the teiid calibration alone had the least effect on posterior estimates, with a maximum increase of 2 My at all nodes (except for the Teiidae-Amphisbaenia split itself, which increased by almost 15 My).

Discussion

In general, our results confirm recent molecular based studies of lacertid phylogeny, including their sister relationship with amphisbaenians. Low taxon sampling within the subfamily Gallotinae hinders any phylogenetic interpretations for the group, apart from being a monophyletic clade that forms the outgroup to the remaining lacertid taxa. The Palearctic clade Lacertini forms a large polytomy in the strict consensus tree that includes the

16
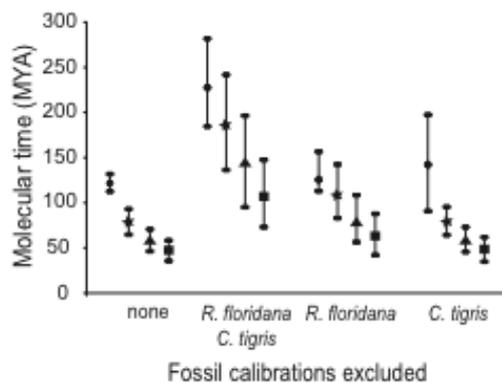
Figure 5
Influences of individual calibration points on node ages. Mean molecular divergence dates, ± 1 standard deviation, for the major lineages estimated using different combinations of fossil calibrations. Divergence dates were calculated using: all four fossil calibrations; all excluding the teiid *Cnemidophorus tigris* and the amphisbaenian *Rhineura floridana*; all except *R. floridana*; and all except *C. tigris*. Evolutionary splits are Teiidae-Amphisbaenia (circle), Amphisbaenia-Lacertidae (star), Gallotinae-Lacertinae (triangle), and Lacertini-Eremiadini (square).

Asian grass lizard *Takydromus sexlineatus* (Figure 2). Relationships among the remaining Palearctic genera are poorly resolved and are therefore not discussed further here, though some biogeographical implications for the clade in general are considered below.

Several well supported sister groups occur within the African subclade Eremiadini (Figure 2). The Saharo-Eurasian group consists of the mainly North African/Asian genera *Ophisops*, *Acanthodactylus*, *Eremias* and *Mesalina*, as well as the Middle Eastern *Omanosaura* and equatorial African genus *Adolfus*. Within the Ethiopian clade, the taxon pairs *Pedioplanis/Tropidosaura* and *Meroles/Ichnotropis* form a distinct southern African cluster, while the remaining genera are distributed primarily in east Africa (with the exception of the singular species of *Poromera* in western central Africa). The restricted distribution of *Poromera* in equatorial forests may be the result of high levels of extinction some time in the past. Indeed, Africa's rainforests have diminished greatly since the early Cenozoic, and during the last 30 My a trend toward increasing aridity, coupled with repeated glacial phases, has left only small remnants of the once extensive blocks of rainforest [41].

Divergence estimates for Lacertidae and their evolutionary implications

Mean dates for the origin of Squamata based on the DM and ULN model (236.9, 238.2 Mya) fall well within estimates given by Vidal and Hedges [10] (221–251 Mya) based on nine nuclear genes, two of which are included in the present study. The split between amphisbaenians and lacertids, on the other hand, is not as well supported. Although their sister relationship is corroborated under all models, node ages vary by over 10 My in the 10% and 20% analyses, the latter case placing the split almost 30 My earlier than the earliest known rhineurid. Previous studies by Vidal and Hedges [10] and Wiens et al. [11] give much older dates for amphisbaenians, pushing their origin back to the late Jurassic-early Cretaceous. It should be noted, however, that Wiens et al. [11] use a different date to calibrate the Amphisbaenia-Lacertidae split based on an older fossil from the early Cretaceous (98 Mya), Hodzhakulia magna [42,43]. This specimen consists only of incomplete maxillaries and dentaries and its purported amphisbaenian affinities have long been in doubt [44,45], making it problematic as a calibration point.

Overall, our dates for the origin of modern lacertids are much earlier than previous estimates, placing them in the late Paleocene, 58–56 Mya. Within the Lacertidae, the majority of divergences occur in the mid- to late Eocene after the Eremiadini split from their palearctic sister clade. The separation of the African clade into its Saharo-Eurasian and Ethiopian genera occurs shortly after, and they continue to diversify until well into the mid-Miocene, some 10 Mya. The relatively young ages of the African lineages are somewhat surprising given the high levels of species richness found in desert clades. Increased rates of speciation in desert lineages may be due to selection pressures experienced in extreme environments. Adaptations to xeric habitat favoring 'r-selected' strategies (e.g. reproducing and dying quickly) could promote a shift towards shortened generation times, thus accelerating diversification [7,46,47]. Unfortunately, very little is known about the ecology of desert lacertids, making it difficult to determine factors underlying their biogeographic patterns. However, recent studies indicate that physiological and life history variables, such as generation time, metabolic rate, body size and clutch size, influence mutation rates in terrestrial vertebrates [48,49], and may affect rates of molecular evolution in reptiles as well [50].

Historical biogeography of Lacertidae

Most authors agree that lacertids originated in Europe, as indicated by the mainly European distribution of the basal Gallotinae [7]. According to our most reliable model (ULN), the majority of the lacertid radiation occurred in the mid-Eocene, 43–46 Mya. During that time, Europe was an archipelago of larger and smaller

17

islands separated by shallow bodies of water [51]. The appearance of land bridges in the Eocene as well as increasing aridity are thought to have played an important role in terrestrial vertebrate migration, and evidence for faunal exchange between Europe and Africa can be seen in the fossil records of mammals and alligators [52,53]. A notable transition in fossil assemblages of squamate reptiles also occurs around the early Eocene in Europe, with large increases in diversity occurring at both the family and species level [[53] and references therein]. Unfortunately, the fossil record for African squamates during that time, particularly for small-bodied lizards, is poor [8] so that comparable estimates of lacertid diversity are unavailable. However, both the warming trend during the late Paleocene-early Eocene and low sea levels presumably made intercontinental dispersal feasible for a wide range of terrestrial vertebrates [53], possibly via land bridges or rafting.

One possible scenario is that lacertids entered North Africa at its northwestern edge via a chain of islands and diversified as they moved towards the southern tip of the continent (Figure 6; map after Popov et al. [54]). A primarily western migration for African lacertids is supported by modern biogeography, since the basal most taxa of both the European and African radiations are found along the western edges of the continents. The basal-most palearctic genus in our analysis (*Podarcis*; ULN, DM, CPP 50% consensus trees) occurs primarily in the western Mediterra-
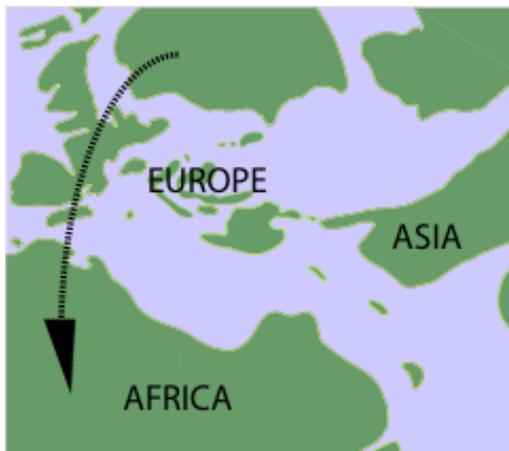
Figure 6
Paleogeographic map of Europe and North Africa in the Late Eocene. Arrow indicates possible lacertid migration route to Africa between southwestern Europe and northwestern Africa via small island chains.

nean region and *Atlantolacerta andreanskyi*, which morphologically and genetically appears basal in the African radiation [7] is restricted to the Atlas Mountains in northern Africa. Taken together, these distributions indicate that southern Iberia and northwest Africa were important areas of divergence for modern lacertids. Similar pattern of dispersal have been hypothesized for other terrestrial fauna, where interchanges of mammals in the Cretaceous and Paleogene occurred along a discontinuous route between southwestern Europe and Africa [55]. Not until the mid-Miocene did a second, more stable land route between southeastern Europe and Asia form, permitting effective movement between the two landmasses [55].

Mayer and Benyr [56] and Arnold et al. [7] proposed the colonization of Africa by Lacertidae in the Miocene over the land bridge connecting Arabia and Africa, which remained up until the early Pliocene [57]. Although our dates for the initial radiation of African lacertids conflict with this hypothesis, this geological event could still have played an important role in the dispersal of certain members of the Saharo-Eurasian clade. Within that group, only *Adolfus* and *Holaspis* (the latter of which is absent in our analysis) are truly African in distribution, while the remaining genera are palearctic. Distributions of *Acanthodactylus*, *Mesalina*, and *Ophisops* in Africa are mainly restricted to the northern Atlantic coast, and the majority of their species, along with *Eremias*, are found in the Middle East and Asia. This pattern suggests that the Saharo-Eurasian lineage may have originated in Eurasia and only partially left the Palearctic, as opposed to secondarily recolonizing the Middle East and Asia from Africa. In fact, the land bridge could have been crossed in the other direction, with the ancestors of modern *Acanthodactylus*, *Mesalina*, and *Ophisops* entering Africa from Arabia once the continents established secondary contact.

An alternative colonization scenario is that the African lineage split from the Lacertini in Europe *prior* to migrating to Africa, and then only later radiated into its component lineages after reaching the African continent. Discovery of a fossil lacertid in Europe with African-like qualities would support this hypothesis. Interestingly, the Baltic amber lizard *Succinilacerta* [58] from mid-Eocene Poland was for some time assigned to the south African genus *Nucras* [59-61], suggesting that it resembles an African lacertid, at least superficially. Unfortunately, most of the diagnostic features separating the European and African clades, including features of the clavicle, tail, ulnar nerve and hemipenis, are not externally visible in preserved specimens [7]. Detailed investigation of this fossil, for example using X-ray Computed Tomography, could reveal internal structures assigning it to one of the modern clades. Other alternatives to fossil evidence may be found

18

in additional taxon sampling for molecular studies. For example, inclusion of the basal African species *Atlantolacerta andreanskyi* in future molecular clock analyses could place a clearer temporal framework around the early evolutionary history of Eremiadini.

Reliability of fossil calibrations

To test the reliability of the oldest squamate calibrations, the Teiidae-Amphisbaenia and the Amphisbaenia-Lacertidae splits, we alternately excluded each of them and compared their respective outcomes. Our results indicate that when all calibrations are combined, the teiid calibration does not have a significant effect on the estimated divergences for lacertids, since its exclusion only marginally alters the ages of the other splits (Figure 5). At the same time, when the teiid calibration is removed, its own divergence from lacertids/amphisbaenians becomes 17.4% older than the oldest-known teiid fossil, whereas removal of the amphisbaenian calibration causes the same split to be 64% older than the prior. Although this result may support the use of fewer calibrations, it should be noted that the use of only two fossil constraints led to unrealistic estimates, pushing the origin of Squamata well into the Permian.

With respect to future studies, we suggest that it may be preferable to constrain calibration points individually depending on the quality of the fossils themselves. For some clades, the quality of different fossils in terms of stratigraphic age or reliable phylogenetic position may be highly variable, with some being easier to constrain confidently based on prior knowledge than others. In such cases, the application of qualitative phylogenetic and stratigraphic criteria as suggested by Reisz & Müller [5,62] and Müller & Reisz [63] may be combined with exponential probability distributions, such that in case of a "good" fossil calibration, the soft bound spans the estimated temporal range in which the split must have occurred. Conversely, in cases of more questionable fossil dates, a 10% or 20% (or any other) upper bound may be applied.

Conclusion

Estimation of evolutionary ages for crown clades such as the lizard family Lacertidae may be hampered by multiple sources of uncertainty, including unknown phylogenetic relationships, lack of an adequate fossil record, and variable evolutionary rates. These are not uncommon obstacles in molecular dating, however they must still be addressed within a statistical framework. Our results highlight the advantages of a Bayesian approach. The methods we describe allow incorporation of prior information in the form of multiple fossil calibrations, while allowing for statistical flexibility and the evaluation of alternative clock models using Bayes factors. We also support the use of a total evidence approach, in which all available molecular

data is combined. Particularly when implemented with multiple calibrations in a Bayesian framework, the simultaneous analysis of multiple loci provides independent constraints on the evolutionary model, thereby avoiding potential biases associated with a single gene or genome [64]. Finally, we stress the importance of communication between paleontologists and molecular biologists in establishing suitable calibrations for more than just the major clades of Metazoa or Tetrapoda. Access to accurate information on divergence dates and paleontological material will allow biologists with diverse study systems to investigate topics such as evolutionary diversification, rates and patterns of morphological change, and historical biogeography at finer phylogenetic scales. In this regard, identifying groups needing additional study and developing plans to enable that study should be a top priority for paleontologists to position themselves as important contributors to the field of molecular dating.

Authors' contributions

CAH collected genetic sequence data, performed the sequence alignment and drafted the manuscript. The original study was conceived by JM, who also participated in data interpretation and helped draft the manuscript. LH and DM designed the bioinformatics program used here and LH carried out all molecular clock analyses. All authors reviewed and approved the final manuscript.

Additional material

Additional file 1

Lacertid clade ages. Mean divergence dates, followed by error ranges, estimated under four different Bayesian molecular clock models using 10% and 20% prior probability distributions. Model abbreviations are Uncorrelated lognormal (ULN), Dirichlet Model (DM), Compound Poisson Process (CPP), and the strict molecular clock (MC). Additional analyses using the ULN model are ULN_1 (excluding the amphisbaenian and teiid calibrations), ULN_2 (excluding the amphisbaenian calibration), ULN_3 (excluding the teiid calibration), mtDNA partition, nDNA partition, and BEAST. Dates are given in millions of years. Nodes are numbered in correspondence to the tree in Figure 1 and calibrated nodes are denoted with an asterisk (*).

Click here for file

[http://www.biomedcentral.com/content/supplementary/1471-2148-9-151-S1.pdf]

19

References

1. Zuckerkandl E, Pauling L: **Evolutionary Divergence and Convergence in Proteins.** In *Evolving Genes and Proteins* Edited by: Bryson V, Vogel H. New York: Academic Press; 1965:97-166.
2. Bromham L, Penny D: **The modern molecular clock.** *Nature Rev Gen* 2003, **4**:216-224.
3. Smith AB, Peterson JJ: **Dating the time of origin of major clades: molecular clocks and the fossil record.** *Annu Rev Earth Planet Sci* 2002, **30**:65-88.
4. Graur D, Martin W: **Reading the entrails of chickens: molecular timescales of evolution and the illusion of precision.** *Trends Genet* 2004, **20**:80-86.
5. Reisz RR, Müller J: **Molecular timescales and the fossil record: a paleontological perspective.** *Trends Genet* 2004, **20**:237-241.
6. Benton MJ, Donoghue PCJ: **Paleontological evidence to date the tree of life.** *Mol Biol Evol* 2007, **24(1)**:26-53.
7. Arnold EN, Arribas O, Carranza S: **Systematics of the Palaearctic and Oriental lizard tribe Lacertini (Squamata: Lacertidae: Lacertinae), with descriptions of eight new genera.** *Zootaxa* 2007, **1430**:1-86.
8. Evans SE: **At the feet of dinosaurs: the early evolutionary history and radiation of lizards.** *Biol Rev* 2003, **78**:513-551.
9. Arnold EN: **Competition, evolutionary change and montane distributions.** In *The Evolving Biosphere* Edited by: Forey PL. British Museum (Natural History), London; 1981:217-228.
10. Vidal N, Hedges SB: **The phylogeny of squamate reptiles (lizards, snakes, and amphisbaenians) inferred from nine nuclear protein-coding genes.** *C R Biologies* 2005, **328**:1000-1008.
11. Wiens JJ, Brandley MC, Reeder TW: **Why does a trait evolve multiple times within a clade? Repeated evolution of snakelike body form in squamate reptiles.** *Evolution* 2006, **60**:123-141.
12. Carranza S, Arnold EN, Amat F: **DNA phylogeny of *Lacerta* (*Iberolacerta*) and other lacertine lizards (Reptilia: Lacertidae): did competition cause long-term mountain restriction?** *System Biodivers* 2004, **2(1)**:57-77.
13. Sanderson MJ: **A nonparameteric approach to estimating divergence times in the absence of rate constancy.** *Mol Biol Evol* 1997, **14**:1218-1231.
14. Sanderson MJ: **R8s: inferring absolute rates of molecular evolution and divergence times in the absence of a molecular clock.** *Bioinformatics* 2003, **19**:301-302.
15. Yang Z, Rannala B: **Bayesian estimation of species divergence times under a molecular clock using multiple fossil calibrations with soft bounds.** *Mol Biol Evol* 2006, **23**:212-226.
16. Drummond AJ, Ho SYW, Phillips MJ, Rambaut A: **Relaxed phylogenetics and dating with confidence.** *PLOS Biol* 2006, **4(5)**:e88.
17. Magallón SA: **Dating lineages: molecular and paleontological approaches to the temporal framework of clades.** *Int J Plant Sci* 2004, **165(Suppl 4)**:S7-S21.
18. Himmelmann L, Metzler D: **TreeTime: An extensible C++ software package for Bayesian phylogeny reconstruction with time-calibration.** *Bioinformatics* 2009 [http://www.zi.biologie.uni-muenchen.de/evol/statgen/software/treetime].
19. Huelsenbeck JP, Ronquist F: **MRBAYES: Bayesian inference of phylogeny.** *Bioinformatics* 2001, **17**:754-755.
20. Drummond AJ, Rambaut A: **BEAST: Bayesian evolutionary analysis by sampling trees.** *BMC Evol Biol* 2007, **7**:214.
21. Thompson JD, Higgins DG, Gibson TJ: **CLUSTAL W: improving the sensitivity of progressive multiple sequence alignments through sequence weighting, position specific gap penalties and weight matrix choice.** *Nucl Acids Res* 1994, **22**:4673-4680.
22. Galtier N, Gouy M, Gautier C: **SeaView and Phylo_win, two graphic tools for sequence alignment and molecular phylogeny.** *Comput Applic Biosci* 1996, **12**:543-548.
23. Farris JS, Källersjö M, Kluge A, Buit C: **Testing significance of congruence.** *Cladistics* 1994, **10**:315-320.
24. Swofford DL: **PAUP* Phylogeny Analysis Using Parsimony (*and other methods), version 40b10.** *Sinauer Association, Inc,* Sunderland, Massachusetts 2002.
25. Yoder AD, Irwin JA, Payseur BA: **Failure of the ILD to determine data combinability for slow loris phylogeny.** *Syst Biol* 2001, **50**:408-424.
26. Kluge AG: **Total evidence or taxonomic congruence: cladistics or consensus classification.** *Cladistics* 1998, **14(2)**:151-158.
27. Sues HD, Olsen PE: **Triassic vertebrates of Gondwanan aspect from the Richmond Basin of Virginia.** *Science* 1990, **249**:1020-1023.
28. Datta PM, Ray S: **Earliest lizard from the Late Triassic (Carnian) of India.** *J Vert Paleontol* 2006, **26**:795-800.
29. Nydam RL, Cifelli RL: **Lizards from the Lower Cretaceous (Aptian-Albian) Antlers and Cloverly formations.** *J Vertebr Paleontol* 2002, **22**:286-298.
30. Sullivan RM: **A new middle Paleocene (Torrejonian) rhineurid amphisbaenian, *Plesiorhineura tsentasi* new genus, new species, from the San Juan Basin, New Mexico.** *J Paleontol* 1985, **59**:1481-1485.
31. Estes R: **Handbuch der Paläoherpetologie, Part 10: Sauria terrestria, Amphisbaenia.** Stuttgart: Gustav Fischer Verlag; 1983.
32. Sanders KL, Lee MSY: **Evaluating molecular clock calibrations using Bayesian analyses with soft and hard bounds.** *Biol Lett* 2007, **3**:275-279.
33. Guindon S, Gascuel O: **A simple, fast, and accurate algorithm to estimate large phylogenies by maximum likelihood.** *Syst Biol* 2003, **52**:696-704.
34. Posada D: **jModelTest: Phylogenetic model averaging.** *Mol Biol Evol* 2008, **25**:1253-1256.
35. Huelsenbeck JP, Larget B, Swofford D: **A compound Poisson process for relaxing the molecular clock.** *Genetics* 2000, **154**:1879-1892.
36. Himmelmann L: **Bayessche Methoden zur Schätzung von Stammbäumen mit Verzweigungszeitpunkten aus molekularen Daten.** In *PhD thesis* Goethe-University Frankfurt am Main, Germany, Department of Computer Science and Mathematics; 2008.
37. Kass RE, Raftery A: **Bayes factors.** *J Am Stat Assoc* 1995, **90**:773-795.
38. Lepage T, Bryant D, Philippe H, Lartillot N: **A general comparison of relaxed molecular clock models.** *Mol Biol Evol* 2007, **24**:2669-2680.
39. Mayer W, Pavlicev M: **The phylogeny of the family Lacertidae (Reptilia) based on nuclear DNA sequences: convergent adaptations to arid habitats within the subfamily Eremiainae.** *Mol Phylogenet Evol* 2007, **44**:1155-1163.
40. Townsend TM, Larson A, Louis E, Macey JR: **Molecular phylogenetics of Squamata: the position of snakes, amphisbaenians, and dibamids, and the root of the squamate tree.** *Syst Biol* 2004, **53**:735-757.
41. Wolfe JA: **Distribution of major vegetation types during the Tertiary.** *Geophys Monogr* 1985, **32**:357-375.
42. Nessov LA: **Rare bony fishes, terrestrial lizards and mammals from the lagoonal zone of the littoral lowlands of the Cretaceous of the Kyzylkumy.** *Yearbook of the All-Union Palaeontological Society, Leningrad* 1985, **28**:199-219.
43. Gao K: **Sineoamphisbaena phylogenetic relationships discussed: reply.** *Can J Earth Sci* 1997, **34**:886-889.
44. Wu X, Russell AP, Brinkman DB: **Discussion: phylogenetic relationships of *Sineoamphisbaena hexatabularis*: further considerations.** *Can J Earth Sci* 1997, **4(6)**:883-885.
45. Kearney M: **Systematics of the Amphisbaenia (Lepidosauria: Squamata) based on morphological evidence from recent and fossil forms.** *Herpetological Monographs* 2003, **17**:1-74.
46. McKinney ML, McNamara KJ: *Heterochrony the Evolution of Ontogeny* New York: Plenum Press; 1991.
47. Smith SA, Donoghue MJ: **Rates of molecular evolution are linked to life history in flowering plants.** *Science* 2008, **322**:86-89.
48. Martin AP, Palumbi SR: **Body size, metabolic rate, generation time, and the molecular clock.** *Proc Natl Acad Sci USA* 1993, **90**:4087-4091.
49. Rand DM: **Thermal habit, metabolic rate and the evolution of mitochondrial DNA.** *Trends Ecol Evol* 1994, **9**:125-131.
50. Bromham L: **Molecular clocks in reptiles: life history influences rates of molecular evolution.** *Mol Biol Evol* 2002, **19(3)**:302-309.
51. Franzen JL: **Mammalian faunal turnover in the Eocene of central Europe.** In *Causes and Consequences of Globally Warm Climates in the Early Paleogene* Edited by: Wing SL, Gingerich D, Schmitz B, Thomas E. Colorado: Geological Society of America; 2003:455-461.
52. Rossmann T, Müller J, Forst M: **First evidence of an alligatorid from Africa and its implications for crocodilian palaeobiogeography.** *Neues Jahrbuch für Geologie und Paläontologie Monatshefte* 2000, **12**:651-668.

53. Augé M: **Lacertilian faunal change across the Paleocene-Eocene boundary in Europe.** In *Causes and Consequences of Globally Warm Climates in the Early Paleogene* Edited by: Wing SL, Gingerich D, Schmitz B, Thomas E. Colorado: Geological Society of America; 2003:441-454.

54. Popov SV, Rögl F, Rozanov AY, Steininger FF, Shcherba IG, Kovac M: **Lithological-Paleogeographic maps of the Paretethys. – 10 maps Late Eocene to Pliocene.** *Courier Forschungsinstitut Senckenberg* 2004, **250**:1-46.

55. Gheerbrant E, Rage J-C: **Paleobiogeography of Africa: how distinct from Gondwana and Laurasia?** *Palaeogeogr, Palaeoclimatol, Palaeoecol* 2006, **241**:224-246.

56. Mayer W, Benyr G: **Albumin-Evolution und Phylogenese in der Familie Lacertidae.** *Annual Naturhistorisches Museum Wien* 1994, **96B**:621-648.

57. Whybrow P: **Geological and faunal evidence from Arabia from mammal "migrations" between Asia and Africa during the Miocene.** *Cour Forsch Inst Senckenberg* 1984, **69**:189-198.

58. Böhme W, Weitschat W: **Redescription of the Eocene lacertid lizard *Nucras succinea* Boulenger, 1917 from Baltic amber and its allocation to *Succinilacerta* n gen.** *Mitteilungen des Geologisch-Paläontologischen Instituts der Universität Hamburg* 1998, **81**:203-222.

59. Klebs R: **Über Bernsteineinschlüsse im allgemeinen und die Coleopteren meiner Bernsteinsammlung.** *Schr physik ökonom Ges Königsberg* 1910, **51**:217-242.

60. Boulenger GA: **A revision of the lizards of the genus *Nucras*, Gray.** *Ann S Afr Mus* 1917, **5**:196-216.

61. Boulenger GA: **Monograph of the Lacertidae 1.** London: Trustees of the British Museum (Natural History); 1920:1-352.

62. Reisz RR, Müller J: **The comparative method for evaluating fossil calibration dates: a reply to Hedges and Kumar.** *Trends in Genetics* 2004, **20**:596-597.

63. Müller J, Reisz RR: **Four well-constrained calibration points from the vertebrate fossil record for molecular clock estimates.** *BioEssays* 2005, **27**:1069-1075.

64. Yang Z, Yoder AD: **Comparison of likelihood and Bayesian methods for estimating divergence times using multiple gene loci and calibration points, with application to a radiation of cute-looking mouse lemur species.** *Syst Biol* 2003, **52**:705-716.

CHAPTER 2:

MORPHOLOGICAL CONVERGENCE IN ARID-DWELLING AFRICAN LACERTID LIZARDS DRIVEN BY ECOLOGICAL AND CLIMATIC FACTORS

ABSTRACT

Studies on the relationship between morphological and ecological variation (ecomorphology) provide a mechanistic link between phenotype and environment. In lizards, strong and predictable patterns of ecomorphology have been found that reveal the selective forces behind adaptation and diversification. However, not all groups of lizards conform to these patterns. The family Lacertidae, spread throughout the Old World, has largely failed to exhibit strong relationships between habitat use and morphology, despite evidence for adaptive radiations and some degree of habitat specialization in Africa. Here we examine morphological variation within and across clades of lacertids in relation to ecology and climate, in an attempt to identify patterns of ecomorphology underlying their evolutionary diversification. Based on measurements of preserved and live animals, we found extensive morphological overlap across biome and substrate types within arid and mesic-dwelling groups. These similarities persist even after application of phylogenetic comparitive methods, indicating strong selective pressures overriding shared ancestry. Particulary among arid-dwelling African clades, a morphological pattern of elongated hindlimbs and robust (deep, wide) heads is shared by independently evolved taxa. Body shape also covaried with site-specific climatic variables in arid regions, with lacertids in more seasonal and extreme environments (for both precipitation and temperature) having relatively smaller heads but long limbs and toes. We suggest that in addition to the selective pressures of foraging mode and prey type on lacertid body shape, extreme climatic conditions contribute to convergent morphologies across independent clades by affecting similar changes in life history. Further studies temporally linking the origin of

derived morphological features to colonization of arid regions will reveal if convergence in African lacertids is driven by development processes.

INTRODUCTION

The extraordinary degree of morphological variation both within and among clades is one of the most striking features of evolution by natural selection (Simpson 1953, Schluter 1998, Carroll 2001). Even closely related species can vary dramatically in body shape and size, and this variation impacts the way they interact with their environments. Ecomorphology, the study of the nature and strength of associations between ecology and morphology, seeks to identify the factors mediating interactions between phenotype and environment, typically through comparative measures of behavior, foraging, locomotion, performance, or some other indicator of ecological function (Losos 1990a, Wainright and Reilly 1994, Luczkovich et al. 1995, Aerts et al. 2002).

The application of phylogenetic hypotheses (i.e. phylogenetic trees) to morphological data also allows us to consider the effects of evolutionary history on interspecific variation. Phylogenetic comparative methods (PCMs) use species relationships derived from independent sources (typically molecular sequence data) to remove the effects of relatedness from covariation in trait values (Felsenstein 1985, Harvey and Pagel 1991, Garland et al. 1992, Miles and Dunham 1993). For most PCMs, the phylogenetic tree is converted into a variance-covariance matrix, in which the diagonals and off-diagonals represent expected and shared amounts of evolutionary change, respectively (Garland et al. 2005). Standard regression or linear contrasts can then be applied to elements in the matrix to extract the portion of variation independent of

relatedness, making them statistically independent and thus appropriate for standard analyses (Grafen 1989, Martins and Housworth 2002).

The integration of PCMs with the greater availability of phylogenetic trees and improved techniques for measuring morphological and ecological traits has led to a resurgence in ecomorphological studies (Schulte et al. 2004). Squamate reptiles, and lizards in particular, have been the main focus of these investigations, providing important insights into the forces driving adaptive radiations and evolutionary diversifications (Pianka 1969, Losos 1990a, Miles 1994, Irschick et al. 1997, Irschick and Losos 1998, Melville and Swain 2000, Herrel et al. 2002). As a whole, lizards present a spectacular array of diversity in both body form and ecology, and encompass several major groups spread across every continent except Antarctica. Among the best known ecomorphological studies are those of Caribbean anoles, whose patterns of body size, shape, diet and behavior are strongly linked to habitat partitioning among perch types (Irschick and Losos 1998, Butler and Losos 2002, Losos 2007). The application of PCMs to this group also revealed that the same sets of ecomorphs (e.g., crown-giant, trunk-crown, trunk-ground) evolved multiple times on each island independently, suggesting that the relationship between ecology and morphology is both strong and predictable (Losos 1992, Irschick et al. 1997, Losos et al. 1998).

However, not all groups of lizard conform to these patterns. The Old World family Lacertidae, with over 300 species in Eurasia and Africa, is widely spread across diverse habitats including equatorial rainforest (*Gastropholis*, *Holaspis*), Asian steppe (*Takydromus*), African savanna (*Pedioplanis*) and extreme desert (*Acanthodactylus*, *Meroles*). Although some species exhibit highly specialized morphologies such as flattened bodies for gliding (*Holaspis* spp., Vanhooydonck et al. 2009), and shovel shaped

24

snouts and fringed toes for sand diving (*Meroles* spp., Arnold 1995), lacertids are generally considered to be morphologically conservative (Arnold 1987, 1989a). This is surprising, as lacertids are as evolutionarily old and widespread as many diverse clades such as Gekkota and Chameleonidae (Vidal and Hedges 2005, Wiens et al. 2006). Particularly in Africa, where lacertids represent a substantial component of the squamate reptile diversity, a large degree of habitat specialization and adaptation is expected.

Several authors have examined the relationship between lacertid morphology and ecology using various types of data (see Table 1). For example, Verwaijen and Van Damme (2007) found a correlation between increased foraging activity and long tails and narrow heads, although with varying significance depending on the evolutionary model used. Vanhooydonck and Van Damme (1999) showed morphological differences according to habitat use (e.g., longer limbs in species in open habitats), but associations disappeared following phylogenetic comparison. Many of these studies relied on incomplete or unresolved phylogenies compiled from molecular and morphological data, and all lacked information on actual branch lengths which can strongly impact the outcomes of PCMs (Martins and Housworth 2002).

While lacertids have been subject to numerous phylogenetic investigations, widespread morphological convergence and variability in molecular markers have hampered the resolution of deeper evolutionary splits (Arnold 1989a, Harris et al. 1998a, Fu 2000). Estimating divergence dates within the family has also been challenging, since lacertids lack an adequate fossil record from which to derive molecular clock calibrations. Fortunately, advances in molecular sequencing and divergence dating have made it possible to apply phylogenetic methods to groups with poorly known evolutionary histories (Drummond et al. 2006, Yang and Rannala 2006). Based on nuclear gene

sequences and improved taxon sampling, Mayer and Pavlicev (2007) showed the African clade consisted of at least three separate radiations into arid habitats, as opposed to a single gradual expansion as reconstructed by morphology (see Arnold 1989a). Short internal branch lengths for these taxa also indicate rapid evolutionary radiations in arid environments, such as for the southern African genera *Meroles* (Harris et al. 1998b) and *Pedioplanis* (Makohka et al. 2007). Based on the relaxed molecular clock analysis of Hipsley et al. (2009), the African clade as a whole was shown to be much older than previously thought, with the majority of the radiation beginning in the mid- to upper Paleogene and continuing to the upper Miocene some 10 million years (My) ago. The relatively young age and high species richness of its arid-dwelling taxa indicate a rapid evolutionary radiation, which is often accompanied by morphological adaptation and diversification (Foote 1997, Schluter 2000).

Given the new information on lacertid history and phylogenetics, we chose to reevaluate their morphology in light of evolutionary relationships and ecological diversity. We use a nested approach in which we analyse morphological variation across the family using museum specimens and general ecology, and within species rich African clades based on measurements and substrate use of live animals in the field. We also investigate the relationship between individual morphology and site-specific climate in arid-dwelling African species, to determine if correlations between body shape and environment are driven by abiotic factors.

MATERIALS AND METHODS

Ecomorphology of lacertid lizards was examined using two independent data sets consisting of measurements taken on ethanol-preserved specimens and live animals in their natural habitats. The morphological variables chosen are ones likely to represent

adaptation to different habitats on the basis of previous field and laboratory studies (e.g.,

Losos and Miles 2002, Harmon et al. 2003, Schulte et al. 2004; also see Table 1). Both

males and females were included in the analyses (since sex could not always be

determined), so that potential differences due to sexual dimorphism are not considered.

We therefore pooled data from males and females to calculate morphological means for

each species. Sampled taxa were also subjected to phylogenetic analysis for the purpose

of applying PCMs, since related taxa are not statistically independent (Felsenstein 1985).

Accession numbers, taxon sampling and sample sizes for the phylogeny and both data

sets are listed in Table 2.

Data set 1. External morphology and ecology of museum specimens

Ten external measurements were taken on ethanol-preserved specimens of

Lacertidae from the Museum für Naturkunde Berlin, Germany. A total of 214 individuals

from 52 species was measured for the following variables using a ruler and digital

calipers to the nearest 0.01mm: (1) snout-vent length (SVL), from the tip of the snout to

the posterior edge of the cloaca, (2) head width, at the widest point posterior to the eyes,

(3) head depth, at the maximal height posterior to the eyes, (4) head length, from the tip

of the snout to the posterior edge of the parietal table, (5) humerus length, from the

intersection of the forelimb and body to the apex of the elbow (6) radius length, from the

apex of the elbow to the wrist joint (7) femur length, from the intersection of the hindlimb

and body to the knee joint (8) tibia length, from the knee joint to the heel, (9) foot length,

from the heel to the base of the 4th digit, and (10) toe length, from the base of the 4th (and

longest) digit to the tip of the claw. Limb measurements were separated into upper and

lower elements (as opposed to total limb length) because of the difficulty of straightening

limbs of preserved specimens. Only adults animals were included, and tail length was not

considered since many individuals had broken or regenerated tails. Between one and nine

individuals were measured per species (Table 2), and all measurements were performed by the same person (K. Brevik). Catalogue numbers and localities of museum specimens are given in Appendix 1.

For ecological descriptions, the collection locality of each specimen was georeferenced to a latitude and longitude. A biome assignment was extracted for each individual using the Terrestrial Ecoregions GIS database (Olson et al. 2001) in ArcGIS v.9.3 (ESRI 2011). Although biome here reflects global distributions of biotic communities and so is not completely independent of species distributions, it provides a useful framework for comparisons among groups and identification of habitats with disparate morphologies (Olson et al. 2001). Individual classifications were used as guidelines for assigning a single biome type to each species. A total of six biomes were represented in the data, capturing large scale variation in climatic zones (e.g., temperate vs tropical) and predominant vegetation (e.g., savanna vs forest). Biome assignments and species means ± 1 standard error for all variables are listed in Appendix 2.

Data set 2. External morphology and site-specific ecology and climate of live animals

To explore specific relationships between morphology and ecology in areas of high species richness (i.e. arid habitats), we conducted fieldwork in Namibia and Sudan in November 2010 and October 2011, respectively (see Figure 1 for sampling localities). Namibia is home to 24 lacertid species in 5 genera, with particularly high species richness and endemism in the Namib and Kalahari Deserts. Sudan, with its hyper arid coastal plains and mountainous regions along the Red Sea coast and Sahara Desert, is also an area of high lacertid diversity (11 species, 7 genera).

At each site, individuals were observed during warm, sunny days when lizards are at active field body temperatures. Substrate type (e.g., loose sand, compact sand, gravel, leaf litter, rock) was recorded at the perch site of each individual prior to disturbance. Although individuals may exploit multiple substrates throughout life, we described the most commonly used type for each individual observed at our study sites. In areas where substrate types frequently overlapped, individuals were scored for both (e.g., loose sand/leaf litter). Lizards were captured by hand or noose and measured directly with a ruler and digital callipers to the neareast 0.01mm. Seven external measurements were taken on live animals by a single person (C. Hipsley): (1) SVL, (2) head width, (3) head depth, (4) head length, (5) forelimb length, from the intersection of the forelimb and body to the tip of the longest finger, (6) hindlimb length, from the intersection of the hindlimb and body to the tip of the longest toe, and (7) toe length. Again, tail length was excluded since many individuals had broken or regenerated tails. All lizards and microhabitats were photographed, and GPS coordinates for each perch site were recorded on a Garmin GPSmap 60cx instrument.

For site-specific climate data, annual temperature and precipitation values were extracted for each coordinate in DIVA-GIS v.7.5 (Hijmans et al. 2001). Nineteen bioclimatic variables (derived from averaged monthly temperature and rainfall values from 1950-2000, Table 3) were downloaded from the WORLDCLIM database at 30 arc-seconds (~1 km^2) resolution (Hijmans et al. 2005; http://www.worldclim.org). These are preferred over monthly values as they represent annual trends, seasonality and extreme or limiting factors related to climate. In total, 80 individuals from 13 species were recorded (Table 1). Morphological measurments, GPS coordinates and substrate assignements for each individual are listed in Appendix 3.

Statistical analyses

All morphological measurements were log transformed prior to analyses. Since body sizes among individuals in this study vary considerably (SVL 28-146mm), we removed the effects of size on shape using Mosimann's (1970) geometric mean method. Although various methods of size adjustment are available (for a review, see Klingenberg 1996), the geometric mean method is most appropriate for interpretations of shape variation across highly heterogenous groups (Butler and Losos 2002). This approach removes the effects of size for each observation using a directly measured index of size, calculated as the arithmetic mean of all log-transformed variables (equal to the log of the geometric mean of the raw variables). The calculated size index (SIZE) is then subtracted from each individual measurement to get a size adjusted value (i.e. the log-ratio). For example, the size adjusted value for humerus length=(log)humerus length–(log)SIZE. Unless otherwise stated, the size adjusted values for species means in Data set 1 and individual values for Data set 2 were used in the following analyses. We chose to focus on individual variation in the latter, as some species were characterized by multiple substrate and climate types.

Multivariate statistical analyses were performed on each data set separately in JMP v.5.1 (SAS Institute, Cary, NC, USA). Principal component analysis (PCA) was used to visualize relationships among variables and identify those contributing the most to morphological variation. To test if morphology signficantly differed among ecological categories, multivariate analysis of variance (MANOVA) was applied to each data set with biome and substrate as factors. Significant groupings were followed by pairwise contrasts within each category.

For field data, multiple regression analysis was performed to explore relationships between morphology and site-specific climate. Partial least squares (PLS) regression was used to assess the relationship between the 19 bioclimatic (predictor) variables and individual morphological (response) variables at each perch site. SVL was excluded from this analysis, as we were primarily interested in body shape variation and did not want differences in body size to overwhelm the explanatory power of other variables (see below). We used k-fold cross-validation to determine the number of axes to retain for interpretation.

Phylogenetic comparative analyses

A phylogenetic tree for comparative analyses of lacertid morphology was constructed based on 1012 base pairs of the nuclear gene RAG-1. Nuclear genes have proven highly successful in resolving higher level squamate relationships (Vidal and Hedges 2005, Townsend et al. 2008), and have been particularly useful in determining the phylogenetic structure of African lacertids (Mayer and Pavlicev 2007). Gene sequences were downloaded from GenBank and aligned and edited in SeaView v.4 (Gouy et al. 2010) for 70 lacertid species and two outgroups (one amphisbaenian, one teiid) (Table 1).

To obtain branch lengths in absolute time, a divergence dating analysis was performed in the Bayesian software BEAST v.1.7.1 (Drummond et al. 2012). Details on the implementation of model parameters and fossil-based calibrations are given in Appendix 4. The resulting 95% maximum clade credibility tree (maximizing the product of the posterior probabilities of all nodes) provided mean branch lengths from the posterior distribution in millions of years. For statistical analyses, the phylogenetic tree was adjusted to match taxon sampling in each data set (a requirement for most PCMs). Taxa present in the phylogeny but not in the morphological sample were pruned from the

31

tree, and taxa sampled for morphology but not phylogeny were added to the tree based on the literature. Details on tree modifications are given in Appendix 5. Final tree topologies for Data sets 1 and 2 are shown in Figure 2.

To detect the presence of phylogenetic signal in the morphological data, we applied Pagel's lambda test in the Geiger package of R (Harmon et al 2008, R Development Core Team 2008). The lambda parameter (λ) transforms the phylogenetic tree by multiplying internal branch lengths by 0 (collapsing the tree into a single polytomy), to test if the resulting phylogeny predicts observed patterns of trait covariance among species. Log-likelihood scores for the above model were compared with the maximum likelihood (ML) model of lambda using a likelihood ratio test. The model of best fit was determined by the p-value calculated from the chi-square distribution.

For phylogenetically independent comparisons with the statistical analyses above, we performed phylogenetic PCA on species means in each data set using the Phytools package in R (Revell 2012). An advantage of phylogenetic PC axes over traditional ones is that they are evolutionarily independent, meaning that the phylogenetic correlation (i.e. the correlation of independent contrasts) between scores on each axis is zero (Revell 2012). Scores from the retained PC axes were projected into a phylomorphospace with related taxa connected through hypothetical ancestors (i.e. internal nodes) estimated by ML.

To compare morphological means among ecological categories (biomes and substrates) while controlling for phylogeny, we also applied a phylogenetic ANOVA in the Geiger package of R (Harmon et al 2008, , R Development Core Team 2008). Phylogenetic ANOVA tests if differences in cross-species values for the dependent

(morphological) variable are larger than expected under an evolutionary model of

Brownian motion (BM) (Garland et al. 1993). For both data sets, morphological variables

were reduced to scores from the first PC axis, to achieve a fully ranked covariance matrix.

For each pairwise contrast, the phylogenetic tree was pruned to match the morphological

taxon sample using the "drop.tip" command. For Data set 2, species means were used

instead of individual values (a requirement for this analyses). For species represented by

more than one substrate type, only the most commonly used substrate was considered and

PC scores were calculated from individuals on that substrate only. For each test, 1 000

BM simulations were performed on the phylogenetic tree using the covariance matrix of

the independent contrasts (Felsenstein 1985, Revell et al. 2007). The p-value was

calculated as the fraction of the simulated data sets in which the F-statistic was equal or

greater to that from the observed data.

RESULTS

Loadings from the non-phylogenetic PCA on morphology are given in Table 4.

The first four components explained over 80% of the variation in each data set (85.8%

and 88.5% respectively), with each component reflecting the influence of different sets of

body and head measurements. In both cases, we retained the first two components since

they explained a large amount of variation (73.2% and 61.8%) and showed little overlap

in variables contributing the most to each component. For Data set 1, PC1 shows foot

length and tibia length loading most strongly and positively, correlated negatively with

SVL. In PC2, the largest values reflect increasing head depth but shortened toe and head

length. For data set 2, the largest values on PC1 reflect head dimensions, with head length

negatively correlated with head width and depth. PC2 shows the largest values for

decreasing toe and hindlimb length, associated with an increase in SVL. Plotting PC

scores for these axes shows extensive overlap in morphological variables across biomes

and substrates (Figure 2). The scatterplot for Data set 1 (Figure 2a) is relatively well

spread compared to that of Data set 2 (Figure 2b), as individuals sampled in the field

represent fewer and generally smaller species.

Lacertid body shape differed significantly among biomes (Wilks's λ 0.06, F 2.93,

p <0.0001), although pairwise contrasts revealed several overlaps in morphology (Table

5). F-tests were nonsignificant (thus rejecting the hypothesis that means for the two

groups are significantly different) for four combinations involving four biomes: desert

and xeric shrublands; temperate grasslands, savannas and shrublands; temperate forest;

and tropical and subtropical grasslands, savannas and shrublands. For Data set 2,

individual morphological values also differed significantly among substrates (Wilks's λ

0.02, F 3.33, p <0.0001), but with eight of the fifteen contrasts being insignificant.

Morphological means in every substrate type except for loose sand overlapped with those

in at least one other substrate.

The PLS on morphological and bioclimatic variables revealed strong interactions

between climate and body shape. The cross validation analysis revealed that 5 axes

resulted in the lowest residual mean squared error term. The first five axes explained 98%

of the variation in climate and 25% of the morphological variation (Table 7). According

to variable ranking, seasonality of precipitation was the most important predictor of

morphological variation. Measurements of the head were negatively correlated with

seasonality. That is, species in more seasonal environments tended to have shorter,

narrower and thinner heads. These were all western Namibian taxa (*Pedioplanis*

namaquensis, P. gaerdesi and *Heliobolus lugubris*) occurring in desert or xeric biomes on

mixed substrate types. In contrast, lengths of the forelimbs, hindlimbs and toes all had

positive loadings with seasonality. Thus, species in highly seasonal environments were

also characterized by relatively longer limbs and toes. This was followed by mean temperature during the wettest quarter and precipitation during the driest month, which were roughly equal in importance. Head width was the most variable morphological factor across climate variables.

Phylogenetic comparative analyses

Relationships in our phylogeny generally reflect those found in previous molecular studies (e.g., Arnold et al. 2007, Mayer and Pavlicev 2007, Hipsley et al. 2009) (for full maximum clade credibility tree, see Appendix 4). However, within the Ethiopian clade (species south of the Sahara Desert), some differences in tree topology are observed. For example, the west African forest genus Poromera is basal to the Ethiopian clade, and two southern African genera, Australolacerta and Ichnotropis, are paraphyletic. Atlantololacerta andreanskyi, hypothesized by Arnold et al. (2007) to be the basal most member of Eremiadini, falls outside of the Saharo-Eurasian group. Estimated divergence dates from our analysis also differ from those in Hipsley et al. (2009), which relied on three out of four of the same fossil calibrations. Here we recover younger ages for every lineage, except for the root age of Teiidae-"Lacertibaenia" (Amphisbaenia+Lacertidae), which was roughly the same (117 My).

Based on the modified tree topologies, Pagel's lambda test showed mixed phylogenetic signal among morphological variables (Table 6). For the first data set, every trait except for toe length, humerus length and head depth covaried strongly with phylogeny, as indicated by lambda values (λ) close to 1. Likelihood ratio tests comparing ML estimates to λ estimates of zero also gave values statistically different from zero (indicating phylogenetic patterning) for those traits. In contrast to Data set 1, variables measured in the field showed almost complete phylogenetic independence. Lambda

estimates for every trait except SVL were not significantly different from zero, meaning no correlation between species.

Results of the phylogenetic PCA differed in variable loadings from the standard PCA for nearly every axis (Table 4). The first four axes accounted for 75.7% and 92.5% of the total variation respectively, and the first two components were retained for plotting in each case. For Data set 1, PC1 reflects an increase in tibia length coupled with a decrease in SVL and head depth. PC2 shows an increase in head depth and decrease in humerus length. For Data set 2, PC1 reflects larger SVL and shorter hindlimb and toe lengths, and PC2 reflects a decrease in head width and increase in forelimb length.

When comparing scatterplots of the PCAs (Figure 3), points from the phylogenetic PCA appear more widespread, as closely related species with dissimilar morphologies are joined by longer branches than those with similar morphologies. The phylogenetic PCA shows some species separated by very long branches, indicating a higher degree of morphological change than expected by evolution through Brownian motion. For Data set 1 (Figure 3c), the most morphologically disparate taxa are those occurring in the wettest and most vegetated biome - tropical and subtropical moist forest. In Data set 2 (Figure 3d), *Nucras intertexta* appears as the most disparate species, most likely due to its relatively large body size and short hindlimbs compared to its closest relatives in the data set. Another distant grouping is formed by members of the *Meroles* clade, which inhabit the most climatically extreme environments of the Namib Desert.

After correcting for phylogeny, several of the morphological differences among ecological categories disappeared. Among biome types, five contrasts became insignificant in the phylogenetic ANOVA, involving all biomes except for desert and

36

xeric shrubland (Table 5a). All morphological differences among substrate types were lost, although two contrasts (compact sand/rock x loose sand/leaf litter and rock) could not be estimated as they only involved two species each (Table 5b).

DISCUSSION

Despite the significant amount of morphological overlap in lacertids between biome and substrate types (Table 5), several evolutionary patterns emerge indicating ecological adaptation. In the standard (non-phylogenetic) PCA of museum specimens (Fig 3a), desert-dwelling forms tended to have elongated hindlimb elements (femur, tibia, toe and foot) and shortened forelimbs relative to body size. A similar pattern was also found by Orriols (2011), who grouped lacertid species by locomotion and habitat type, with desert forms characterized as fast runners or ground dwellers in open areas. Lacertids in tropical and subtropical moist forests also group together (Figure 3a, lower left quadrant), as they are slightly larger bodied with longer forelimbs than hindlimbs (e.g., *Gastropholis* and *Adolfus*).

The application of PCMs led to a tighter ecological clustering among species, but with some overlap remaining within the arid and mesic biomes. Species lie along a positive slope (Fig 3c), where taxa inhabiting more moist or temperate biomes and having longer bodies and forelimbs fall in the lower left quadrant, while those inhabiting deserts and arid regions fall in the upper right, indicating relatively short bodies and long hindlimbs. This pattern highlights the negative relationship of SVL, head and forelimb measurements to hindlimb length. Head variables also appear to scale allometrically, with longer heads (accompanied by longer SVLs) becoming more narrow and flat (Table 4). This applies mainly to mesic forms inhabiting forests in temperate, Mediterranean, and tropical regions (e.g., *Gastropholis*, *Poromera*, *Algyroides*).

In contrast to mesic lacertids, arid-dwelling species tend to be smaller in size, yet have slightly wider and deeper skulls. McBrayer (2004) found a similar pattern in desert and savanna dwelling lacertids like *Meroles suborbitalis* and *Pedioplanis lineoocellata*, which is expected for sit-and-wait foragers concentrating on larger and harder prey types (Schoener 1971, Herrel et al. 1996, Pough et al. 2001). Indeed, both of these species feed on beetles, grasshoppers and locusts (Branch 1998), which require large gapes and jaw musculature to produce sufficient bite force (Herrel et al. 1999, Verwaijen and Van Damme 2007). Although one would expect associated changes in other elements of the skull related to feeding such as the jaw and quadrate bones, strong links between skull morphology and diet in lacertids are still lacking (McBrayer 2004, Verwaijen and Van Damme 2007).

Variation in lacertid limb morphology, however, has been linked to foraging mode in previous studies. Even among closely related species, hindlimb length has been shown to be an important factor distinguishing sit-and-wait from active foragers (McBrayer and Wylie 2009). In lizards, hindlimb length is a strong predictor of sprint speed (Losos 1990b, Miles 1994, Bauwens et al. 1995, Bonine and Garland 1999), which is necessary for sit-and-wait foragers to successfully ambush prey (Huey and Pianka 1981, Vanhooydonck et al. 2007). Locomotor morphology is also known to vary with substrate type (Garland and Losos 1994, Miles 1994), although we found significant overlaps in morphologies across our field sites (Table 5, Figure 3b). In general, species moving on compact sand and leaf litter (e.g., *Heliobolus*, *Ichnotropis* and some *Pedioplanis*) tended to have shorter bodies and limbs but wider and deeper heads. Lacertids living on loose sand such as *Meroles anchietae* and *M. cuneirostris* were slightly longer in SVL with longer hindlimbs than forelimbs. The only truly saxicolous

species at our field sites, *Pedioplanis rubens*, had relatively long bodies and limbs, a pattern which has been related to improved sprinting and climbing in other saxicolous lizards (Goodman et al. 2008).

Convergence among arid-dwelling lizards was also supported by phylogenetic comparisons of the field data, with body shape overlapping on every type in our sample (Table 5). Species and community convergence in desert lizards has been studied extensively by Pianka and others (Pianka 1986, Pianka 2000, Lamb et al. 2003, Melville et al. 2006, Sherbrooke et al. 2007) across multiple families and continents. Significant similarities in microhabitat occupation and morphology across even distantly related taxa in North America and Australia suggests that deserts exert a selective pressure often overriding the inertia of phylogeny (Melville et al. 2006). The results of Pagel's lambda test on our field data also support this view, since nearly every trait measured failed to show phylogenetic signal (Table 6). The strong phylogenetic signal of SVL in the field data is most likely driven by members of the southern African clade (*Ichnotropis*, *Pedioplanis* and *Meroles*), which are much smaller bodied than the rest of the sampled taxa. This observation led us to exclude SVL as a variable in our climate analyses, as it may have masked relationships between other morphological variables and climate.

Overall, climatic variables were shown to be a significant driver of morphological disparity and convergence. Together they account for a quarter of the morphological variation in our data set, with the most important factors being precipitation seasonality, mean temperature of the wettest quarter and precipitation of the driest month (Table 7). All morphological measurements scale similarly with these factors, with head dimensions negatively correlated with limb and toe lengths. The only exception is head length in relation to precipitation of the driest month, where it scales negatively with head width

and depth. The only field site we visited with variation in this factor (all other areas receiving zero rain during the driest month) was the Erkowit Plateau along the Red Sea coast in northern Sudan, where we sampled *Acanthodactylus boskianus*. This region also had the highest values for temperature seasonality, precipitation of the driest and coldest quarter and the lowest values for precipitation seasonality.

Although Erkowit is relatively dry (annual rainfall ~170mm), the hills receive winter mists supporting *Euphorbia candelabra* trees and other Ethiopian highland vegetation (Mawson and Williams 1984). These features allow it to host high levels of biodiversity, as supported by our observations of numerous geckos, agamids, colubrid snakes, chameleons, burrowing skinks and ranid frogs in the same area. Interestingly, *A. boskianus* was also found to be the most variable in morphology across our sample sites and occurred on a variety of substrates, including compact sand and gravel, leaf litter and rock, and on loose sand. It is therefore tempting to conclude that substrate variation alone drives morphological disparity in arid habitats. However, the largest values for the top climatic variables in our model (Table 7) occur across multiple substrate types, including compact sand and leaf litter, gravel and rock. Furthermore, lacertid body shape did not differ significantly across substrates, thus emphasizing the impacts of the climatic variables. We therefore suggest that climate itself, particularly related to moisture and the interaction between extreme temperatures and precipitation, has significant effects on lacertid morphology. In this case, extreme climate may drive morphological convergence through similar pressures on life history across independent clades. Indeed, some arid-dwelling lacertids appear to be short-lived compared to their temperate counterparts (Branch 1998), possibly reflecting an "r-selected" strategy in response to extreme environmental conditions (Sandercock et al. 2005). This compression of development

may lead to similar morphological features, as illustrated by the typically paedomorphic head shapes of some of the arid-dwelling taxa (Arnold et al. 2007).

Further studies of qualitative traits in Lacertidae, not just quantitative, may reveal other features of the skull and body directly affected by changes in environment. In order to show that these features are evolutionarily related to climate, we need to temporally link their origins with historical climatic events. Furthermore, since the African radiation consists of three independent invasions of deserts with unique geological histories (Mayer and Pavlicev 2007, Hipsley et al. 2009), it is possible to test if the same suite of morphological features (and possibly developmental processes) evolved in response to separate climatic events. Properly performed divergence dating and extensive morphological analyses (potentially via X-ray Computed Tomography) will contribute greatly to this endeavor.

TABLE 1. Traits studied in relation to interspecific morphological variation in Lacertidae. PCMs indicates the use of Phylogenetic Comparative Methods.

Traits	Sampling	PCMs	Significance	Reference
bite force	live, museum	yes	poor	McBrayer 2004
foraging mode	museum	yes	mixed	McBrayer and Wylie 2009
foraging mode, bite force	live, museum	yes	mixed	Verwaijen and Van Damme 2007
habitat use	live, museum	yes	no	Vanhooydonck and Van Damme 1999
habitat use	museum	yes	mixed	Orriols 2011
speed, gait	live	yes	mixed	Vanhooydonck et al. 2002
sprint speed	live	yes	no	Verwaijen and Van Damme 2008
sprint, climbing speed	live	yes	no	Vanhooydonck and Van Damme 2001

TABLE 2. Species included in phylogenetic and morphological analyses of Lacertidae, with GenBank accession numbers and sample sizes (N) for each data set. Data set 1 includes museum specimens and Data set 2 is based on live animals in the field. RAG-1 numbers followed by an asterik (*) denote unpublished sequences.

Species	RAG-1	Data set 1 (N)	Data set 2 (N)
Acanthodactylus boskianus	EF632206	6	9
Acanthodactylus busacki		2	
Acanthodactylus erythrurus	HQ616540		
Acanthodactylus scutellatus	EF632207	6	
Adolfus africanus	HQ616552		
Adolfus jacksoni	HQ616558	6	
Algyroides fitzingeri	GQ142157	4	
Algyroides moreoticus	EF632209	4	
Algyroides nigropunctatus	EF632210	3	
Anatololacerta danfordi	EF632224	5	
Anatololacerta oertzeni	GQ142159		
Apathya cappadocica	EF632223	3	
Archaeolacerta bedriagae	EF632211	6	
Aspidoscelis tigris	AY662620		
Atlantolacerta andreanskyi	HQ616538	2	
Australolacerta australis	DQ871208		
Australolacerta rupicola	ADW5*		
Congolacerta asukului	HQ616555		
Congolacerta vaureselli	HQ616561		
Dalmatolacerta oxycephala	EF632228	5	
Darevskia valentini	EF632212		
Dinarolacerta mosorensis	EF632227		
Eremias arguta	EF632213	2	
Eremias pleskei	EF632214	6	
Gallotia galloti	EF632215		
Gastropholis prasina	HQ616543	1	
Gastropholis vittata	HQ616542	1	
Heliobolus lugubris	EF632216	2	21
Heliobolus spekii	EF632217	4	
Hellenolacerta graeca	EF632225	6	
Holaspis guentheri	HQ616546		
Holaspis laevis	EF632218		
Iberolacerta cyreni	HQ616539		
Iberolacerta horvathi	EF632219		
Iberolacerta monticola	EF632220	2	
Ichnotropis capensis	DQ871206	2	6
Ichnotropis squamulosa	EF632221	5	
Iranolacerta brandtii	GQ142162	1	
Lacerta agilis	EF632222	9	

Lacerta viridis		2	
Latastia longicaudata	EF632229	8	2
Meroles anchietae			1
Meroles cuneirostris	ABL18*		13
Meroles knoxii	DQ871205		
Meroles reticulatus	DQ871202	7	
Meroles suborbitalis	DQ871203	1	2
Mesalina guttulata	EF632231	8	
Mesalina rubropunctata	EF632232	6	
Nucras intertexta			2
Nucras lalandii	EF632233	3	
Nucras tessellata		4	
Omanosaura jayakari	EF632234	1	
Ophisops elegans	EF632235	3	
Parvilacerta fraasii	GQ142158		
Parvilacerta parva	EF632236	6	
Pedioplanis gaerdesi			4
Pedioplanis inornata		1	5
Pedioplanis laticeps	DQ871185	1	
Pedioplanis lineoocellata		4	
Pedioplanis namaquensis		6	6
Pedioplanis rubens			4
Pedioplanis undata	EF632237	2	5
Philochortus spinalis	EF632238	3	
Phoenicolacerta kulzeri	GQ142161		
Phoenicolacerta laevis	EF632226	6	
Podarcis muralis	HQ616541	3	
Poromera fordii	EF632240	3	
Psammodromus algirus	EF632241	6	
Psammodromus hispanicus	EF632242	6	
Pseuderemias brenneri		8	
Pseuderemias smithii	EF632243		
Rhineura floridana	AY662618		
Takydromus amurensis	EF632244		
Takydromus sexlineatus	EF632245	5	
Tiera dugesii	EF632246		
Tiera perspicillata	GQ142155		
Timon lepidus	EF632247	1	
Timon pater		5	
Timon tangitanus	HQ616537		
Tropidosaura cottrelli	ACJ1*		
Tropidosaura essexi	ACK1*		
Tropidosaura gularis	EF632248		
Tropidosaura montana	2_ABZ2*		
Zootoca vivipara	EF632249	6	

TABLE 3. Bioclimatic variables extracted for each individual in Data set 2 from the Worldclim database (Hijmans et al. 2005).

Variable	Description
Bio1	Annual mean temperature
Bio2	Mean diurnal temperature range (mean of monthly maximum temperature minus minimum temperature)
Bio3	Isothermality (Bio2/Bio7 * 100)
Bio4	Temperature seasonality (standard deviation of monthly temperature)
Bio5	Minimum temperature of the coldest month
Bio6	Maximum temperature of the warmest month
Bio7	Temperature range (maximum temperature of the warmest month minus minimum temperature of the coldest month)
Bio8	Mean temperature of wettest quarter (i.e. mean temperature of four consecutive wettest months)
Bio9	Mean temperature of driest quarter
Bio10	Mean temperature of warmest quarter
Bio11	Mean temperature of coldest quarter
Bio12	Annual precipitation
Bio13	Precipitation of wettest month
Bio14	Precipitation of driest month
Bio15	Precipitation seasonality (standard deviation of monthly precipitation)
Bio16	Precipitation of driest quarter
Bio17	Precipitation of wettest quarter
Bio18	Precipitation of warmest quarter
Bio19	Precipitation of coldest quarter

TABLE 4. Loadings from the first four principal components of morphological variables in a) Data set 1, and b) Data set 2. Results of the non-phylogenetic PCA are on the left and phylogenetic PCA on the right. All PCAs were performed on species means except for the non-phylogenetic PCA for Data set 2, which was performed on individual morphological values. Variables contributing the most to each axis are in bold.

	Non-phylogenetic				Phylogenetic			
a) Data set 1	PC1	PC2	PC3	PC4	PC1	PC2	PC3	PC4
SVL	**-0.378**	-0.100	**0.340**	**0.675**	**-0.697**	-0.201	0.095	0.401
Head width	-0.251	0.236	-0.092	**-0.535**	-0.597	0.494	0.145	**-0.366**
Head depth	-0.322	**0.671**	**-0.344**	0.133	**-0.719**	**0.518**	-0.041	0.128
Head length	-0.240	**-0.288**	-0.117	0.028	-0.453	-0.363	**-0.550**	0.352
Humerus length	-0.091	-0.244	**0.377**	-0.255	-0.141	**-0.664**	0.580	-0.346
Radius length	-0.134	-0.209	0.062	-0.184	-0.324	-0.358	-0.485	**-0.554**
Femur length	0.162	-0.063	0.232	-0.244	0.655	-0.060	**-0.557**	-0.102
Tibia length	**0.458**	0.136	0.036	-0.014	**0.788**	0.317	-0.070	-0.124
Toe length	0.232	**-0.433**	**-0.706**	0.162	0.674	-0.182	0.209	**0.388**
Foot length	**0.564**	0.295	0.212	0.233	0.820	0.079	0.095	-0.016
Eigenvalue	0.010	0.002	0.001	0.001	3.865	1.397	1.273	1.038
% variance	59.407	13.818	6.854	5.733	38.646	13.974	12.734	10.383

b) Data set 2	PC1	PC2	PC3	PC4	PC1	PC2	PC3	PC4
SVL	-0.321	**0.509**	0.024	0.138	**0.786**	0.426	0.076	-0.237
Head width	**0.411**	-0.049	**-0.695**	**-0.430**	-0.018	**-0.847**	**-0.486**	-0.096
Head depth	**0.664**	0.394	**0.369**	0.249	0.689	-0.209	0.380	**0.534**
Head length	**-0.406**	0.086	**-0.395**	0.429	0.712	-0.080	0.145	**-0.644**
Forelimb length	-0.346	0.113	0.355	**-0.692**	0.244	**0.532**	**-0.772**	0.184
Hindlimb length	-0.041	**-0.464**	0.030	0.263	**-0.869**	0.094	0.030	-0.321
Toe length	0.039	**-0.590**	0.312	0.044	**-0.896**	0.220	0.245	0.054
Eigenvalue	0.004	0.003	0.002	0.001	3.217	1.290	1.065	0.906
% variance	33.693	28.130	18.190	8.531	45.954	18.426	15.213	12.941

TABLE 5. F-test scores across pairs of a) biome types in Data set 1 and b) substrate types in Data set 2. Values below the diagonal were calculated on the size-adjusted morphological variables. Values above the diagonal were calculated from the phylogenetic ANOVA on scores from the first PC axis. Values in bold are statistically significant ($p < 0.05$) and indicate a lack of morphological similarity. N/A refers to phylogenetic contrasts that could not be calculated for comparisons involving only two species.

a) Data set 1						
Biome	Desert & xeric shrublands	Mediterranean forests, woodlands & scrub	Temperate grasslands, savannas & shrublands	Temperate forest	Tropical & subtropical grasslands, savannas & shrublands	Tropical & subtropical moist forests
Desert & xeric shrublands	-	**18.634**	2.2355	**11.008**	0.2366	**15.5**
Mediterranean forests, woodlands & scrub	**1.113**	-	1.9071	**5.228**	**11.929**	4.2543
Temperate grasslands, savannas & shrublands	0.153	**0.629**	-	5.3163	1.6722	4.1591
Temperate forest	**0.778**	**0.585**	0.428	-	5.2071	0.1391
Tropical & subtropical grasslands, savannas & shrublands	0.265	**1.631**	0.287	**1.007**	-	**8.083**
Tropical & subtropical moist forests	**2.562**	**1.474**	**1.647**	**0.784**	**2.725**	-

b) Data set 2						
Substrate	compact sand/gravel	compact sand/ leaf litter	compact sand/rock	loose sand	loose sand/leaf litter	rock
compact sand/gravel	-	0.046	0.5538	0.1122	1.7278	0.098
compact sand/leaf litter	0.062	-	0	0.0754	0.1271	0.0907
compact sand/rock	0.011	0.058	-	1.6421	N/A	N/A
loose sand	**1.137**	**1.528**	**0.86**	-	22.319	0.1706
loose sand/leaf litter	0.168	**0.232**	0.113	**0.451**	-	N/A
rock	0.099	0.171	0.122	**0.439**	**0.223**	-

TABLE 6. Results of Pagel's lambda test for phylogenetic signal in morphological variables in a) Data set 1 and b) Data set 2. Lambda (λ) was estimated for each variable under a Maximum Likelihood model (ML), and log likelihood (LL) values are given for models with λ=0 (phylogenetic independence) and λ=ML. A LL ratio test was used to compare models. Significant values (p<0.05) are in bold.

Variable	Lambda (λ=ML)	LL (λ=0)	LL (λ=ML)	LL Ratio	p value
a) Data set 1					
SVL	0.8531	87.99	93.51	11.05	**0.0009**
Head width	0.4164	100.60	104.34	7.47	**0.006**
Head depth	0.3820	85.40	86.33	1.85	0.17
Head length	0.9825	106.22	121.47	30.50	**<0.0001**
Humerus length	<0.0001	113.71	113.71	<0.0001	1
Radius length	0.8594	115.67	118.14	4.94	**0.02**
Femur length	0.7596	114.92	116.95	4.05	**0.04**
Tibia length	0.9734	84.55	101.26	33.43	**<0.0001**
Toe length	<0.0001	94.84	94.84	<0.0001	1
Foot length	0.8749	73.65	87.70	28.11	**<0.0001**
b) Data set 2					
SVL	1.0000	25.94	28.36	4.8454	**0.03**
Head width	0.9237	25.59	27.38	3.5761	0.06
Head depth	0.7913	23.11	23.93	1.6359	0.20
Head length	<0.0001	38.15	38.15	0.0000	1
Forelimb length	0.4864	32.16	32.54	0.7570	0.38
Hindlimb length	1.0000	25.15	26.37	2.4323	0.11
Toe length	<0.0001	24.96	24.96	<0.0001	1

TABLE 7. Bioclimatic variables in order of importance for predicting morphological variation of lacertids in arid-dwelling African clades. Model coefficients of the size adjusted morphological variables are given for each variable. Full explanations of Bioclim variables are given in Table 3.

Bioclim variable	Impor-tance	Head width	Head depth	Head length	Forelimb length	Hindlimb length	Toe length
BIO15	2.853	-0.714	-0.228	-0.060	0.331	0.143	0.480
BIO8	1.324	-0.240	-0.009	-0.111	0.006	0.232	0.341
BIO14	1.212	-0.242	-0.107	0.020	0.092	0.032	0.141
BIO13	1.152	0.023	0.063	0.004	0.056	-0.125	-0.162
BIO12	1.138	0.073	0.068	0.021	0.044	-0.155	-0.215
BIO16	1.103	0.028	0.056	0.010	0.059	-0.131	-0.168
BIO4	1.064	-0.195	0.018	-0.035	0.047	0.042	0.088
BIO7	1.045	-0.142	0.028	-0.089	-0.006	0.144	0.212
BIO17	1.038	-0.170	-0.045	-0.028	-0.005	0.127	0.204
BIO3	1.013	-0.031	-0.085	-0.002	0.028	0.054	0.122
BIO18	1.002	-0.107	0.003	-0.011	0.099	-0.060	-0.022
BIO2	0.949	-0.107	-0.051	-0.076	0.009	0.166	0.276
BIO19	0.786	-0.126	-0.023	0.023	0.023	0.002	0.019
BIO5	0.690	-0.091	0.025	-0.017	-0.025	0.059	0.055
BIO10	0.689	-0.065	0.030	0.003	-0.007	0.003	-0.020
BIO11	0.678	0.079	0.025	0.031	-0.046	-0.032	-0.098
BIO9	0.656	0.072	0.019	0.042	-0.046	-0.042	-0.109
BIO1	0.639	-0.032	0.024	0.013	-0.010	-0.012	-0.044
BIO6	0.629	0.016	0.002	0.038	-0.014	-0.039	-0.081

FIGURE 1. Lacertid sampling sites for Data set 2 in a) Sudan, and b) Namibia.
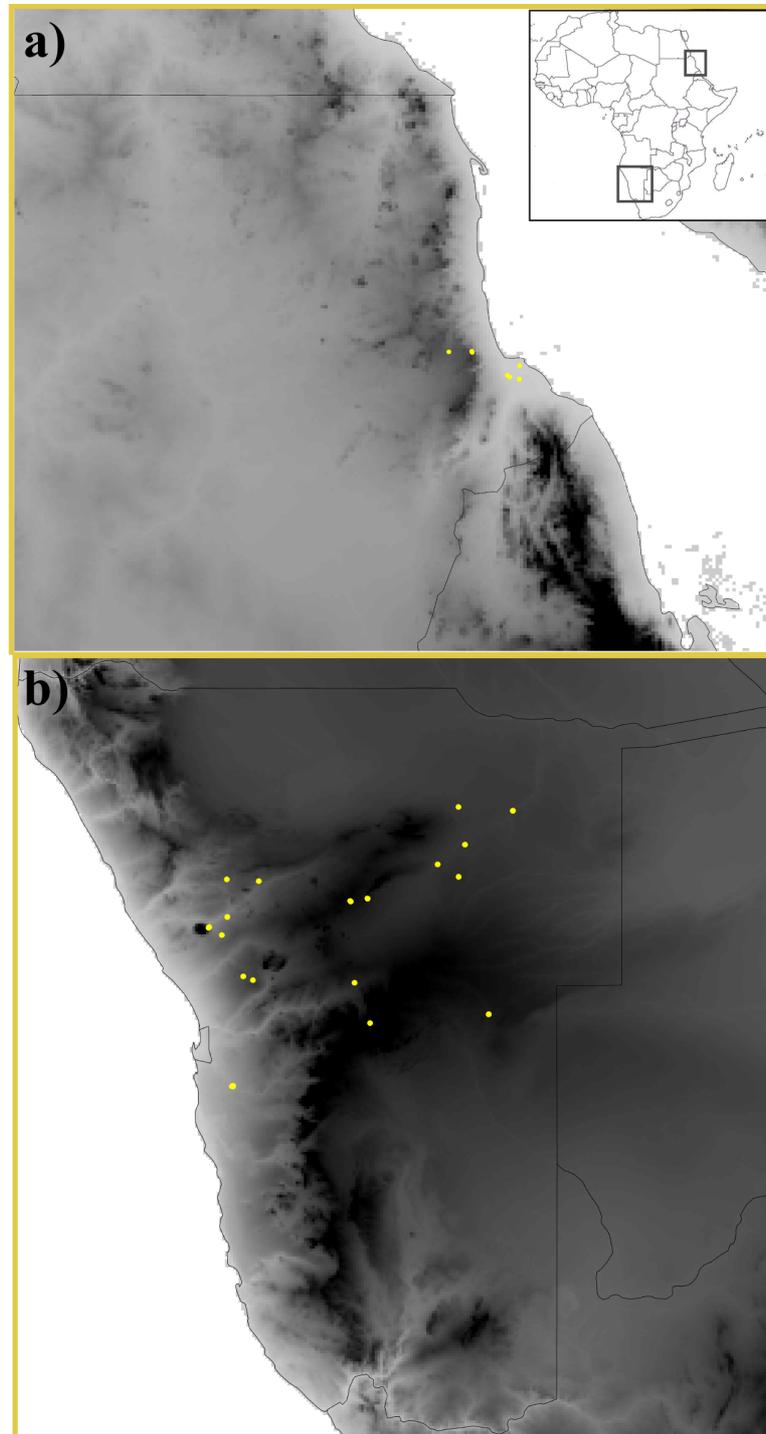
FIGURE 2. Time-calibrated molecular phylogenies used in the comparative analyses of lacertid taxa in a) Data set 1, and b) Data set 2. Details on the construction of each tree are given in Appendix 5. The x axis is in millions of years.
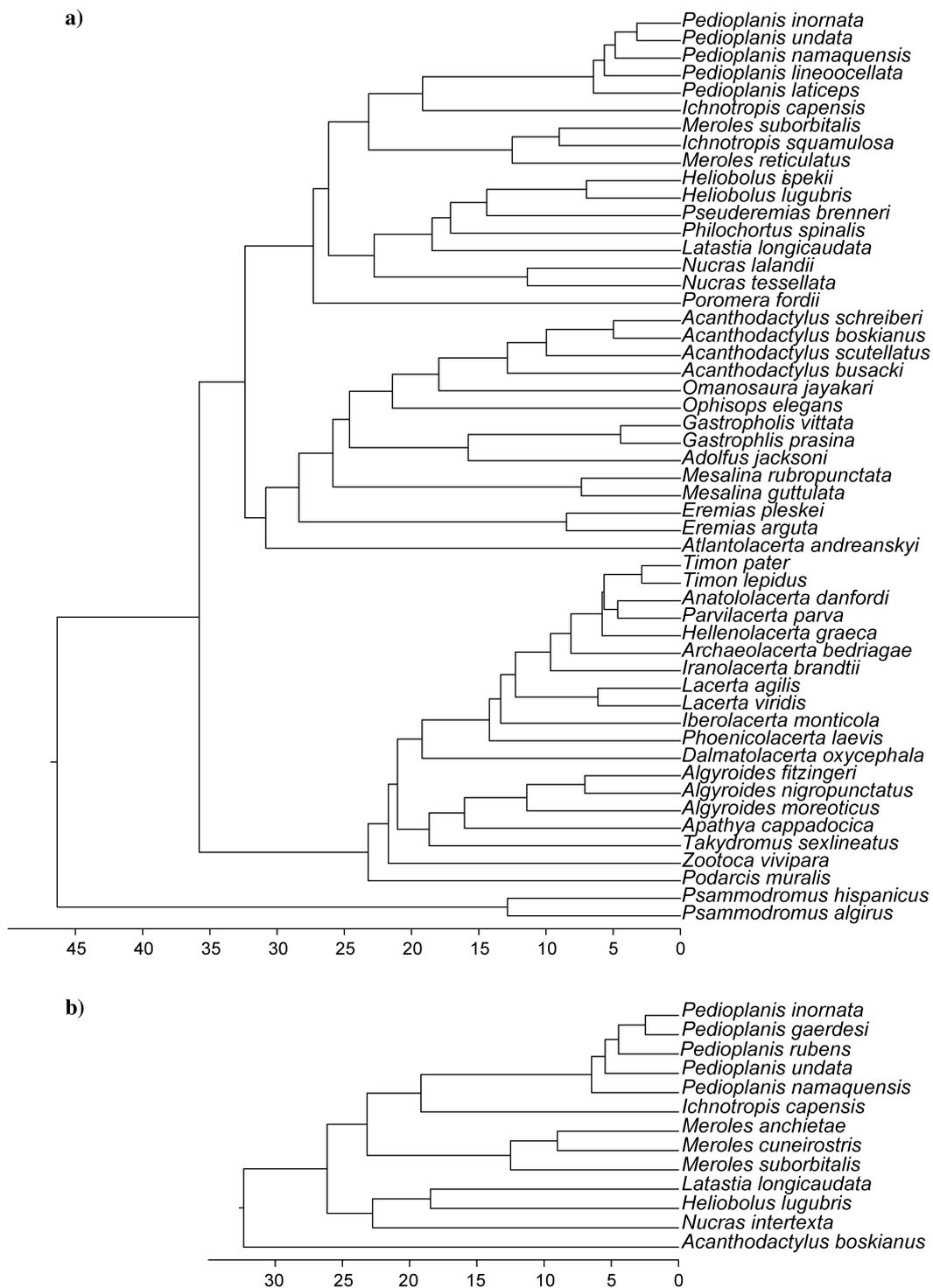
FIGURE 3. Morphological variation in Lacertidae along the first two principal components axes. Scatterplots of scores from the non-phylogenetic PCA are shown above and phylomorphospace plots from the phylogenetic PCA are shown below. Coloured points represents phenotypic values for species in Data set 1 (a, c). Scatterplots for Data set 2 are scores of individuals (b) and species (d). Colours represent different ecological categories. In the phylomorphospace plots (c and d), black lines connect related species through hypothetical ancestors, denoted by black points.
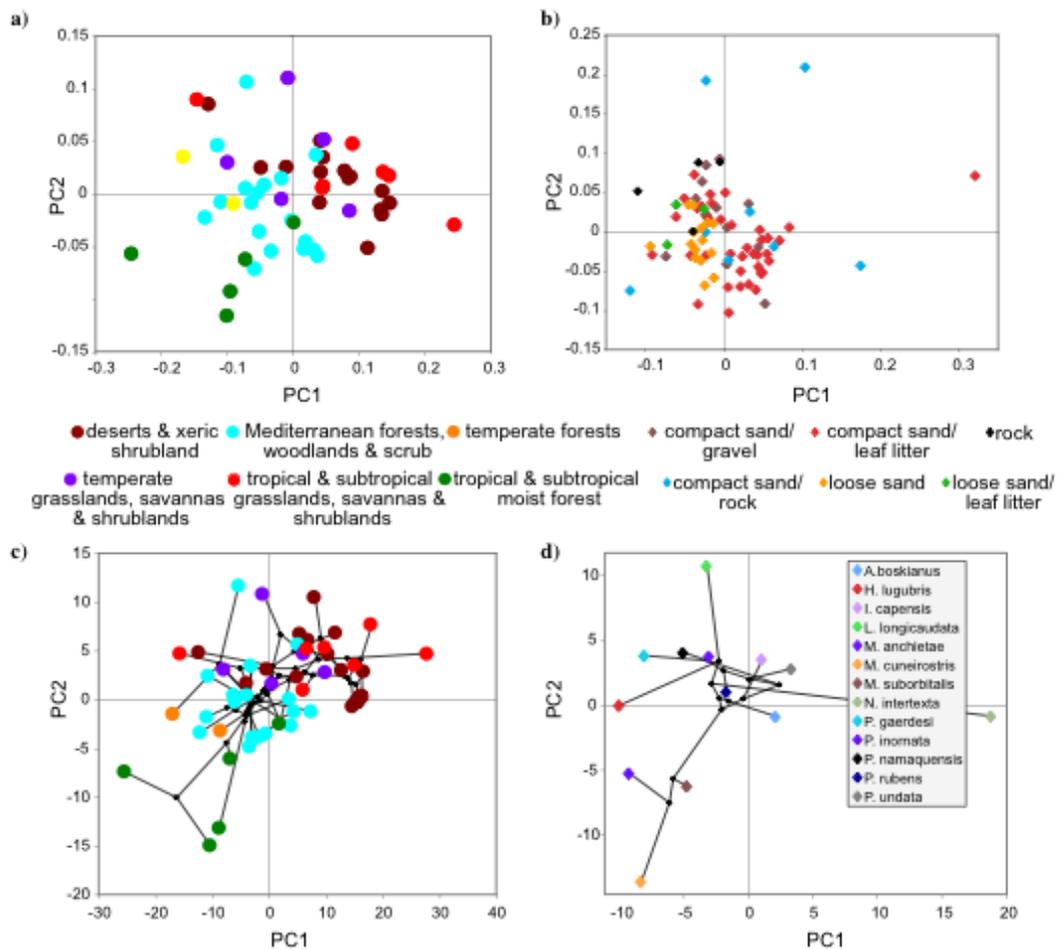
APPENDIX 1. Data set 1 taxon sampling. Catalogue numbers and localities of museum specimens from the Museum für Naturkunde Berlin, Germany (ZMB).

Species	Catalogue no.	Locality
Acanthodactylus boskianus	ZMB 70855	Tunis, Tunisia
Acanthodactylus boskianus	ZMB 14879	Tunis, Tunisia
Acanthodactylus boskianus	ZMB 15168	Sinai, Egypt
Acanthodactylus boskianus	ZMB 70857	Aden, Yemen
Acanthodactylus boskianus	ZMB 27404	Aden, Yemen
Acanthodactylus boskianus	ZMB 70856	Aden, Yemen
Acanthodactylus busacki	ZMB 76683	Tamri, Morocco
Acanthodactylus busacki	ZMB 76684	Tamri, Morocco
Acanthodactylus schreiberi	ZMB 18131	Republic of Cyprus
Acanthodactylus schreiberi	ZMB 18131	Republic of Cyprus
Acanthodactylus schreiberi	ZMB 18132	Republic of Cyprus
Acanthodactylus schreiberi	ZMB 18132	Republic of Cyprus
Acanthodactylus schreiberi	ZMB 18133	Republic of Cyprus
Acanthodactylus schreiberi	ZMB 18133	Republic of Cyprus
Acanthodactylus scutellatus	ZMB 31857	Oued Ed-Dahab-Lagouira, West Sahara
Acanthodactylus scutellatus	ZMB 31857	Oued Ed-Dahab-Lagouira, West Sahara
Acanthodactylus scutellatus	ZMB 31857	Oued Ed-Dahab-Lagouira, West Sahara
Acanthodactylus scutellatus	ZMB 31857	Oued Ed-Dahab-Lagouira, West Sahara
Acanthodactylus scutellatus	ZMB 31857	Oued Ed-Dahab-Lagouira, West Sahara
Acanthodactylus scutellatus	ZMB 31857	Oued Ed-Dahab-Lagouira, West Sahara
Adolfus jacksoni	ZMB 48254	Arusha, Tanzania
Adolfus jacksoni	ZMB 22437	Idjwi Island, Democratic Republic of the Congo
Adolfus jacksoni	ZMB 22437	Idjwi Island, Democratic Republic of the Congo
Adolfus jacksoni	ZMB 22438	Idjwi Island, Democratic Republic of the Congo
Adolfus jacksoni	ZMB 22773	Idjwi Island, Democratic Republic of the Congo
Adolfus jacksoni	ZMB 24504	Kibongoto, Tanzania
Algyroides fitzingeri	ZMB 73926	Sardinia, Italy
Algyroides fitzingeri	ZMB 71090	Sassari, Italy
Algyroides fitzingeri	ZMB 10568	Sassari, Italy
Algyroides fitzingeri	ZMB 71091	Sassari, Italy
Algyroides moreoticus	ZMB 18777	Kefalonia, Greece
Algyroides moreoticus	ZMB 18414	Kefalonia, Greece
Algyroides moreoticus	ZMB 18414	Kefalonia, Greece
Algyroides moreoticus	ZMB 18414	Kefalonia, Greece
Algyroides nigropunctatus	ZMB 47122	Pestani, Macedonia
Algyroides nigropunctatus	ZMB 47123	Pestani, Macedonia

Algyroides nigropunctatus	ZMB 47124	Pestani, Macedonia
Anatololacerta danfordi	ZMB 49256	Ikaria, Greece
Anatololacerta danfordi	ZMB 18072	Bulghar Dagh, Turkey
Anatololacerta danfordi	ZMB 28558	Mt.Erciyes, Turkey
Anatololacerta danfordi	ZMB 28558	Mt.Erciyes, Turkey
Anatololacerta danfordi	ZMB 13496	Ikaria, Greece
Apathya cappadocica	ZMB 31152	Taurus Mts., Turkey
Apathya cappadocica	ZMB 45846	Kiranardi, Turkey
Apathya cappadocica	ZMB 45847	Kiranardi, Turkey
Archaeolacerta bedriagae	ZMB 39056	Sardinia, Italy
Archaeolacerta bedriagae	ZMB 69156	Sardinia, Italy
Archaeolacerta bedriagae	ZMB 69158	Sardinia, Italy
Archaeolacerta bedriagae	ZMB 69157	Sardinia, Italy
Archaeolacerta bedriagae	ZMB 39021	Corsica, France
Archaeolacerta bedriagae	ZMB 36521	Corsica, France
Atlantolacerta andreanskyi	ZMB 76685	Oukaïmeden, Morocco
Atlantolacerta andreanskyi	ZMB 76686	Oukaïmeden, Morocco
Dalmatolacerta oxycephala	ZMB 24576	Dalmatia, Croatia
Dalmatolacerta oxycephala	ZMB 42347	Hutovo Blato, Bosnia and Herzegovina
Dalmatolacerta oxycephala	ZMB 35883	Kupari, Croatia
Dalmatolacerta oxycephala	ZMB 38540	Hutovo Blato, Bosnia and Herzegovina
Dalmatolacerta oxycephala	ZMB 38540	Hutovo Blato, Bosnia and Herzegovina
Eremias arguta	ZMB 37829	Lotus Mountain, China
Eremias arguta	ZMB 37830	Mt. Taishan, China
Eremias pleskei	ZMB 42956	Zvartnots, Armenia
Eremias pleskei	ZMB 42957	Zvartnots, Armenia
Eremias pleskei	ZMB 42958	Zvartnots, Armenia
Eremias pleskei	ZMB 42959	Zvartnots, Armenia
Eremias pleskei	ZMB 42960	Zvartnots, Armenia
Eremias pleskei	ZMB 42961	Zvartnots, Armenia
Gastropholis prasina	ZMB 18087	Usambara Mts., Tansania
Gastropholis vittata	ZMB 74300	Tendaguru, Tanzania
Heliobolus lugubris	ZMB 5713	Otjimbingwe, Namibia
Heliobolus lugubris	ZMB 5713	Otjimbingwe, Namibia
Heliobolus spekii	ZMB 48327	Mazimbu, Tanzania
Heliobolus spekii	ZMB 48326	Dakawa, Tanzania
Heliobolus spekii	ZMB 48325	Mazimbu, Tanzania
Heliobolus spekii	ZMB 48324	Mazimbu, Tanzania
Hellenolacerta graeca	ZMB 18412	Langhada Pass, Greece
Hellenolacerta graeca	ZMB 18412	Langhada Pass, Greece

Hellenolacerta graeca	ZMB 18412	Langhada Pass, Greece
Hellenolacerta graeca	ZMB 29251	Taygetos, Greece
Hellenolacerta graeca	ZMB 18779	Taygetos, Greece
Hellenolacerta graeca	ZMB 18779	Taygetos, Greece
Iberolacerta monticola	ZMB 42422	Puerto De Navacerrada, Spain
Iberolacerta monticola	ZMB 42421	Puerto De Navacerrada, Spain
Ichnotropis capensis	ZMB 15564	Muliro, DRC
Ichnotropis capensis	ZMB 25829	Kalahari, Namibia
Ichnotropis squamulosa	ZMB 6615	Tete, Mozambique
Ichnotropis squamulosa	ZMB 53010	Tete, Mozambique
Ichnotropis squamulosa	ZMB 53021	Makonde Plateau, Tanzania
Ichnotropis squamulosa	ZMB 53022	Makonde Plateau, Tanzania
Ichnotropis squamulosa	ZMB 53020	Makonde Plateau, Tanzania
Iranolacerta brandtii	ZMB 37965	Lake Urmia, Iran
Lacerta agilis	ZMB 69379	Lebus, Germany
Lacerta agilis	ZMB 69383	Lebus, Germany
Lacerta agilis	ZMB 69381	Lebus, Germany
Lacerta agilis	ZMB 69384	Lebus, Germany
Lacerta agilis	ZMB 69374	Lebus, Germany
Lacerta agilis	ZMB 69375	Lebus, Germany
Lacerta agilis	ZMB 69372	Lebus, Germany
Lacerta agilis	ZMB 69373	Lebus, Germany
Lacerta agilis	ZMB 69382	Lebus, Germany
Lacerta viridis	ZMB 47085	Lake Dojran, Macedonia
Lacerta viridis	ZMB 47086	Lake Dojran, Macedonia
Latastia longicaudata	ZMB 22443	Kibwezi, Kenya
Latastia longicaudata	ZMB 22444	Kibwezi, Kenya
Latastia longicaudata	ZMB 22444	Kibwezi, Kenya
Latastia longicaudata	ZMB 18201	Menaballa, Ethiopia
Latastia longicaudata	ZMB 19822	Daba`as Djibouti
Latastia longicaudata	ZMB 19822	Daba`as Djibouti
Latastia longicaudata	ZMB 19798	Zeila, Somalia
Latastia longicaudata	ZMB 19798	Zeila, Somalia
Meroles reticulatus	ZMB 74646	Conception Bay, Namibia
Meroles reticulatus	ZMB 74647	Conception Bay, Namibia
Meroles reticulatus	ZMB 74648	Conception Bay, Namibia
Meroles reticulatus	ZMB 74649	Conception Bay, Namibia
Meroles reticulatus	ZMB 74650	Conception Bay, Namibia
Meroles reticulatus	ZMB 74651	Conception Bay, Namibia
Meroles reticulatus	ZMB 74652	Conception Bay, Namibia

Meroles suborbitalis	ZMB 74653	Lüderitz, Namibia
Mesalina guttulata	ZMB 38633	Tedzhen River, Turkmenistan
Mesalina guttulata	ZMB 38633	Tedzhen River, Turkmenistan
Mesalina guttulata	ZMB 15306	Tripoli, Libya
Mesalina guttulata	ZMB 38825	Imam Baba, Turkmenistan
Mesalina guttulata	ZMB 38633	Tedzhen River, Turkmenistan
Mesalina guttulata	ZMB 38633	Tedzhen River, Turkmenistan
Mesalina guttulata	ZMB 38443	Tedzhen River, Turkmenistan
Mesalina guttulata	ZMB 38443	Tedzhen River, Turkmenistan
Mesalina rubropunctata	ZMB 24410	Temassinin, Algeria
Mesalina rubropunctata	ZMB 24410	Temassinin, Algeria
Mesalina rubropunctata	ZMB 24470	Biskra, Algeria
Mesalina rubropunctata	ZMB 24470	Biskra, Algeria
Mesalina rubropunctata	ZMB 24470	Biskra, Algeria
Mesalina rubropunctata	ZMB 18327	Uadi el Talha, Libya
Nucras lalandii	ZMB 23913	Cape Colony, South Africa
Nucras lalandii	ZMB 13555	Transvaal, South Africa
Nucras lalandii	ZMB 7032	Durban, South Africa
Nucras tessellata	ZMB 1044	Tete, Mozambique
Nucras tessellata	ZMB 25831	Kalahari, Namibia
Nucras tessellata	ZMB 1043	Tete, Mozambique
Nucras tessellata	ZMB 71093	Tete, Mozambique
Omanosaura jayakari	ZMB 50029	Masafi, United Arab Emirates
Ophisops elegans	ZMB 38789	Tell Halaf, Syria
Ophisops elegans	ZMB 75338	Armavir, Armenia
Ophisops elegans	ZMB 75339	Armavir, Armenia
Parvilacerta parva	ZMB 38906	Spitak, Armenia
Parvilacerta parva	ZMB 38906	Spitak, Armenia
Parvilacerta parva	ZMB 38906	Spitak, Armenia
Parvilacerta parva	ZMB 38903	Spitak, Armenia
Parvilacerta parva	ZMB 38903	Spitak, Armenia
Parvilacerta parva	ZMB 38903	Spitak, Armenia
Pedioplanis inornata	ZMB 27522	Warmbad, Namibia
Pedioplanis laticeps	ZMB 23443	Warmbad, Namibia
Pedioplanis lineoocellata	ZMB 23151	Tau Pan, Botswana
Pedioplanis lineoocellata	ZMB 23151	Tau Pan, Botswana
Pedioplanis lineoocellata	ZMB 23151	Tau Pan, Botswana
Pedioplanis lineoocellata	ZMB 23142	Lüderitz, Namibia
Pedioplanis namaquensis	ZMB 5714	Otjimbingwe, Namibia
Pedioplanis namaquensis	ZMB 5714	Otjimbingwe, Namibia

Pedioplanis namaquensis	ZMB 5714	Otjimbingwe, Namibia
Pedioplanis namaquensis	ZMB 5714	Otjimbingwe, Namibia
Pedioplanis namaquensis	ZMB 5715	Otjimbingwe, Namibia
Pedioplanis namaquensis	ZMB 5715	Otjimbingwe, Namibia
Pedioplanis undata	ZMB 73917	Gobabis, Namibia
Pedioplanis undata	ZMB 73917	Gobabis, Namibia
Philochortus spinalis	ZMB 10270	Adali, Ethiopia
Philochortus spinalis	ZMB 19752	Odamuda, Somalia
Philochortus spinalis	ZMB 19790	Zeila, Somalia
Phoenicolacerta laevis	ZMB 14110	Gülek, Turkey
Phoenicolacerta laevis	ZMB 14110	Gülek, Turkey
Phoenicolacerta laevis	ZMB 14110	Gülek, Turkey
Phoenicolacerta laevis	ZMB 38354	Bolkar Dagi, Turkey
Phoenicolacerta laevis	ZMB 38354	Bolkar Dagi, Turkey
Phoenicolacerta laevis	ZMB 20942	Mount Erciyes, Turkey
Podarcis muralis	ZMB 38690	Naples, Italy
Podarcis muralis	ZMB 38690	Naples, Italy
Podarcis muralis	ZMB 38690	Naples, Italy
Poromera fordii	ZMB 21235	Bipindi, Cameroon
Poromera fordii	ZMB 59398	Bipindi, Cameroon
Poromera fordii	ZMB 15222	Yaounde, Cameroon
Psammodromus algirus	ZMB 36603	Linares de Riofrío, Spain
Psammodromus algirus	ZMB 36603	Linares de Riofrío, Spain
Psammodromus algirus	ZMB 36603	Linares de Riofrío, Spain
Psammodromus algirus	ZMB 36603	Linares de Riofrío, Spain
Psammodromus algirus	ZMB 36603	Linares de Riofrío, Spain
Psammodromus algirus	ZMB 36603	Linares de Riofrío, Spain
Psammodromus hispanicus	ZMB 38655	Linares de Riofrío, Spain
Psammodromus hispanicus	ZMB 38655	Linares de Riofrío, Spain
Psammodromus hispanicus	ZMB 38655	Linares de Riofrío, Spain
Psammodromus hispanicus	ZMB 38655	Linares de Riofrío, Spain
Psammodromus hispanicus	ZMB 38655	Linares de Riofrío, Spain
Psammodromus hispanicus	ZMB 38655	Linares de Riofrío, Spain
Pseuderemias brenneri	ZMB 8119	Barawa, Somalia
Pseuderemias brenneri	ZMB 8120	Barawa, Somalia
Pseuderemias brenneri	ZMB 8121	Barawa, Somalia
Pseuderemias brenneri	ZMB 8122	Barawa, Somalia
Pseuderemias brenneri	ZMB 8123	Barawa, Somalia
Pseuderemias brenneri	ZMB 39142	Barawa, Somalia
Pseuderemias brenneri	ZMB 39143	Barawa, Somalia

Pseuderemias brenneri	ZMB 39144	Barawa, Somalia
Takydromus sexlineatus	ZMB 39054	Bogor, Java
Takydromus sexlineatus	ZMB 39054	Bogor, Java
Takydromus sexlineatus	ZMB 39054	Bogor, Java
Takydromus sexlineatus	ZMB 39054	Bogor, Java
Takydromus sexlineatus	ZMB 39054	Bogor, Java
Timon lepidus	ZMB 1004	Montpellier, France
Timon pater	ZMB 24565	Algiers, Algeria
Timon pater	ZMB 14869	Tunis, Tunisia
Timon pater	ZMB 14869	Tunis, Tunisia
Timon pater	ZMB 19617	Algiers, Algeria
Timon pater	ZMB 15562	Annaba, Algeria
Zootoca vivipera	ZMB 22954	Föhr, Germany
Zootoca vivipera	ZMB 22954	Föhr, Germany
Zootoca vivipera	ZMB 31592	Bützow, Germany
Zootoca vivipera	ZMB 31592	Bützow, Germany
Zootoca vivipera	ZMB 31592	Bützow, Germany
Zootoca vivipera	ZMB 29132	Kaunas, Lithuania

APPENDIX 2. Data set 1 summary. Mean morphological variables ± 1 standard error (mm), sample sizes (N) and biome assignments for 52 lacertid species in Data set 1.

Species	N	SVL	Head length	Head width	Head depth	Humerus length	Radius length	Femur length	Tibia length	Foot length	Toe length	Biome
Acanthodactylus boskianus	6	61.08 ± 3.34	14.48 ± 0.7	9.2 ± 0.49	7.76 ± 0.37	7.24 ± 0.49	6.51 ± 0.43	11.35 ± 0.54	10.6 ± 0.51	6.6 ± 0.27	12.25 ± 0.59	Deserts & Xeric Shrublands
Acanthodactylus busacki	2	56.5 ± 3.5	13.19 ± 0.88	9.16 ± 1.08	6.71 ± 0.73	6.85 ± 0.06	5.9 ± 0.43	10.73 ± 0.23	9.81 ± 0.71	5.95 ± 0.33	11.08 ± 0.7	Deserts & Xeric Shrublands
Acanthodactylus schreiberi	6	77.83 ± 2.1	18.87 ± 0.66	12.56 ± 0.47	10.43 ± 0.59	9.53 ± 0.28	9.28 ± 0.3	14.93 ± 0.57	13.81 ± 0.74	8.67 ± 0.39	15.95 ± 0.28	Mediterranean Forests, Woodlands & Scrub
Acanthodactylus scutellatus	6	54.83 ± 1.45	13.28 ± 1.19	9.06 ± 0.38	7.01 ± 0.32	7.24 ± 0.31	6.15 ± 0.19	11.03 ± 0.33	10.67 ± 0.38	6.32 ± 0.2	12.58 ± 0.28	Deserts & Xeric Shrublands
Adolfus jacksoni	6	70.33 ± 1.78	16.95 ± 1.06	10.58 ± 0.72	7.18 ± 0.48	8.45 ± 0.49	7.73 ± 0.47	11.14 ± 0.4	9.45 ± 0.56	5.76 ± 0.41	12.43 ± 0.58	Tropical & Subtropical Moist Forests
Algyroides fitzingeri	4	38.13 ± 1.2	8.61 ± 0.07	5.63 ± 0.13	4 ± 0.11	4.33 ± 0.13	3.44 ± 0.18	5.5 ± 0.3	4.5 ± 0.16	3 ± 0.23	5.92 ± 0.08	Mediterranean Forests, Woodlands & Scrub
Algyroides moreoticus	4	42.5 ± 1.19	10.46 ± 0.29	6.52 ± 0.15	4.82 ± 0.12	4.85 ± 0.18	4.31 ± 0.09	6.81 ± 0.22	5.83 ± 0.13	3.7 ± 0.09	7.55 ± 0.24	Mediterranean Forests, Woodlands & Scrub
Algyroides nigropunctatus	3	66 ± 1.73	17.23 ± 0.45	10.4 ± 0.22	8.7 ± 0.36	7.8 ± 0.38	7.35 ± 0.26	11.41 ± 0.55	9.53 ± 0.36	5.85 ± 0.3	12.79 ± 0.77	Mediterranean Forests, Woodlands & Scrub
Anatololacerta danfordi	5	57.6 ± 1.63	13.93 ± 0.19	8.57 ± 0.16	6.06 ± 0.14	7.4 ± 0.43	6.34 ± 0.26	10.4 ± 0.25	9.5 ± 0.25	5.41 ± 0.13	11.31 ± 0.25	Mediterranean Forests, Woodlands & Scrub
Apathya cappadocica	3	67.67 ± 2.19	15.94 ± 0.56	10.6 ± 0.12	6.62 ± 0.32	8.06 ± 0.34	6.95 ± 0.26	11.74 ± 0.28	10.78 ± 0.16	6.4 ± 0.26	12.85 ± 0.67	Mediterranean Forests, Woodlands & Scrub
Archaeolacerta bedriagae	6	65 ± 1.86	16.06 ± 0.67	9.98 ± 0.54	7.1 ± 0.51	8.23 ± 0.43	7.13 ± 0.26	12.78 ± 0.31	10.96 ± 0.48	6.33 ± 0.24	14.14 ± 0.48	Mediterranean Forests, Woodlands & Scrub
Atlantolacerta andreanskyi	2	43 ± 2	9.48 ± 0.46	5.89 ± 0.06	4.02 ± 0.14	4.33 ± 0.53	3.79 ± 0.4	6.42 ± 0.4	4.8 ± 0.43	2.94 ± 0.2	5.71 ± 0.11	Mediterranean Forests, Woodlands & Scrub
Dalmatolacerta oxycephala	5	57.8 ± 3.07	14.43 ± 0.82	8.87 ± 0.54	5.66 ± 0.34	6.84 ± 0.43	6.36 ± 0.37	10.38 ± 0.73	8.86 ± 0.64	4.89 ± 0.26	9.74 ± 0.63	Mediterranean Forests, Woodlands & Scrub
Eremias arguta	2	55 ± 4	13.06 ± 1.04	9.29 ± 0.9	7.89 ± 1.11	6.42 ± 0.69	6.09 ± 0.55	9.49 ± 0.65	9.49 ± 1.11	5.98 ± 0.5	9.32 ± 0.58	Temperate Grasslands, Savannas & Shrublands
Eremias pleskei	6	50.08 ±	12.23 ±	7.71 ±	6.87 ±	6.78 ±	5.62 ±	9.43 ±	9.13 ±	5.82 ±	9.79 ±	Temperate Grasslands, Savannas &

60

		1.54	0.39	0.22	0.3	0.26	0.31	0.29	0.33	0.15	0.2	Shrublands
Gastropholis prasina	1	105	27.61	12.78	10.84	12.10	11.82	15.42	12.40	7.97	20.00	Tropical & Subtropical Moist Forests
Gastropholis vittata	1	81	19.08	10.96	8.62	7.77	8.34	9.81	8.60	4.20	11.97	Tropical & Subtropical Moist Forests
Heliobolus lugubris	2	53.5 ± 0.5	13.57 ± 0.14	7.72 ± 0.08	6.47 ± 0.03	7.6 ± 0.76	6.24 ± 0.1	11.36 ± 0.12	10.81 ± 0.28	6.97 ± 0.71	12.13 ± 0.16	Deserts & Xeric Shrublands
Heliobolus spekii	4	43.25 ± 1.6	10.28 ± 0.23	6.6 ± 0.15	5.32 ± 0.17	5.41 ± 0.15	4.93 ± 0.19	9.04 ± 0.49	9.33 ± 0.27	5.53 ± 0.38	9.97 ± 0.28	Tropical & Subtropical Grasslands, Savannas & Shrublands
Hellenolacerta graeca	6	66.17 ± 1.92	15.86 ± 0.55	9.68 ± 0.36	6.63 ± 0.31	7.96 ± 0.4	6.81 ± 0.27	11.1 ± 0.33	9.52 ± 0.39	5.06 ± 0.2	11.94 ± 0.63	Mediterranean Forests, Woodlands & Scrub
Iberolacerta monticola	2	61.5 ± 3.5	14.47 ± 1.43	8.91 ± 0.74	6.65 ± 0.99	7.64 ± 0.47	6.38 ± 0.28	10.6 ± 0.71	8.75 ± 0.84	5.12 ± 0.4	10.61 ± 1.25	Mediterranean Forests, Woodlands & Scrub
Ichnotropis capensis	2	49 ± 3	12 ± 0.15	7.68 ± 0.07	5.69 ± 0.03	6.26 ± 0.01	5.85 ± 0.02	9.74 ± 1	8.56 ± 0.81	5.46 ± 0.1	9.13 ± 0.86	Tropical & Subtropical Grasslands, Savannas & Shrublands
Ichnotropis squamulosa	5	54.1 ± 1.75	13.27 ± 0.37	8.5 ± 0.18	7.13 ± 0.1	6.88 ± 0.21	6.84 ± 0.18	10.79 ± 0.45	10.47 ± 0.38	7.04 ± 0.32	11 ± 0.55	Tropical & Subtropical Grasslands, Savannas & Shrublands
Iranolacerta brandtii	1	70.00	14.53	9.17	7.41	7.01	6.98	11.27	9.69	5.99	12.09	Temperate Grasslands, Savannas & Shrublands
Lacerta agilis	9	69 ± 1.95	14.54 ± 0.31	10.03 ± 0.22	8.44 ± 0.22	8.01 ± 0.3	6.92 ± 0.22	9.68 ± 0.3	7.7 ± 0.24	5.02 ± 0.1	9.92 ± 0.21	Temperate forest
Lacerta viridis	2	104.5 ± 0.5	25.84 ± 0.77	17.16 ± 0.64	15.67 ± 0.19	10.29 ± 0.36	10.97 ± 0.04	19.05 ± 0.83	15.51 ± 0.04	9.65 ± 0.31	18 ± 1	Mediterranean Forests, Woodlands & Scrub
Latastia longicaudata	8	82.25 ± 3.22	19.39 ± 0.6	11.66 ± 0.42	10.06 ± 0.34	8.87 ± 0.39	8.56 ± 0.35	14.47 ± 0.58	14.3 ± 0.58	8.69 ± 0.19	14.66 ± 0.54	Deserts & Xeric Shrublands
Meroles reticulatus	7	35.57 ± 4.17	10.39 ± 0.87	6.09 ± 0.58	4.41 ± 0.43	5.06 ± 0.58	4.16 ± 0.48	7.08 ± 0.76	7.17 ± 0.62	5.33 ± 0.47	8.57 ± 0.9	Deserts & Xeric Shrublands
Meroles suborbitalis	1	49.50	12.22	9.10	6.44	6.04	6.34	8.71	10.96	5.60	12.00	Deserts & Xeric Shrublands
Mesalina guttulata	8	49.94 ± 0.98	11.49 ± 0.36	7.37 ± 0.24	5.32 ± 0.2	5.76 ± 0.23	5.33 ± 0.15	8.46 ± 0.37	8.43 ± 0.41	5.09 ± 0.19	9.38 ± 0.33	Deserts & Xeric Shrublands
Mesalina rubropunctata	6	52.08 ± 0.58	13.27 ± 0.33	9.12 ± 0.34	6.48 ± 0.14	6.77 ± 0.14	6.11 ± 0.18	9.76 ± 0.36	8.83 ± 0.16	5.41 ± 0.26	9.49 ± 0.22	Deserts & Xeric Shrublands
Nucras lalandii	3	85.33 ±	13.98 ±	9.16 ±	8.58 ±	7.36 ±	5.99 ±	8.74 ±	8.88 ±	5.47 ±	8.86 ±	Tropical & Subtropical Grasslands,

Species	n											Habitat
		7.51	1.31	0.62	0.98	0.64	0.6	0.61	0.72	0.49	0.45	Savannas & Shrublands
Nucras tessellata	4	73.13 ± 3.71	15.07 ± 0.83	9.9 ± 0.29	8.04 ± 0.37	7.98 ± 0.53	7.25 ± 0.43	11.1 ± 0.69	10.1 ± 0.37	6.21 ± 0.54	11.21 ± 0.62	Deserts & Xeric Shrublands
Omanosaura jayakari	1	129	30.29	22.38	18.96	16.28	14.98	21.93	18.56	10.84	19.93	Deserts & Xeric Shrublands
Ophisops elegans	3	45 ± 2.08	10.46 ± 0.63	7 ± 0.38	5.19 ± 0.57	5.63 ± 0.19	5.46 ± 0.16	8.33 ± 0.86	8.42 ± 0.25	5.16 ± 0.41	9.95 ± 0.37	Temperate Grasslands, Savannas & Shrublands
Parvilacerta parva	6	48.75 ± 1.28	10.7 ± 0.37	6.92 ± 0.2	6.18 ± 0.31	5.28 ± 0.1	4.69 ± 0.35	7.5 ± 0.23	6.36 ± 0.22	3.75 ± 0.15	8.31 ± 0.17	Temperate Grasslands, Savannas & Shrublands
Pedioplanis inornata	1	54	14.41	8.85	6.25	7.05	7.01	12.28	11.46	7.52	12.00	Deserts & Xeric Shrublands
Pedioplanis laticeps	1	68	16.29	12.34	8.55	10.78	7.84	13.46	13.51	8.55	15.11	Deserts & Xeric Shrublands
Pedioplanis lineoocellata	4	51 ± 2.86	12 ± 0.81	7.55 ± 0.35	5.74 ± 0.54	6.57 ± 0.35	6.26 ± 0.56	10.38 ± 0.79	10.67 ± 0.78	6.68 ± 0.32	9.55 ± 0.79	Tropical & Subtropical Grasslands, Savannas & Shrublands
Pedioplanis namaquensis	6	50.33 ± 0.92	11.02 ± 0.2	6.35 ± 0.19	4.99 ± 0.11	5.81 ± 0.17	5.2 ± 0.12	9.23 ± 0.27	8.67 ± 0.24	5.47 ± 0.1	10.65 ± 0.18	Deserts & Xeric Shrublands
Pedioplanis undata	2	53.5 ± 1.5	12.51 ± 0.07	7.14 ± 0.44	5.63 ± 0.04	6.79 ± 0.19	6.01 ± 0.53	10.37 ± 0.9	10.35 ± 0.21	6.6 ± 0.21	10.6 ± 0.6	Deserts & Xeric Shrublands
Philochortus spinalis	3	45.67 ± 4.1	10.36 ± 0.41	6.34 ± 0.42	5.22 ± 0.76	5 ± 0.55	4.54 ± 0.29	7.65 ± 0.22	7.99 ± 0.45	4.42 ± 0.31	8.7 ± 0.3	Tropical & Subtropical Grasslands, Savannas & Shrublands
Phoenicolacerta laevis	6	65.08 ± 1.24	16.97 ± 0.61	11 ± 0.44	8.84 ± 0.37	8.15 ± 0.27	7 ± 0.26	11.73 ± 0.65	10.33 ± 0.36	5.74 ± 0.29	14.03 ± 0.52	Mediterranean Forests, Woodlands & Scrub
Podarcis muralis	3	61.17 ± 4.57	15.42 ± 1.48	9.79 ± 0.86	7.77 ± 0.91	7.01 ± 0.67	6.4 ± 0.51	9.26 ± 0.76	8.93 ± 0.95	6.34 ± 0.32	13 ± 1.15	Mediterranean Forests, Woodlands & Scrub
Poromera fordii	3	58.33 ± 1.2	15.22 ± 0.4	9.21 ± 0.37	7.11 ± 0.51	8.03 ± 0.39	7.22 ± 0.39	11.19 ± 0.53	10.24 ± 0.11	5.77 ± 0.58	11.59 ± 0.47	Tropical & Subtropical Moist Forests
Psammodromus algirus	6	67.33 ± 1.89	15.49 ± 0.36	9.84 ± 0.3	6.83 ± 0.36	7.94 ± 0.27	7.37 ± 0.21	11.24 ± 0.17	10.88 ± 0.22	6.45 ± 0.24	13.68 ± 0.65	Mediterranean Forests, Woodlands & Scrub
Psammodromus hispanicus	6	37 ± 1.59	9.24 ± 0.39	5.25 ± 0.2	4.07 ± 0.2	4.46 ± 0.16	4.1 ± 0.3	6.11 ± 0.26	5.52 ± 0.21	3.73 ± 0.25	6.76 ± 0.25	Mediterranean Forests, Woodlands & Scrub
Pseuderemias brenneri	8	46.5 ± 0.8	12.17 ± 0.22	7.02 ± 0.11	5.34 ± 0.11	6.46 ± 0.13	5.29 ± 0.11	10.56 ± 0.32	11.26 ± 0.25	7.4 ± 0.19	12.94 ± 0.27	Tropical & Subtropical Grasslands, Savannas & Shrublands
Takydromus	5	42.8 ±	10.36 ±	5.29 ±	4.54 ±	5.33 ±	5.01 ±	6.54 ±	5.59 ±	3.17 ±	7.58 ±	Tropical & Subtropical Moist Forests

sexlineatus		1.36	0.36	0.15	0.13	0.12	0.13	0.26	0.19	0.2	0.41	
Timon lepidus	1	146	35.45	25.44	17.61	19.94	16.84	25.79	22.64	13.97	26.11	Mediterranean Forests, Woodlands & Scrub
Timon pater	5	133.2 ± 5.06	32.72 ± 1.98	21.98 ± 1.63	17.36 ± 1.22	15.97 ± 1.26	14.44 ± 0.59	22.59 ± 1.29	19 ± 0.9	10.81 ± 0.58	20.44 ± 1.01	Mediterranean Forests, Woodlands & Scrub
Zootoca vivipera	6	51.83 ± 0.79	10.99 ± 0.17	7.31 ± 0.28	5.66 ± 0.12	6.03 ± 0.26	5.43 ± 0.18	7.84 ± 0.4	6.41 ± 0.26	4.18 ± 0.05	8.32 ± 0.32	Temperate forest

APPENDIX 3. Data set 2 summary. Morphological variables (mm), GPS coordinates and substrate assignments for 80 lacertid individuals in Data set 2.

Species	SVL	Head length	Head width	Head depth	Forelimb length	Hindlimb length	Toe length	Latitude	Longitude	Substrate
Acanthodactylus boskianus	57	13.51	7.72	6.39	20	42	10.62	18.44895	37.70258	compact sand/gravel
Acanthodactylus boskianus	71	16.85	9.2	8.08	25	49	12.02	18.44895	37.70258	compact sand/gravel
Acanthodactylus boskianus	70	16.75	9.43	7.51	24	50	11.99	18.61609	37.70661	loose sand
Acanthodactylus boskianus	66.5	14.77	9.04	7.21	21	42	10.09	18.49674	37.55706	loose sand/leaf litter
Acanthodactylus boskianus	77	17.63	10.43	9.04	26	56	15.77	18.49674	37.55706	loose sand/leaf litter
Acanthodactylus boskianus	78	18.33	10.74	9.48	23	55	14.55	18.47501	37.58359	loose sand/leaf litter
Acanthodactylus boskianus	70.5	15.5	9.1	7.48	23	43	11.28	18.79587	37.11529	compact sand/rock
Acanthodactylus boskianus	61.5	14.09	8.3	6.95	21	42	11.72	18.79587	37.11529	compact sand/rock
Acanthodactylus boskianus	73	16.3	9.99	7.58	24	50	13.53	18.78182	37.12107	compact sand/rock
Heliobolus lugubris	53	12.79	7.13	5.63	23	42.5	11.5	-20.38295	15.435083	compact sand/gravel
Heliobolus lugubris	58	13.87	9.15	6.98	23	43.5	13.77	-20.355717	14.94455	compact sand/gravel/leaf litter
Heliobolus lugubris	53.5	13.79	8.8	6.95	24	49	15.79	-20.938967	14.952933	compact sand/gravel/leaf litter
Heliobolus lugubris	52.5	13.48	8.12	6.99	23	47	14.12	-20.937833	14.953933	compact sand/gravel/leaf litter
Heliobolus lugubris	52.5	13.07	7.51	6.15	22	46	14.27	-21.91975	15.345233	compact sand/gravel/leaf litter
Heliobolus lugubris	51.5	12.52	7.94	7.15	20	42	12.18	-21.959733	16.9025	compact sand/gravel/leaf litter
Heliobolus lugubris	51.5	12.85	8.4	7.63	22	53	14.28	-21.959083	16.903583	compact sand/gravel/leaf litter
Heliobolus lugubris	51	13.12	8.05	6.47	21	42.5	12.38	-22.584933	17.139183	compact sand/gravel/leaf litter
Heliobolus lugubris	51.5	13.19	8.23	6.78	21	43	14.26	-22.5848	17.139483	compact sand/gravel/leaf litter
Heliobolus lugubris	55	13	8.16	6.96	22	42.5	11.5	-22.448133	18.95815	compact sand/gravel/leaf litter

Heliobolus lugubris	58	12.37	7.55	5.76	21	38	10.04	-22.450783	18.9588	compact sand/gravel/leaf litter
Heliobolus lugubris	52.5	12.76	7.73	5.65	21	41	11.4	-22.448367	18.958633	compact sand/gravel/leaf litter
Heliobolus lugubris	52	13.16	8.66	7.05	22	46	13.9	-22.451267	18.957783	compact sand/gravel/leaf litter
Heliobolus lugubris	54.5	13.4	9.48	7.37	21	44	12.09	-20.12285	18.1752	compact sand/gravel/leaf litter
Heliobolus lugubris	56	8.21	9.72	13.89	22	44	12.99	-20.12295	18.175483	compact sand/gravel/leaf litter
Heliobolus lugubris	55	13.89	9.99	8.02	21	43	12.46	-20.12285	18.1752	compact sand/gravel/leaf litter
Heliobolus lugubris	54	12.6	7.43	6.03	21	39	10.06	-19.2326	18.496033	compact sand/gravel/leaf litter
Heliobolus lugubris	56	14.13	9.59	8.06	23	49	13.86	-19.290117	19.329133	compact sand/gravel/leaf litter
Heliobolus lugubris	59.5	13.51	8.22	6.69	23	45	13.5	-19.29115	19.326217	compact sand/gravel/leaf litter
Heliobolus lugubris	62.5	13.15	8.41	7.05	22.5	44.5	12.19	-19.816433	18.595617	compact sand/gravel/leaf litter
Heliobolus lugubris	54.5	13.65	8.88	7.3	20.5	45	13.66	-20.3171	18.497117	compact sand/gravel/leaf litter
Ichnotropis capensis	60	12.43	8.03	6.55	22.5	39	10.91	-19.289933	19.328683	compact sand/gravel
Ichnotropis capensis	52	12.29	6.69	6.19	20	39.5	9.66	-19.28965	19.328883	compact sand/gravel
Ichnotropis capensis	60	13.28	8.31	6.49	19	36	11.17	-19.28965	19.328883	compact sand/gravel
Ichnotropis capensis	57	12.68	8.24	6.87	30	37	10.78	-19.290117	19.329133	compact sand/gravel
Ichnotropis capensis	53.5	12.57	7.57	6.07	20	40	10.25	-19.81725	18.595833	compact sand/gravel/leaf litter
Ichnotropis capensis	53	13.24	7.53	6.16	19.5	33	11.08	-20.3171	18.497117	compact sand/gravel/leaf litter
Latastia longicaudata	79	16.73	9.08	7.73	26	53.5	14.34	18.44769	37.70028	compact sand/gravel/leaf litter
Latastia longicaudata	64	14.68	7.47	6.31	24.5	47	13.77	18.78886	36.83171	compact sand/gravel/leaf litter
Meroles anchietae	46	11.22	8.18	5.62	19	36	10.82	-23.5684	15.042583	loose sand
Meroles cuneirostris	64	16.97	12.49	8.31	23	49	14.85	-23.5696	15.0411	loose sand
Meroles cuneirostris	60.5	17.19	11.66	8.77	23	51	13.89	-23.5696	15.0411	loose sand
Meroles cuneirostris	53	14.27	10.18	6.62	20	44	11.8	-23.570867	15.0411	loose sand
Meroles cuneirostris	66	12.4	17.19	8.4	23	52	14.99	-23.569333	15.04105	loose sand
Meroles cuneirostris	50	13.4	9.25	6.75	19	52	10.81	-23.5657	15.0382	loose sand
Meroles cuneirostris	58	15.68	11.31	7.61	23	50	14.46	-23.569833	15.04095	loose sand
Meroles cuneirostris	54.5	14.1	9.74	6.65	20	44	11.8	-23.570133	15.040983	loose sand
Meroles cuneirostris	51	13.3	9.34	6.81	20	42	11.22	-23.570133	15.040983	loose sand
Meroles cuneirostris	49	14.04	9.39	6.73	20	41.5	11.81	-23.5711	15.041167	loose sand
Meroles cuneirostris	51	15.16	10.56	7.01	22	50	13.15	-23.571267	15.041183	loose sand

Meroles cuneirostris	55	15.57	10.69	7.69	22	48	12.92	-23.55995	15.031383	loose sand
Meroles cuneirostris	50	13.75	9.56	6.74	20	41	10.66	-23.56495	15.0236	loose sand
Meroles cuneirostris	53	15.05	10.07	6.83	22	47	12.82	-23.567283	15.022833	loose sand
Meroles suborbitalis	61	14.97	10.21	7.15	24	49	13.88	-23.559483	15.041567	compact sand/gravel
Meroles suborbitalis	61	15.44	10.38	7.77	23	45	12.27	-23.556317	15.041683	compact sand/gravel
Nucras intertexta	69	13.85	8.61	10.81	22.5	33	10.55	-20.123133	18.175383	compact sand/gravel/leaf litter
Nucras intertexta	80	16.7	10.1	8.28	26	37	10.22	-20.314833	18.497933	compact sand/gravel/leaf litter
Pedioplanis gaerdesi	51	12.72	7.66	5.63	20.5	39	11.16	-21.096367	14.674483	compact sand/gravel/leaf litter
Pedioplanis gaerdesi	46	11.33	7.44	5.08	19	38	11.29	-21.098067	14.674533	compact sand/gravel/leaf litter
Pedioplanis gaerdesi	44.5	10.15	6.13	3.81	19	36	9.71	-21.098317	14.6742	compact sand/gravel/leaf litter
Pedioplanis gaerdesi	43	10.06	6.23	4.78	16.5	32	8.72	-21.09845	14.673817	compact sand/gravel/leaf litter
Pedioplanis inornata	45.5	10.3	5.62	5	17	31	8.6	-21.861583	15.199083	compact sand/rock
Pedioplanis inornata	48.5	11.06	7.03	4.92	18	33	9.83	-21.859483	15.19795	compact sand/rock
Pedioplanis inornata	44	11.16	6.48	5.18	18	34	9.59	-21.861033	15.199183	compact sand/rock
Pedioplanis inornata	45.5	11.47	6.55	5.54	18	37	10.33	-21.861583	15.199083	compact sand/rock
Pedioplanis inornata	45	10.91	6.3	5.6	18.5	34.5	9.42	-21.861417	15.199183	compact sand/rock
Pedioplanis namaquensis	45	10.31	6.09	4.96	16	30	9.33	-21.220067	14.868983	compact sand/gravel
Pedioplanis namaquensis	51	11.73	6.81	5.19	17	33	9.31	-21.220067	14.868983	compact sand/gravel
Pedioplanis namaquensis	51.5	10.8	6.46	4.22	17	33.5	9.84	-21.219417	14.87035	compact sand/gravel
Pedioplanis namaquensis	40	9.58	5.46	4.76	15	32	10.11	-21.219417	14.87035	compact sand/gravel
Pedioplanis namaquensis	43	9.73	5.79	4.6	16	33	9.38	-21.097967	14.674583	compact sand/gravel/leaf litter
Pedioplanis namaquensis	47	10.94	6.38	5.26	18	35	11.09	-21.107517	14.664367	compact sand/gravel/leaf litter
Pedioplanis rubens	57	11.65	7.35	4.96	18	34	9.73	-20.65215	17.099833	rock
Pedioplanis rubens	51	12.16	7.39	4.9	20	37.5	10.17	-20.652283	17.099967	rock
Pedioplanis rubens	49.5	12.16	7.67	5.31	19	34	10.25	-20.655283	17.101317	rock
Pedioplanis rubens	47	11.54	7.48	4.89	19	35	9.77	-20.654083	17.1033	rock

Pedioplanis undata	55.5	12.48	7.49	5.84	19.5	34	8.81	-20.700317	16.844483	compact sand/gravel/leaf litter
Pedioplanis undata	51.5	12.34	6.68	5.48	27.5	35.5	9.49	-20.700283	16.8445	compact sand/gravel/leaf litter
Pedioplanis undata	51	12.98	8.02	5.72	20	37	9.57	-20.689633	16.836783	compact sand/gravel/leaf litter
Pedioplanis undata	53.5	12.28	7.56	5.52	19	45	9.2	-20.688717	16.837083	compact sand/gravel/leaf litter
Pedioplanis undata	53.5	12.11	7.8	5.93	19	32	8.9	-20.688683	16.83665	compact sand/gravel/leaf litter

APPENDIX 4. Phylogenetic and molecular clock analysis.

Evolutionary relationships and divergence dates for Lacertidae were estimated within a Bayesian framework in BEAST (Drummond et al. 2012). We applied the best-fit model, GTR with a proportion of invariant sites and gamma distributed rate heterogeneity (GTR+I+G), as determined by jModelTest 0.1.1 (Posada 2008; Guindon and Gascuel 2003), and a relaxed molecular clock with an uncorrelated lognormal distribution of evolutionary rates among branches (Drummond et al. 2006). Default settings for all priors were retained, except for the tree prior that was set to the Yule Process (speciation), as recommended by Drummond et al. (2007). Minimum and maximum constraints for four nodes were chosen based on evidence from the fossil record (see below). A preliminary run was used to optimize parameters and generate an input tree. The final analysis was run for 107 generations, with trees sampled every 1 000 generations over four separate chains. The first 2 000 trees of each run were discarded as burn in, and the remaining 32 000 trees (combined from the four chains) were combined in LogCombiner 1.5.2 and analyzed in Tracer 1.4.1 (Rambaut and Drummond 2008). The effective sample size was >100 for all parameters, suggesting that the results accurately represent the target joint posterior distribution. The maximum clade credibility tree (based on a posterior probability threshold of 0.95) is shown below, with time in millions of years:

Psammodromus_hispanicus
Psammodromus_algirus
Gallotia_galloti
Poromera_fordii
Nucras_lalandii
Latastia_longicaudata
Philochortus_spinalis
Pseuderemias_smithii
Heliobolus_spekii
Heliobolus_lugubris
Australolacerta_rupicola
Meroles_suborbitalis
Meroles_knoxii
Ichnotropis_squamulosa
Meroles_reticulatus
Meroles_cuneirostris
Australolacerta_australis
Tropidosaura_essexi
Tropidosaura_cottrelli
Tropidosaura_gularis
Tropidosaura_montana
Pedioplanis_laticeps
Pedioplanis_undata
Ichnotropis_capensis
Eremias_pleskei
Eremias_arguta
Mesalina_rubropunctata
Mesalina_guttulata
Ophisops_elegans
Omanosaura_jayakari
Acanthodactylus_erythrurus
Acanthodactylus_scutellatus
Acanthodactylus_boskianus
Gastropholis_vittata
Gastropholis_prasina
Adolfus_africanus
Adolfus_jacksoni
Congolacerta_vauereselli
Congolacerta_asukului
Holaspis_laevis
Holaspis_guentheri
Atlantolacerta_andreanskyi
Phoenicolacerta_laevis
Phoenicolacerta_kulzeri
Iberolacerta_horvathi
Darevskia_valentini
Iberolacerta_monticola
Iberolacerta_cyreni
Lacerta_agilis
Iranolacerta_brandtii
Archaeolacerta_bedriagae
Timon_tangitanus
Timon_lepidus
Anatololacerta_danfordi
Anatololacerta_oertzeni
Parvilacerta_parva
Parvilacerta_fraasii
Hellenolacerta_graeca
Dalmatolacerta_oxycephala
Tiera_perspicillata
Tiera_dugesii
Algyroides_fitzingeri
Algyroides_nigropunctatus
Dinarolacerta_mosorensis
Algyroides_moreoticus
Apathya_cappadocica
Takydromus_sexlineatus
Takydromus_amurensis
Zootoca_vivipara
Podarcis_muralis
Rhineura_floridana
Aspidoscelis_tigris

Cretaceous	Pal	Eoc	Oligo	Mio	Plio

120　　　100　　　80　　　60　　　40　　　20　　　0

69

APPENDIX 5. Phylogenetic trees for comparative analyses.

Since missing taxa can greatly affect the results of phylogenetic comparative analyses (Harvey & Pagel 1991, Blackburn & Gaston 1998), the above tree was modified to match taxon sampling in Data sets 1 and 2, respectively. For each data set, missing taxa were inserted into the tree in Mesquite v.2.75 (Maddison and Maddison 2009) based on available morphological and molecular information. Species in Data set 1 that had morphological data but not sequence data were positioned in the phylogeny as follows: *Timon pater* replaced *Timon tangitanus*, as these species form a monophyletic clade including *T. lepidus* (Arnold 1973, Ahmadzadeh et al. 2012); *Pseuderemias brenneri* replaced *P. smithii* (Arnold 1986); *Lacerta viridis* was added as sister taxon to *L. agilis* (Godinho et al. 2005); *Nucras tessellata* was added as sister to *N. lalandii* (Broadley 1972); *Acanthodactylus busacki* replaced *A. erythrurus* and *A. schreiberi* was added as sister to *A. boskianus* (Salvador 1982, Arnold 1983, Harris and Arnold 2000); *Pedioplanis inornata*, *P. lineoocellata* and *P. namaquensis* were added to the existing *P. laticeps* and *P. undata* as (((*P. laticeps*(((*P. lineoocellata*((*P. namaquensis*(*P. inornata*, *P. undata*)))) based on the molecular phylogeny of Makokha *et al.* (2007). Inserted branches were stretched to the tips to retain an ultrametric structure. Sister species were given equal branch lengths and approximate node ages of inserted *Pedioplanis* species were informed by the molecular clock analysis of Makokha *et al.* (2007).

The same procedure above was applied to the tree topology of Data set 2 with the following changes: *Meroles anchietae* replaced *M. reticulatus*, as these species are more closely related to each other than to the remaining *Meroles* species (Lamb and Bauer 2003); *Nucras intertexta* replaced *N. lalandii* (Broadley 1972); *Pedioplanis namaquensis* replaced *P. laticeps*, and *P. gaerdesi*, *P. inornata* and *P. rubens* were added to the *Pedioplanis* clade in the branching order (((*P. namaquensis*(((*P. undata*((*P. rubens*(*P.*

inornata, *P. gaerdesi*)))) based on Makokha *et al*. (2007), which also informed branch lengths. Taxa in each phylogeny not represented in the morphological data sets were pruned from the tree in Mesquite.

Fossil calibrations

Taxon sampling differed slightly from our previous study (Hipsley et al. 2009), so that the fossils chosen here for molecular clock calibrations have also changed. The previous node for the origin of Squamata (represented by the split between *Sphenodon punctatus* and the remaining taxa) was removed, in order to avoid the bias that a very long branch may introduce (see Magallón 2010). We also added a new calibration, based on an early Miocene lacertid fossil (see below).

For each fossil calibration, we used a maximum and minimum bound with uniform probability, such that the divergence could have occurred at any point during the selected time interval. We chose this approach over the implementation of "soft" bounds (but see Yang and Rannala 2006, Drummond et al. 2006), as in our opinion the lacertid fossil record is not sufficiently sampled to inform the shape of the probability curve (e.g., exponential, lognormal). Instead, we used the age of the oldest fossil of a lineage as the minimum bound for that node, and the maximum bound was calculated as the minimum plus 10%. Although this approach is not justified paleontologically (through phylogenetic bracketing or preservation potential; e.g., Reisz and Müller 2004; Müller and Reisz 2005, Benton and Donoghue 2007; Donoghue and Benton 2007; Benton et al. 2009), there is at present no practical way to estimate curve parameters (Ho and Phillips 2009). We therefore chose a conservative approach with the fewest assumptions on the probability of origination for each calibrated node.

All fossil-based calibrations are presented below following the guidelines of Parham et al. (2012), outlining five steps to justify the phylogenetic position and age of each specimen:

1) Museum numbers of specimen(s) that demonstrate all of the relevant characters and provenance data should be listed. Referrals of additional specimens to the focal taxon should be justified.

2) An apomorphy-based diagnosis of the specimen(s) or an explicit, up-to-date, phylogenetic analysis that includes the specimen(s) should be referenced.

3) Explicit statements on the reconciliation of morphological and molecular data sets should be given.

4) The locality and stratigraphic level (to the best of current knowledge) from which the calibrating fossil(s) was/were collected should be specified.

5) Reference to a published radioisotopic age and/or numeric time scale and details of numeric age selection should be given.

(i) Teiidae (*Aspidoscelis tigris–Rhineura floridana*: 113 Ma minimum, 124.3 Ma maximum)

1) OMNH (Oklahoma Museum of Natural History) 60764, holotype of *Ptilotodon wilsoni* consisting of a broken right dentary with six tooth positions and four complete teeth (Nydam and Cifelli 2002).

2) Represents the oldest known teiid based on the presence of thick cementum at the bases of the teeth, together with deep, subcircular replacement pits at the tooth bases (Nydam and Cifelli 2002). Differs from other Early Cretaceous teiids described by Winkler et al. (1990) in having less robust teeth, tooth crowns with well developed anterior and posterior expansions, a shorter subdental shelf, and lacking medial striae.

3) This fossil has not been included in a phylogenetic analysis.

4) Howard McLeod Correctional Center (OMNH V706), Tomato Hill, Atoka County, Oklahoma.

5) Late/Upper Aptian to Middle Albian (125.0 - 99.6 Ma) floodplain of claystone and sandstone in the Antlers Formation of Oklahoma. Yields microvertebrates from 1-1.5 m below the dinosaur-bearing horizon (Nydam and Cifelli 2002).

(ii) Amphisbaenia (*Rhineura floridana–Gallotia galloti*: 64.2Ma minimum, 70.6 Ma maximum)

1) NMMNH (New Mexico Museum of Natural History and Science) P-12347 (originally described under catalogue number UNM NP-596), holotype of *Plesiorhineura tsentasi* (Sullivan 1985), comprised of the medial part of the right ramus.

2) Oldest known rhineurid amphisbaenian, based on subpleurodont tooth morphology, positioning of the teeth on the dentary, and juxtaposition of the dentary, coronoid and splenial bones (Sullivan 1985). To date, all North American fossil forms belong to the family Rhineuridae (Kearney 2003).

3) This fossil has not been included in a phylogenetic analysis.

4) Torreon Wash (Bureau of Land Management and University of New Mexico locality 77-184), Deer Mesa Quadrangle, San Juan County, New Mexico.

5) Upper part of the Nacimiento Formation, "Pantolambda Zone," middle Paleocene (Torrejonian). Torreon Wash is considered to be "middle Torrejonian" and part of the "To2" zone (Lofgren et al. 2004). Correspondingly, correlations based on pollen from the Nacimiento Formation suggest the fossil bearing zones are at least 62 Ma (Williamson et al. 2008).

(iii) *Lacerta viridis* group (*Lacerta agilis-Iranolacerta brandtii*: 18.1 Ma minimum, 19.9 Ma maximum)

1) Pb (National Museum, Prague, Czech Republic) 02054 consisting of fused frontals, and Pb 02055 consisting of a fragment of the single left frontal (Čerňanský 2010).

2) Čerňanský (2010) compared the above fossils to material from extant *L. viridis*, *L. agilis* and *Timon lepidus* (formerly *L. lepida*), and to Rauscher's (1992) descriptions of *Podarcis muralis* and *Zootoca vivipara*. The frontals were found to be indistinguishable from those of the extant *L. viridis* group (including *L. viridis* [sensu stricto], *L. bilineata*, *L. media*, *L. pamphylica*, *L. trilineata*, *L. strigata*, and *L. schreiberi*), on the basis of the following features: large size, light ornamentation of the dorsal surface formed by small grooves and protuberances, robust and narrow relative to length, anterior portion before the sulcus interfacialis longer than the posterior one (approximately 3:2), narrow prefrontal facets on anterior lateral margins which are straight and not arched, massively developed crista cranii frontale on the ventral surface, and entire posterior margin contacting the parietal (Čerňanský (2010).

3) The fossil has not been included in a phylogenetic analysis, however members of the *L. viridis* group have been subject to both morphological and molecular phylogenetic analyses (Arnold 1973, Godinho et al. 2005, Böhme et al. 2006). The green lizard group is currently divided into *L. viridis* (sensu stricto) and its sister species *L. bilineata*, with the latter possibly situated within the former based on mitochondrial and nuclear DNA (Godinho et al. 2005). Other members of this polytomy include *L. media*, *L. pamphylica*, *L. trilineata*, *L. strigata*, and *L. schreiberi*, although exact relationships among these species remain unresolved (Arnold et al. 2007).

4) The Dolnice locality consists of lower/early Miocene (Ottnangian) lake sediments, belonging to the MN-zone 4b (sensu Mein 1990) in the westernmost part of the Cheb basin near the town of Cheb in western Bohemia, Czech Republic. Fossils are derived from greenish, calcareous marls and limnic clay silts and are interpreted as marginal,

riparian facies (Fejfar & Kvaček 1993). The fossil-bearing deposits are exposed at several sites in the roof of the local, main, brown coal seam of the basin. In addition to lacertids, the locality has yielded a rich abundance of other fossil lizards, such as chameleonids, cordylids, and anguids (e.g., Klembara 1979, 1981; Roček 1984).

5) The Ottnangian stage represents the middle Burdigalian (c. 18.1-17.2 Ma) within the regional stratigraphic concept for the Central Paratethys.

(iv) *Timon* group (*Timon lepidus/T. tangitanus–Anatololacerta/Parvilacerta*): 5.3 Ma minimum, 5.8 Ma maximum)

1) Holotype material of *"Lacerta" ruscinensis,* consisting of a dentary and a caudal vertebra, described by Depéret (1890).

2) According to Depéret (1890) and confirmed by Mlynarski (1956), the material is almost indistinguishable in size and shape from modern *Timon lepidus*, which still occurs in the same area today. Unfortunately no images were included in the text, so direct comparisons to other material cannot be made here.

3) This fossil has not been included in a phylogenetic analysis.

4) The late Pliocene Basin of Roussillon, France, today corresponding to a plain with the city of Perpignan in the center. The Roussillon Basin was formed following the posterior transgression in the early Pliocene that resulted in widespread flooding and formation of several marginal basins in the Mediterranean area (Clauzon 1990, Gibert and Martinell 1998). This area has yielded abundant and diverse fossil macro- and microfauna, including molluscs and rodents (Gilbert et al. 2007).

5) Lower Villafranchian of the European Neogene Mammal timescale, zone NM 16. The lower boundary is dated to 5.28 Ma (Late Pliocene).

CHAPTER 3:

EFFECTS OF CENOZOIC ARIDIFICATION ON TAXONOMIC AND MORPHOLOGICAL DIVERSIFICATION OF AFRICAN LACERTID LIZARDS (LACERTIDAE)

ABSTRACT

African lizards from the family Lacertidae exhibit an unusual pattern of species richness in which their highest diversity occurs in arid regions north and south of the equator, as opposed to lower latitudes. Compared to their palearctic sister taxa, arid-dwelling taxa also appear to be evolutionarily derived in terms of morphology and phylogenetic position, indicating a relatively young but rapid radiation. To determine if arid environments promote taxonomic and morphological evolution in this group, we tested if patterns of diversification were associated with historical climatic events. A combination of phylogenetic, ecological and morphological approaches was used to estimate timing and rates of speciation and extinction for the major lineages, and test if ancestral transitions in ecology, morphology, and rates of diversification temporally coincide with paleoclimatic events in the Cenozoic. We found that ancestral shifts to arid habitat were correlated with several derived osteological traits, many of which appear to have functional or adaptive purposes. Patterns of taxomic diversification also followed significant climate change events in the Oligocene and Miocene related to the transition from closed, mesic forests to open, dry habitats in Africa. An overall slowing of diversification rates towards the present indicates an early adaptive radiation in response to historical climate change, possibly via heterochronic processes. Shortened life histories in response to extreme climatic conditions in Africa could explain the apparent paedomorphic features and increased diversification rates through shorter generation times. Although African lacertids have successfully diversified under extreme conditions, it is unclear if they will survive predicted changes in climate that may drive them over their thermal maxima.

The family Lacertidae consists of small bodied, mainly terrestrial lizards distributed throughout the Old World. Phylogenetically it is divided into two subfamilies, the basal-most Gallotinae, restricted to the Canary Islands and parts of the Mediterranean, and the common and widespread Lacertinae covering Europe, Asia and Africa. The latter is divided into two subclades, the predominantly palearctic Lacertini and the African Eremiadini (Arnold et al. 2007). In terms of genera, the African radiation makes up over half of the entire family, and in species number nearly 60% (www.lacerta.de), making Eremiadini the most diverse lacertid clade. At the same time, many of its members are also considered to be the most derived both morphologically (Arnold 1981, 1991) and evolutionarily (Lamb and Bauer 2003, Arnold et al. 2007, Mayer and Pavlicev 2007), indicating significant heterogeneity in the evolutionary processes underlying their diversification.

In contrast to the global pattern of increasing biodiversity towards the tropics (Hillebrand 2004), African lacertids are most species rich in arid habitats north and south of the equator, despite being spread throughout the continent (www.lacerta.de). Genera in arid regions of Africa tend to be taxonomically diverse (e.g., *Acanthodactylus*, *Pedioplanis*), while those with tropical equatorial distributions are geographically restricted and species poor (e.g., *Holaspis*, *Poromera*). According to morphology, the clade shows a continuous monophyletic trend from mesic to xeric forms, with equatorial forest taxa (e.g., *Gastropholis*, *Adolfus*, *Holaspis*) arising basally (Arnold 1989b, Harris et al. 1998a). In contrast, molecular-based phylogenies indicate multiple, independent radiations into arid environments across the group (Mayer and Pavlicev 2007, Hipsley et al. 2009). According to this pattern, if the primitive condition is mesic (as suggested by outgroup comparison), invasions of arid habitats have occurred at least three times during

their evolution: in the Saharo-Eurasian clade (*Acanthodactylus*, *Eremias*, *Mesalina*, *Ophisops*), the Northeast African clade (*Latastia*, *Philochortus*, *Heliobolus*) and the southern African clade (*Meroles*, *Ichnotropis*, *Pedioplanis*) (Mayer & Pavlicev 2007). In the latter group, lacertid diversity reaches its peak in southern Africa, where over two-thirds of lacertid species are endemic (Branch 1998, Makokha et al. 2007).

The high species richness and endemicity of arid-dwelling lacertids is surprising, given that they represent the youngest and most derived taxa in the clade (Harris et al. 1998b, Arnold 1991, Lamb and Bauer 2003). According to the molecular clock study by Hipsley et al. (2009), the Eremiadini arose in the mid-Eocene around 45 million years ago (Mya) and shortly thereafter radiated in both northern and southern Africa. Some of its most derived arid and desert-dwelling forms like *Meroles* and *Ichnotropis* did not appear until the early Miocene, about 20 Mya (Hipsley et al. 2009). In addition, this study and others (e.g., Makokha et al. 2007, Mayer and Pavlicev 2007) found significant heterogeneity in substitution rates across genes, genomes and branches, indicating unevenness in the evolutionary processes affecting lineages. Discrepancies between rates of molecular and morphological change have also been reported for the southern African genera *Meroles* (Harris et al. 1998b) and *Pedioplanis* (Makokha et al. 2007), suggesting rapid morphological evolution in response to aridification.

The role of climate change in evolutionary radiations has been investigated in a wide array of groups, including angiosperms (Egan and Crandall 2008), corals (Chadwick-Furman 1996, Simpson et al. 2011), freshwater fish (Near et al. 2005), insects (Carsten and Knowles 2007) and aquatic invertebrates (Crame 2000). Among terrestrial vertebrates, patterns of global diversity are strongly linked with paleoclimatic events in the Cenozoic - the period from 65 Mya to today when modern plants and animals first

appeared (Barnosky et al. 2003, Delsuc et al. 2004, Weir and Schluter 2004, Blois and Hadly 2009). For example, the lineage including modern horses underwent dramatic morphological transformations of the teeth (for grass grazing), limbs (lengthening for efficient running) and toes (digital reduction) as their habitats shifted from predominantly tropical, closed forests in the late Paleocene to open, dry grassland in the late Eocene-early Oligocene (Simpson 1951, Prothero and Shubin 1989). In addition to morphological transformation, paleoclimatic events can also affect diversification rates directly. This is well illustrated by the fossil record of early hominoids, which experienced repeated pulses of expansion and extinction following mid-Miocene warming and end-Miocene cooling, respectively (Folinsbee and Brooks 2007).

While most of the aforementioned studies inferred diversity dynamics from paleontological evidence (e.g., fossil occurrence data, comparative anatomy of preserved parts, paleoecology), many groups lack an adequate fossil record from which to derive temporal patterns of evolutionary change. Squamate reptiles in particular, the group including snakes, lizards and amphisbaenians, are poorly known from the Cenozoic of Africa, mainly due to their small body sizes and collection biases towards mammals and birds (Augé 2003, Evans 2003). Lacertid lizards especially suffer from this bias, as so far only one fossil has been described from the African clade (Rage 1976). However, the advent of recent statistical methods now permit the reconstruction of historical evolutionary events even in the absence of a good fossil record (Paradis et al. 2004, Rabosky 2006, Harmon et al. 2008, Alfaro et al. 2009). These methods typically use branch lengths derived from molecular phylogenies to estimate net rates of diversification (Magallón and Sanderson 2001) or speciation rates under various levels of extinction (Rabosky 2006). The tempo and mode of lineage accumulation can then be compared to a constant model of evolution (e.g., the birth-death model; Kendall 1948, Nee et al. 1994),

to test if diversification rates are constant over time or lineages (Pybus and Harvey 2000). Such approaches can then be combined with information about the biogeographical and phenotypic histories of clades to test if changes in diversification rates coincide with climatic events or morphological evolution (Zink and Slowinski 1995; Kadereit et al. 2004; Weir and Schluter 2004).

Applying the above methods to Lacertidae to investigate the evolutionary context of their African radiation requires a robust time-calibrated phylogeny from which to calculate rates of diversification. Several authors have attempted to date the major lineages, but estimates for the origin of the African clade vary from the mid-Miocene, 12-16 Mya (Carranza et al. 2004, Arnold et al. 2007) to the mid-Eocene, 38-48 Mya (Hipsley et al. 2009). In Chapter 2, we reevaluated lacertid divergence times using a conservative approach to prior modelling (i.e. uniform probability curves) and a modified set of four fossil calibrations. Compared to our previous study (Hipsley et al. 2009), we recovered younger ages for nearly every lineage, placing the origin of Eremiadini at the end-Eocene, 36 Mya. This overall pull of evolutionary splits towards the recent is most likely due to the exclusion of the rhynchocephalian *Sphenodon punctatus* as outgroup to Squamata. According to some estimates, these groups may be separated by up to 100 million years (My) (Vidal and Hedges 2005, Wiens et al. 2006, Hugall et al. 2007). Such a long branch can dramatically bias molecular clock estimates, as it may encompass a vast number of combinations of substitution rate and time (Anderson and Swofford 2004, Magallón 2010).

Regardless of the exact date, modern lacertids are an essentially Cenozoic group, as indicated by their long fossil record in Europe (Estes 1983) and other molecular dating studies (e.g., Vidal and Hedges 2005, Wiens et al. 2006). The Cenozoic period is

characterized by multiple dramatic climatic changes, many of which are thought to have influenced the evolution of African biota (Table 1). In the early Cenozoic, Africa experienced its greatest extent of tropical and subtropical forests and its highest temperatures at the Paleocene-Eocene Thermal Maximum (~55 Mya; Zachos et al. 2008). Global cooling at the end of the Eocene (~34 Mya) transformed the continent from lush forests and woodlands to increasingly open habitat, resulting in massive faunal turnover (Bobe 2006). Significant tectonic rearrangements and the closing of the Tethys Sea at the Oligocene-Miocene boundary (~24 Mya) also increased aridification, while the reconnection of Eurasia with Africa opened exchange routes for flora and fauna (Augé 2003). Rainfall in Africa was significantly reduced and external factors such as tectonic uplift, cooling and drying led to the formation of deserts across the continent. The Namib Desert in southwestern Africa formed following the development of the Benguela Current in the late Miocene (Siesser 1980), and multiple episodes of aridity and sand deposition shaped the Sahara and Kalahari Deserts around 7 and 1 Mya, respectively (Stokes et al. 1997, Schuster et al. 2006).

The individual geological histories of the arid regions, combined with independent radiations of lacertids in Africa, provide a unique opportunity for comparative tests of climate-driven evolution in this group. Using a combination of phylogenetically-based approaches, we test if ancestral transitions in morphology, ecology and rates of speciation and extinction temporally coincide with paleoclimatic events. Specifically, we test the hypothesis that bouts of increasing aridity in the Cenozoic increase rates of diversification in Lacertidae, and that radiations into arid environments promote morphological diversification. Although lacertids lack fossil evidence directly placing them in arid regions of Africa at any certain time in the past, we

use ancestral state reconstructions of arid-adapted cranial traits and ecology as a proxy for paleoenvironment, thus providing a timeframe for the origins of shifts to drier habitats.

MATERIALS AND METHODS

Scoring of cranial characters

The cranial anatomy of 46 lacertid species was investigated using high resolution X-ray Computed Tomography (CT). Taxon sampling included up to four species from each genus of Eremiadini, 1-2 species from each genus of the basal-most clade Gallotinae (*Gallotia+Psammodromus*), and 1-2 species from 4 genera of Lacertini. Adult specimens were obtained from the Museum für Naturkunde Berlin, Germany, the Zoologisches Forschungsmuseum Alexander Koenig in Bonn, Germany, and from private persons or breeders (see Appendix 1 for specimen details). Between one and four specimens were examined per species. For CT scanning, whole preserved lizards were removed from ethanol, wrapped in plastic bubble wrap, and transferred to a dry 15ml or 50ml centrifuge tube stabilized in a metal clamp. CT scans were performed at the Museum für Naturkunde Berlin, using a Phoenix|x-ray Nanotom (GE Sensing & Inspection Technologies GmbH, Wunstorf, Germany) with a 180 kV high-power nanofocus tube and a tungsten target. Reconstructions were performed in Datos|x-reconstruction software (GE Sensing & Inspection Technologies GmbH phoenix|x-ray) and three-dimensional volumes were visualized in VGStudio Max 2.1 (Volume Graphics, Heidelberg, Germany).

To describe interspecific variation in the lacertid skull, osteological cranial characters were scored based on the CT images. The cranium of each individual was isolated from the mandibles and vertebral column in VGStudio Max using the region grower tool, which chooses all voxels in the volume within a given range of grey values

(corresponding to differences in bone density). Since the region grower will not cross large sutures or gaps, it can be used to isolate individual bones, here the mandibles and vertebrae, and remove them from the volume leaving only the cranium.

The characters chosen were based on the morphological analyses of Arnold (1983, 1989a, b, 1991) and Arnold et al. (2007). These studies identified over a dozen derived cranial osteological traits that appear related to life in arid habitats, such as a complex septomaxilla, flattening of the snout, and an overall decrease in ossification accompanied by fusion of some cranial bones (Figure 1). In total, 19 characters were scored for each species as discrete, binary traits (Table 2, Appendix 2). For binary codings, the value of the number itself (a 0 or 1) is unrelated to character polarity. Character distributions are given in Appendix 3.

Phylogenetic analysis and ancestral state reconstruction

The time-calibrated molecular phylogeny was taken from Chapter 2, based on 1012 bp of the nuclear gene RAG-1 for 72 species (70 lacertid species and 2 outgroups). Ancestral state reconstructions were performed on a modified tree to match taxon sampling in the CT data. When possible, species not represented in the phylogeny took the place of their next closest relatives, based on previous studies. For example, the missing phylogenetic position of Omanosaura cyanura was substituted by that of its congener O. jayakari (Harris et al. 1998a). Acanthodactylus maculatus took the place of A. erythrurus based on a combined analysis of molecular and morphological data by Harris and Arnold (2000). Darevskia valentini was replaced by D. mixta according to microsatellite repeat similarity (Grechko et al. 2007), and Pseuderemias brenneri took the place of P. smithii (Szczerbak 1989). Taxa not represented in the CT data were pruned from the tree, leaving a total of 46 terminal taxa with matching phylogenetic and

morphological data. All tree modifications were made in Mesquite v.2.75 (Maddison and Maddison 2009).

Ancestral state reconstructions were also performed in Mesquite (Maddison and Maddison 2009). To identify evolutionary transitions to arid environments that may be linked to patterns of diversification, we reconstructed ancestral habitat type onto the phylogeny using maximum likelihood (ML) and unordered parsimony. For ML, the Markov k-state 1 parameter (Mk1; Lewis 2001) was used as the evolutionary model, in which changes between states are equally probable. Habitat was characterized for each species as arid or mesic based on species distributions and biome assignments of museum specimens (see Chapter 2 for biome extraction methods). For this analysis, an arid assigment was reserved for species inhabiting xeric or hyper-arid habitats like aeolian desert and coastal dunes (e.g., *Meroles cuneirostris*), as well as dry, open areas with sparse vegetation including tropical and subtropical grasslands, savannas and shrublands (e.g., *Heliobolus spekii, Ichnotropis capensis*). All other species were considered mesic. The outgroup taxon to Lacertidae, *Rhineura floridana*, was retained for this analysis only for character polarity and scored as mesic, as its members inhabit tropical and semitropical regions of the world (Gans 2005). Although we recognize these categories as ecologically broad, species within arid and mesic biomes were shown to overlap morphologically in Chapter 2, indicating similar selective pressures despite differences in structural vegetation. Habitat assignments for each species are listed in Appendix 2.

To determine which traits are coupled with arid environments, we tested for evolutionary associations between osteological characters and habitat using Pagel's (1994) correlation method in Mesquite (Maddison and Maddison 2009). This method tests for the independent evolution of two binary characters by calculating the likelihood of models in which transition rates of each character are either dependent or independent

of the state of the other. The fit of each model to the observed data was compared using likelihood ratio tests, and the model of best fit was determined as that with a log likelihood at least two times greater than the chi-square variate with one degree of freedom (Pagel 1994). Following recommendations of Maddison and Maddison (2009) and Wiedenhoeft et al. (2008), one likelihood estimate and 500 replicates were implemented for each test. Osteological characters significantly associated with habitat type were reconstructed onto the phylogeny to look for patterns in the timing and sequence of morphological transitions. To identify potentially adaptive or functional character complexes, we further tested for evolutionary correlations among those traits using Pagel's correlation method as described above.

Estimation of diversification rates

Based on the complete time-calibrated phylogeny for Lacertidae, patterns of diversification were explored using likelihood methods in the Laser package of R (Rabosky 2006, R Development Core Team 2008). For all tests, we assumed a pure-birth model of diversification, as molecular phylogenies have been shown to give innacurate rates of extinction (Rabosky 2010, Simpson et al. 2011). First, patterns of species accumulation were visualized by constructing lineage-through-time plots for the entire family and for the major subclades separately. Under a constant evolutionary model (i.e. a pure-birth process with no extinction), species are expected to accumulate at a loglinear rate. Deviations from this pattern suggest historical rate variation, thus rejecting a model of constant diversification (Fordyce 2010). Second, net rates of diversification were estimated for the family and its subclades using discrete-shift methods. Within a given time interval, a truncated exponential distribution was fitted to the number of observed branching events and branch lengths (Nee et al. 1992, Nee 2001, Simpson et al. 2011). By "sliding" the time window from the root of the tree to the present, episodes of increasing

or decreasing diversification can be identified. This process was implemented by iterating the yuleWindow function in Laser (Rabosky 2006) over the timescale of Lacertidae, and estimating rates of diversification within a 5 My window for the family as a whole and 1.5 My window for each subclade. A minimum of one node within each time window is required for rate estimation, since the rate is calculated as the number of nodes divided by the sum of all branch lengths within that interval (Simpson et al. 2011).

Since incomplete sampling can affect phylogeny-based estimates of diversification (Brock et al. 2011), we also conducted a Monte Carlo Constant Rates (MCCR) test (Pybus and Harvey 2000) on our data set. The MCCR test is based on the gamma statistic (γ) of Pybus and Harvey (2000), which is commonly used to detect if a clade has undergone early or late diversification during its history (see McPeek 2008). The gamma statistic describes the distribution of branching times across the tree, following the assumption that clades have diversified at a constant rate. A negative gamma value indicates that the majority of branching events occurs early in the tree and decreases towards the present. A positive gamma values indicates that divergences are concentrated more towards the tips of the tree. To test if incomplete taxon sampling biases observed patterns of diversification in Lacertidae, we computed the gamma statistic for the entire family and compared it to a null distribution of gamma values for a set of randomly pruned trees. This was performed with a MCCR test of 5 000 repetitions and a clade size for Lacertidae of 305 species (www.lacerta.de). If the gamma value for the actual tree falls within the null distribution, we can reject the idea that random and incomplete sampling is driving observed patterns of divergence events.

The complete phylogenetic analysis from Chapter 2 resulted in a well supported tree topology for the major lineages (<0.95 posterior probabilities; Chapter 2, Appendix 4). Within the Eremiadini, two major groups correspond to distinct geographical regions: the Saharo-Eurasian clade in southern Europe, parts of the Middle East and Asia and northern Africa, and the Ethiopian (i.e. south of the Sahara) clade, with taxa in western, eastern and southern Africa. Evolutionary ages range from the mid-Eocene for the crown clade of Lacertidae to more recent splits in the Pliocene for members of *Tropidosaura* and *Gastropholis*. The African radiation as a whole is estimated to have arisen in the early Oligocene and split into its component clades 27-31 Mya. The majority of branching events occurs in the Miocene, when nearly all of the African genera arise.

Optimization of habitat type onto the phylogeny suggests that mesic habitat is the most likely ancestral state for lacertids, according to both ML and parsimony reconstructions (Figure 2). ML support for a mesic condition at the basal node of Lacertidae was 0.85, and for the two basal-most clades (Gallotini and Lacertini) was 0.98 and 0.79, respectively. All members of the Gallotinae and palearctic Lacertini retain the mesic condition, while a total of six transitions to arid habitat occur within the African Eremiadini. Within the Ethiopian clade, three independent shifts to arid habitat occur from the late Oligocene to early Miocene, 27-18 Mya. The earliest transition is seen in the predominantly east African group of *Nucras* and allies, followed by the southern African genera *Ichnotropis*, *Meroles* and *Pedioplanis*. Within the Saharo-Eurasian clade, three additional transitions to arid habitat are observed between the early Oligocene to late Miocene: *Eremias* and *Mesalina* 28 and 26 Mya respectively, and *Omanosaura* and *Acanthodactylus*, about 21 Mya (Figure 2). Although two genera in the Ethiopian clade

87

are paraphyletic (*Australolacerta* and *Ichnotropis*), modifying tree topology to enforce monophyly does not affect the overall pattern.

The evolution of several anatomical characters was also shown to be highly correlated with shifts to arid environments. Out of 19 osteological traits examined, 11 were significantly associated with habitat type according to Pagel's correlation test (Table 3). When the origins of those characters are mapped onto the phylogeny, several morphological trends can be observed (Figure 3). Common features of nearly all arid-dwelling African taxa include a depressed snout (1), complex septomaxilla (5), developed frontal processes (6), fused frontals (8), reduced supraocular osteoderms (12), a square-shaped parietal table (18) and thin frontals (19). Correlation tests among characters also revealed several evolutionary patterns. Out of 55 pairwise tests, 36 character pairs were significantly evolutionarily associated (Table 4). For example, characters (8) and (19), frontal fusion and thin frontals, are commonly gained in tandem in arid groups like the Saharo-Eurasian and south African *Meroles*/*Ichnotropis squamulosa* clades. In contrast, some features are regularly reversed in tandem in mesic-dwelling taxa, such as the condition of the premaxillary process (16) and nasal openings (17). No single trait evolved entirely independently, indicating possibly few origins of suites of correlated traits.

Patterns of diversification

Lineage-through-time plots for Lacertidae and its subclades show a steady increase in species accumulation over time, with a slowing towards the present (Figure 4). The palearctic Lacertini have a slightly steeper slope of increase than the African Eremiadini (Figure 4a), corresponding to higher diversification rates for sampled taxa. Within the African clade, rates of diversification between the Saharo-Eurasian and

Ethiopian clades are similar, with the radiation of the latter beginning approximately 3 My later but reaching a larger number of taxa (Figure 4b). The largest period of gain for the Ethiopian clade occurs within the early Miocene from 25 to 16 Mya. Net rates of diversification within each time window also show a general decrease in diversification towards the present (Figure 5). The family as a whole undergoes four major peaks of diversification, three of which occur in the Oligocene and one in the mid-Miocene (Figure 4a). Within the subclades of Lacertidae, the African Eremiadini begin with very high rates of diversification early in their radiation (late Oligocene), followed by two major peaks in the early and late Miocene (Figure 2b). Net diversification for the Ethiopian and Saharo-Eurasian clades is represented by steeply decreasing rates in the late Oligocene and late Miocene, respectively (Figure 2b). An overall decrease in net diversification rates towards the present was also supported by a negative gamma statistic (γ =-4.225235, p < 0.0001). When compared to gamma values calculated over the set of randomly pruned trees, the observed gamma still fell within the null distribution (critical γ =-4.796709), allowing us to reject the hypothesis that incomplete sampling biases diversification patterns of Lacertidae.

Patterns of diversification in Lacertidae exhibit some synergy with paleoclimatic events observed during the history of the Cenozoic (see Table 1, Figures 2, 5). The family as a whole arises in the early-middle Eocene, during a time of sustained warming conditions in Europe (Zachos et al. 2008). They experience a peak in diversification in the late Oligocene (26-28 Mya) as they radiate into the main African subclades. This also coincides with increasing aridity in Africa and a transition from closed and wet forests to open, arid grasslands (Janis 1993, Strömberg 2011). Although the family experiences an overall decline over the early Miocene, it peaks again just before the mid-Miocene Climatic Optimum, after which it steadily declines. However, the Eremiadini experience

89

another peak in the late Miocene (Figure 5), precisely at the time of the formation of the Benguela current along the southwestern African coast (Siesser 1980, Richardson et al. 2001).

Molecular estimates for the origin of Lacertidae and their component clades fall well within the Cenozoic, with the majority of their radiations occurring in the Oligocene and early Miocene (Figure 2). This pattern is also supported by the lacertid fossil record in Europe, which reaches back to the Palaeocene over 50 Mya (Estes 1983). Our estimated divergences for the palearctic and African clades are significantly older than in previous studies (e.g., Carranza et al. 2004, Arnold et al. 2007), all of which relied on a single molecular clock calibration based on a very young island formation (El Hierro Island, 1 Mya). The use of island ages to date endemic taxa has been shown be misleading in several studies (Buckley et al. 2009, Chapple et al. 2009, den Tex et al. 2010), as island endemics can be much older than their respective islands (for a review, see Heads 2011). We therefore find our estimated dates more reliable, as they are based on multiple independent fossil-derived calibrations and rigorous divergence dating methods (see Hipsley et al. 2009, Chapter 2).

Mesic origins of Lacertidae as suggested by ancestral state reconstruction are corroborated by the fossil record in Europe (Estes 1983) and current distribution of its basal most clade Gallotinae (*Gallotia + Psammodromus*; Arnold et al. 2007). A primitive mesic condition is also supported by the tropical and subtropical distribution of its outgroup, Amphisbaenia, here represented by the North American species *Rhineura floridana*. Although the sister relationship between lacertids and amphisbaenians has been contentious in the past, recent fossil evidence strongly links the two groups via

Cryptolacerta hassiaca from the Eocene Messel locality of Germany, which was then

subtropical rainforest (Müller et al. 2011). Given these independent lines of evidence, we

therefore consider the evolutionary shift to arid and xeric habitat in Lacertidae to be a

derived state. However, several taxa in the African radiation retain the plesiomorphic

condition, such as *Poromera* in restricted regions of West Africa and the equatorial forest

clade including *Adolfus*, *Congolacerta*, *Gastropholis*, and *Holaspis* (Figure 2).

Interestingly, these taxa also represent the most species poor genera of the entire radiation

(www.lacerta.de). Whether this is an artifact of poor taxon sampling or a result of

increased extinction in the past is difficult to discern, as so far we lack statistical methods

for reliably estimating extinction rates from molecular phylogenies alone (Rabosky 2010,

Simpson et al. 2011).

Our finding of multiple independent radiations into arid habitat rejects previous

morphology-based hypotheses of a monophyletic trend towards xeric forms (Arnold

1989a, 2004). Evolutionary shifts to arid habitat were also accompanied by a suite of

cranial traits (Table 3, Figure 3). These species are generally characterized as having a

dorsoventally flattened snout with large, dorsally exposed nasal openings, a well

developed anterior projection of the septomaxilla and a long, slender nasal process of the

premaxilla, thin, hourglass shaped fused frontals with well developed anterior descending

processes, reduced or fenestrated supraocular osteoderms, a square-shaped parietal not

extending over the supraoccipital, and a well developed quadratojugal process of the

jugal bone.

Correlated patterns of loss and gain in arid-dwelling lacertids are also strong

indicators of functional and/or adaptive relationships among traits. Over half of the traits

significantly associated with shifts to arid habitat were also highly correlated with each

other (Table 4), providing evidence for coadapted character complexes in response to arid lifestyles. For example, Arnold (1989a) suggested that lacertids evolve larger eyes as an adaptation for visual acuity in deserts, thus narrowing the inter-orbital area. Fusion of the frontal bones would therefore counteract the resulting weakness, as would interdigitating cranial bones. Well developed frontal processes embracing the maxillae may also funtion in this sense, to increase strength in the snout. A general lightening of the skull, as seen in features like the reduction of supraocular osteoderms and extent of the parietal table, may also be related to external characteristics typical of arid forms. In Chapter 2, we showed that lacertids in arid environments tended to have short bodies with relatively long hindlimbs and robust (deep and wide) heads. Taken together, many of these osteological and external features produce a paedomorphic appearance resembling juveniles from the palearctic clade (pers. obs., Arnold 1989a, Barahona & Barbadillo 1998). If arid-dwelling lacertids indeed experience shortened life histories, as suggested by the annual life cycle of some desert species (Branch 1998), then such juvenile characteristics may be the result of changes in developmental timing (i.e. heterochrony) leading to allometric growth (see McKinney and McNamara 1991, Klingenberg 1998).

Heterochrony in response to extreme environmental conditions is well known in modern groups such as frogs and salamanders (Emerson 1986, Collins et al. 1993, Denöel et al. 2005, Tejedo et al. 2010), and has also been documented in the fossil record in relation to climate change (Roček 1995). Increasing aridification of Africa since the Cenozoic may therefore drive morphological evolution in Eremiadini by inducing heterochronic transformations. At the same time, desertification would have been a strong selective force on new variants, leading to the extinction of some species and rapid speciation of others through shortened generation times. This would explain the generally longer branch lengths of the African taxa compared to their sister group Lacertini (Arnold

et al. 2007), as well as changes in many morphological traits in conjuction with shifts to arid habitat.

Patterns of diversification estimated from the molecular phylogeny support the impacts of historical climate change on lacertid evolution. Both species accumulation and net rates of diversification show that the Oligocene was an important time for lacertid radiations in Africa. The Oligocene is often considered a significant period of transition for many fauna, representing a link between the tropical world of the Eocene and the more modern cool and dry ecosystems of the Miocene (Prothero 1993). Increases in diversification around this time have been reported in other African groups such as birds (Fuchs et al. 2006), mammals (Kappelman et al. 2003) and even lizards (Cordylidae; Stanley et al. 2011). Relatively high temperatures and low precipitation towards the late Oligocene promoted the expansion of grasslands and shrinking of tropical forests in Africa (Lunt et al. 2007, Strömberg 2011), creating new habitats where niches were available. This scenario generally follows Arnold's (1981) speciation model for desert lacertids, in which fluctuating climatic conditions and increasing aridification triggered rapid diversification through repeated bouts of habitat fragmentation and ecological displacement. Indeed, Eremiadini and the Ethiopian radiation experience their highest diversification rates in the early Miocene leading up to the mid-Miocene Climatic Optimum (Figure 5b), when temperatures reached the highest levels of the Neogene (Flowers and Kennett 1994).

Significant shifts in habitat and morphology in African lacertids are also seen in the late Oligocene-early Miocene, leading to the appearance of several derived traits in arid-dwelling taxa (Figures 3-4). Although we lack the fossil evidence to directly place lacertids in Africa at this time, the appearance of nearly a dozen traits coinciding with

shifts to arid habitat strongly suggests taxonomic and morphological diversification occurred together with increasing aridification. The second peak for African lacertids in the late Miocene 9-11 Mya also coincides with the formation of the Benguela current, responsible for the extreme xeric conditions and unique coastal fog belts of the Namib Desert (Siesser 1980). The extension of the Benguela current along the Namib coast has also been linked to rapid radiations of its many endemic taxa, including plants, arachnids, insects, amphibians and other reptiles (Simmons et al. 1998, Steckel et al. 2010). Interestingly, the progressive aridification and seasonality of this period may have also led to increased extinction and restricted distributions of forest-dwelling chameleons in southern Africa, as suggested by the long branches observed in these lineages and lack of extant sister species (Tolley et al. 2008).

In addition to increasing diversification related to historical climate, lacertid lizards also show a general decline in rates towards the present (Figures 4-5). This pattern is a common feature of adaptive radiations and is also predicted under scenarios of morphological innovation (Foote 1997, Schluter 2000, Losos and Miles 2002, Harmon et al. 2003). However, since we are currently unable to untangle the effects of speciation and extinction with molecular data alone, it is difficult to interpret slowing rates in light of climatic or evolutionary events. Neverthless, the link between evolution and historical climate as seen in this and other groups (e.g., Delsuc et al. 2004, Weir and Schluter 2004, Egan and Crandall 2008, Tolley et al. 2008) emphasizes the potential influences of current and future climate change on biodiversity. Evolutionary responses to current global climate change have already been witnessed in a number of taxa, including birds, insects and plants (Parmesan and Yohe 2003). The common assumption for reptiles, and especially lizards, is that they will be relatively invulnerable to global warming as they are already tolerate extreme climatic conditions and can conform to ambient temperatures

(Huey and Pianka 1977, Bauwens et al. 1996, Kearney et al. 2009). However, Sinervo et al. (2010) recently showed widespread extinction in 34 families of lizards and predicted that nearly one-fourth of lizard species would go extinct according to global climate models for the year 2080. So while arid regions appear to be important centers of reptile evolution, expected changes in global climate may exceed the abilities of arid-dwelling lizards to adapt and persist.

TABLE 1. Paleoclimatic events in the Cenozoic with potential effects on African biota. Epoch intervals follow the International Commission on Stratigraphy's International Stratigraphic Chart (2010).

Epoch	Time (Mya)	Event	Climatic effects	References
Pleistocene	2.5-0.01	Pleistocene glaciation	Fluctuating glaciation, increases in African climate variability and aridity leading to more varied and open habitat	de Menocal 2004
Pliocene	3	Pliocene-Pleistocene boundary	Global cooling and drying, expansion of savanna and warm-temperate forests in Africa	Blois and Hadly 2009, Salzmann et al. 2009
Miocene	7	Formation of the Sahara Desert	Onset of recurrent desert conditions in the Sahara followed by numerous wet and dry periods, culminating in the present desert conditions 4k years ago	Schuster et al. 2006
	10	Development of Benguela current	Increased glaciation in Antarctica leading to cold upwelling along the west African coast, intensified aridity in the Namib Desert and fynbos regions of South Africa	Siesser 1980, Richardson et al. 2001
	14	Middle Miocene extinction	Wave of extinctions of terrestrial and aquatic life following a major cooling period 14.8-14.1 Mya	Böhme 2003
	17-15	Mid-Miocene Climatic Optimum	Increased seasonality, aridification of mid-latitude continental regions including Africa	Retallack 1992, Flowers and Kennett 1994
	23	Mi-1 glaciation	Brief but intense glacial maximum following preceding interval of extreme global warmth in the late Oligocene	Naish and Carter 2003
Oligocene	28-23	Late Oligocene	Global expansion of grasslands and regression of tropical broad leaf forests to the equator, appearance of herbivorous megafauna in Africa	Janis 1993, Strömberg 2011
	34	Oi-1 glaciation	Substantial deep-sea cooling and development of Antarctic ice sheet followed by 400k years of glaciation	Lear et al. 2004
Eocene	35	End Eocene Climatic Optimum (EndECO)	Rapid cooling and sea level decline, Antarctica reaches present position causing cold upwelling, continental interiors dry, forests shrink, grasses begin to expand	Zachos et al. 2008
	40	Middle Eocene Climatic Optimum (MECO)	Significant reversal of mid-Eocene cooling trend, over 4°C increase over 600k years	Bohaty and Zachos 2003
	53-49	Early Eocene Climatic Optimum (EECO)	Global temperatures reach a long-term maximum for the Cenozoic, followed by sustained warming conditions	Zachos et al. 2008

TABLE 2. Osteological characters used in ancestral state reconstructions of Lacertidae, based on Arnold (1983, 1989a, b, 1991) and Arnold et al. (2007).

Char No.	Character description
1	*Angle of snout*. Less than 45° (0); greater than 45° (1)
2	*Number of premaxillary teeth*. 7 (0); more than 7 (1)
3	*Pterygoid teeth*. Absent (0); present (1)
4	*Dorsal skull surface*. Smooth (0); rugose (1)
5	*Anterior projection of septomaxilla*. Slight or absent (0); distinct (1)
6	*Anterior descending process of frontal bone*. Reduced or absent (0); present and well developed (1)
7	*Frontoparietal suture*. Simple (0); complex (1)
8	*Frontal bones*. Separate (0); fused (1)
9	*Postfrontal and postorbital bones*. Separate (0); fused (1)
10	*Pineal fontanelle*. Absent (0); present (1)
11	*Ossification of temporal scales*. Little or none (0); extensive (1)
12	*Supraocular osteoderms*. Medial fringe or fenestrated, reduced (0); complete (1)
13	*Quadrato-jugal process on jugal bone*. Absent (0); present (1)
14	Parietal and squamosal bones. Not contacting (0); contacting (1)
15	*Dorsoanterior portion of supraoccipital*. Visible in dorsal view (0); covered by parietal (1)
16	*Nasal process of premaxilla*. Broad and short (0); slender and long (1)
17	*Nasal opening of skull*. Small, anteriorly exposed (0); large, dorsally exposed (1)
18	*Parietal table*. Square shaped, or more wide than long (0); anteroposteriorly elongated, longer than wide (1)
19	*Frontal bones*. Hourglass shaped in dorsal view, pinched between the orbits (0); lateral walls forming straight lines in dorsal view, not pinched between the orbits (1)

TABLE 3. Results of Pagel's (1994) correlation analyses of osteological characters and habitat type for Lacertidae. A significant correlation (indicated in bold) indicates dependence of evolutionary transitions in morphology on ancestral habitat type (arid or mesic). Character numbers and states match those in Table 2. The derived state of characters undergoing transitions with shifts in habitat was determined from the ML and parsimony reconstructions.

Character description	Char No.	p-value	arid state	arid condition
angle of snout	1	**0.02**	0	<45°
premaxillary teeth	2	0.162		
pterygoid teeth	3	0.254		
dorsal skull surface	4	0.204		
septomaxilla projection	5	**0.03**	1	distinct
frontal process	6	**0.02**	1	well developed
frontoparietal suture	7	0.076		
frontal bones	8	**0.018**	1	fused
postorbital and postfrontal bones	9	1		
pineal fontanelle	10	0.22		
temporal osteoderms	11	0.319		
supraocular osteoderms	12	**<0.001**	0	reduced or fenestrated
jugal process	13	**0.002**	1	present
parietal and squamosal bones	14	0.052		
dorsoanterior supraoccipital	15	**0.046**	0	visible in dorsal view
nasal process of premaxilla	16	**0.012**	1	slender, long
nasal opening of skull	17	**0.006**	1	large, dorsally exposed
parietal table	18	**0.002**	0	square or wide
frontals thickness	19	**0.01**	0	hourglass-shaped

TABLE 4. Results of Pagel's (1994) correlation analyses of osteological characters. A significant correlation (indicated in bold) indicates dependence of evolutionary transitions in one character on the ancestral state of the other character at that node. Character numbers match those in Table 2.

Char. No.	1	5	6	8	12	13	15	16	17	18	19
1	-	0.4	**0.03**	**0.02**	**<0.001**	0.052	**0.040**	**0.020**	**<0.001**	0.05	**<0.001**
5		-	**0.04**	0.06	0.6	0.52	0.64	0.49	0.11	**0.03**	0.33
6			-	**<0.001**	0.05	**0.044**	**0.030**	**<0.001**	**<0.001**	**<0.001**	**<0.001**
8				-	**<0.001**	**<0.001**	**0.040**	0.07	**<0.001**	**<0.001**	**<0.001**
12					-	**<0.001**	**<0.001**	**0.010**	**0.02**	0.52	**<0.001**
13						-	**0.010**	**0.040**	**0.04**	0.7	**<0.001**
15							-	0.71	0.15	**0.020**	0.26
16								-	**<0.001**	0.11	**0.01**
17									-	0.05	**<0.001**
18										-	**0.002**
19											-

FIGURE 1. X-ray computed tomographic rendered skulls of a) the mesic-dwelling palearctic lacertid *Podarcis muralis*, with principal dorsal bones labeled, and b) the arid-dwelling north African lacertid *Acanthodactylus boskianus*, showing common derived features. Figure modeled after Arnold (1989a).
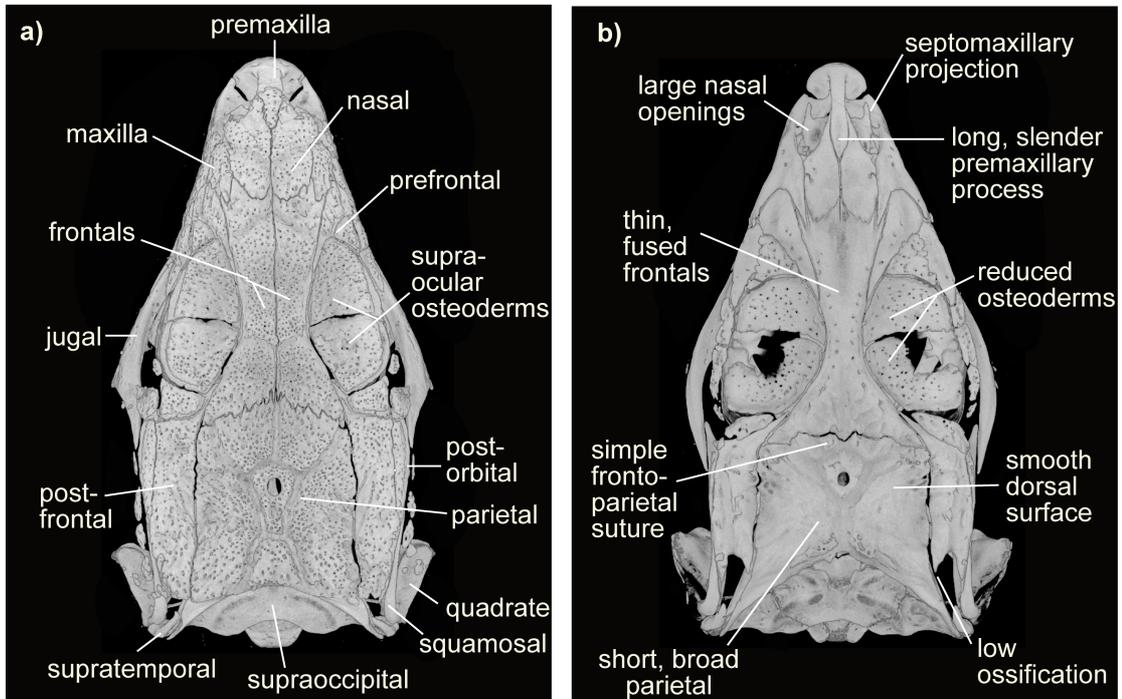
FIGURE 2. Time-calibrated Bayesian phylogeny for Lacertidae based on 1012 bp of the nuclear gene *RAG-1*. Branch colors represent habitat optimizations based on parsimony, with maximum likelihood estimates indicated by pie charts at each node. Habitat type was characterized for terminal taxa as mesic (green) or arid (blue). Vertical gray bands in this and subsequent figures denote geologic sub-epochs, abbreviated as early (E), middle (M) and late (L). The amphisbaenian *Rhineura floridana* was used as outgroup to Lacertidae and scored as mesic in ancestral state reconstructions, although it is not shown here.
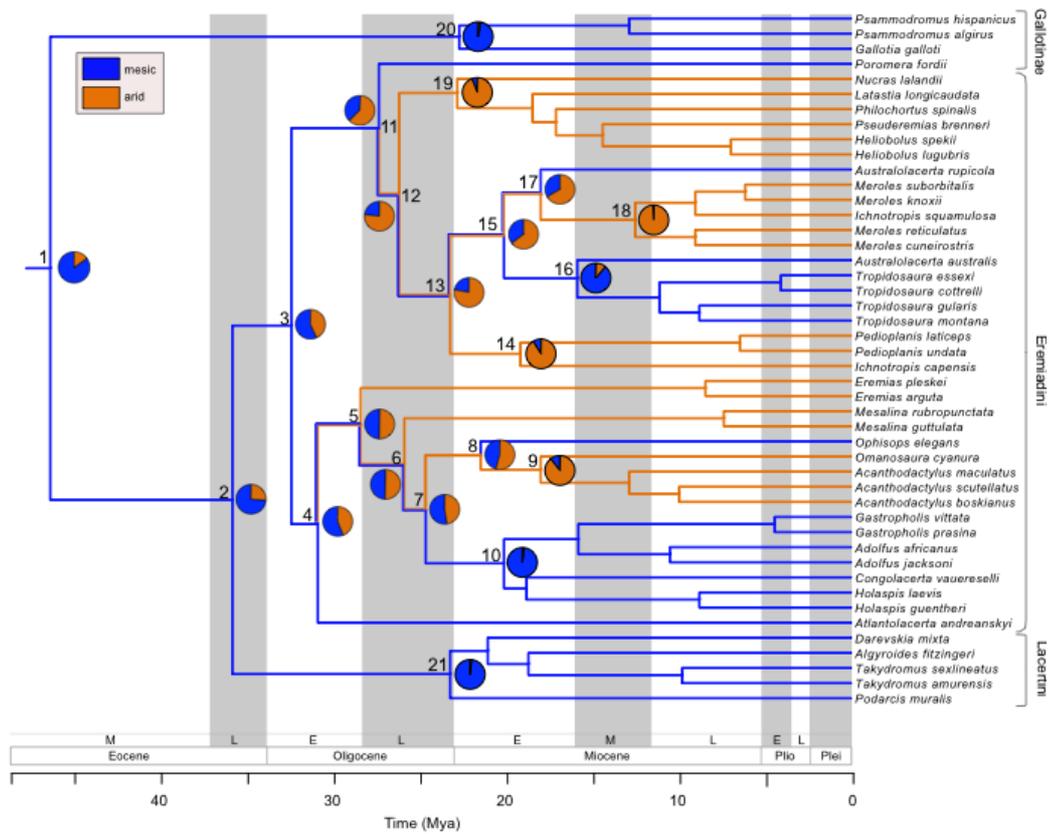
FIGURE 3. Ancestral character state reconstructions of osteological cranial characters found to be significantly correlated with transitions to arid habitat. Locations of gains and losses in character states are placed according to maximum parsimony. Characters are listed in Table 3.
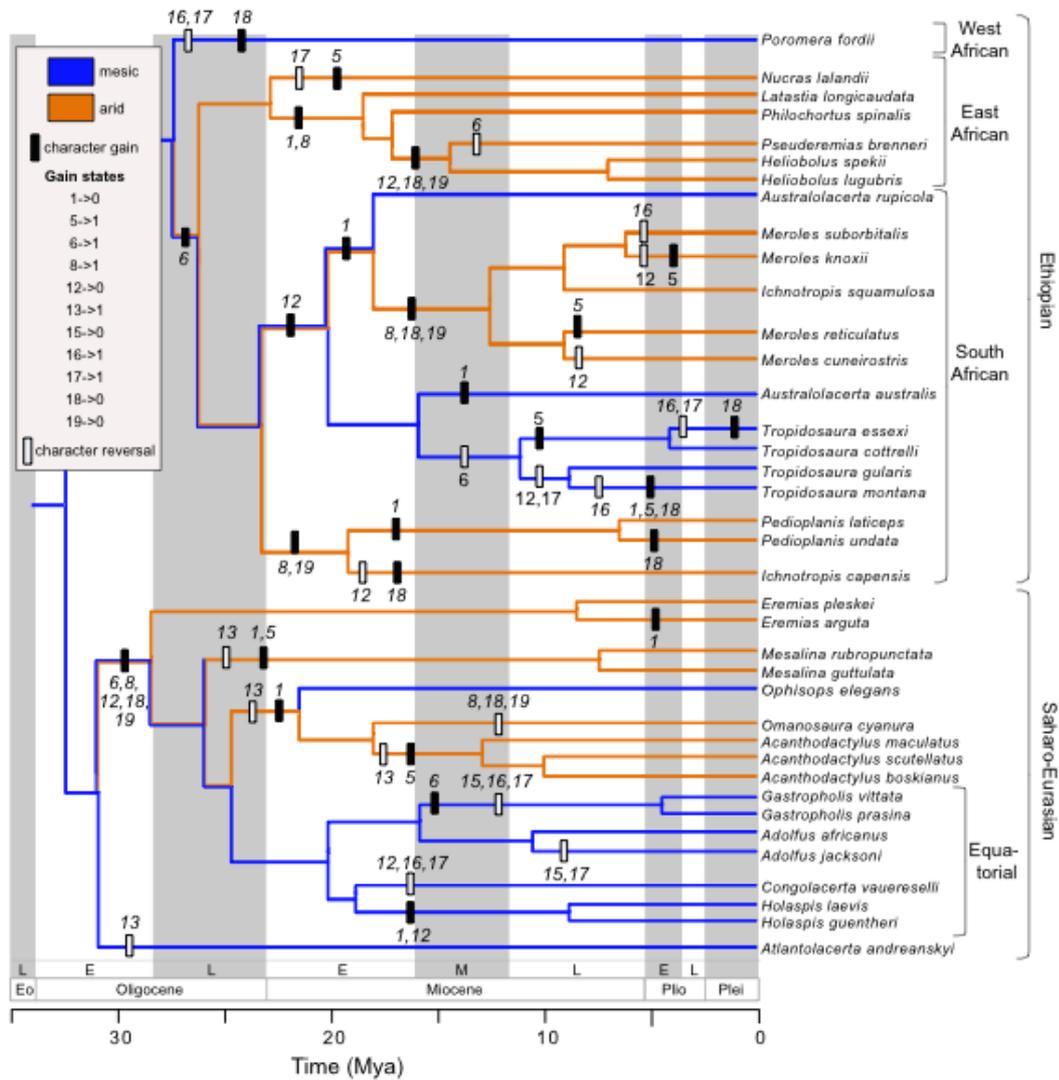
FIGURE 4. Lineage-through-time plots for a) the family Lacertidae and two of its main clades, and b) the African subclade Eremiadini, split into its component groups.
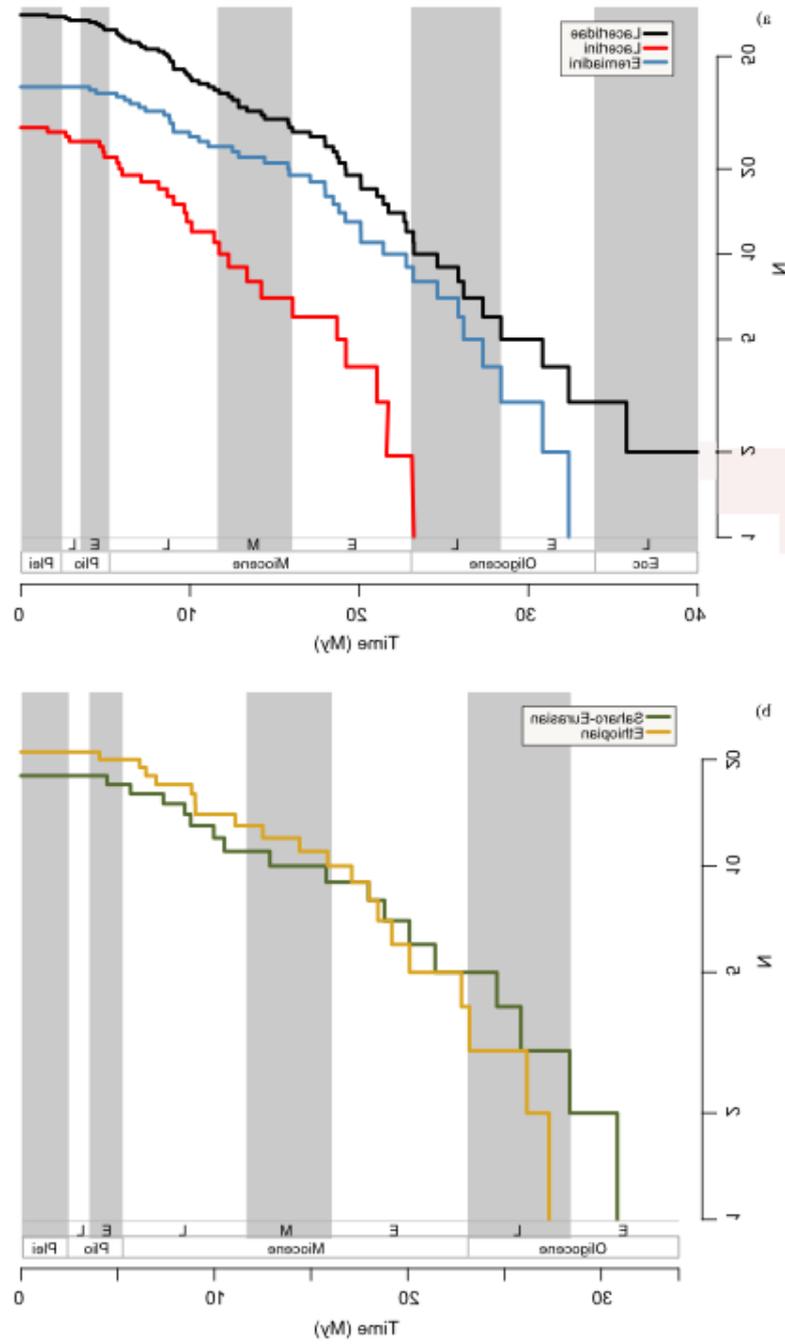
FIGURE 5. Net rate of diversification estimated from the molecular phylogeny for a) Lacertidae and b) its subclades.
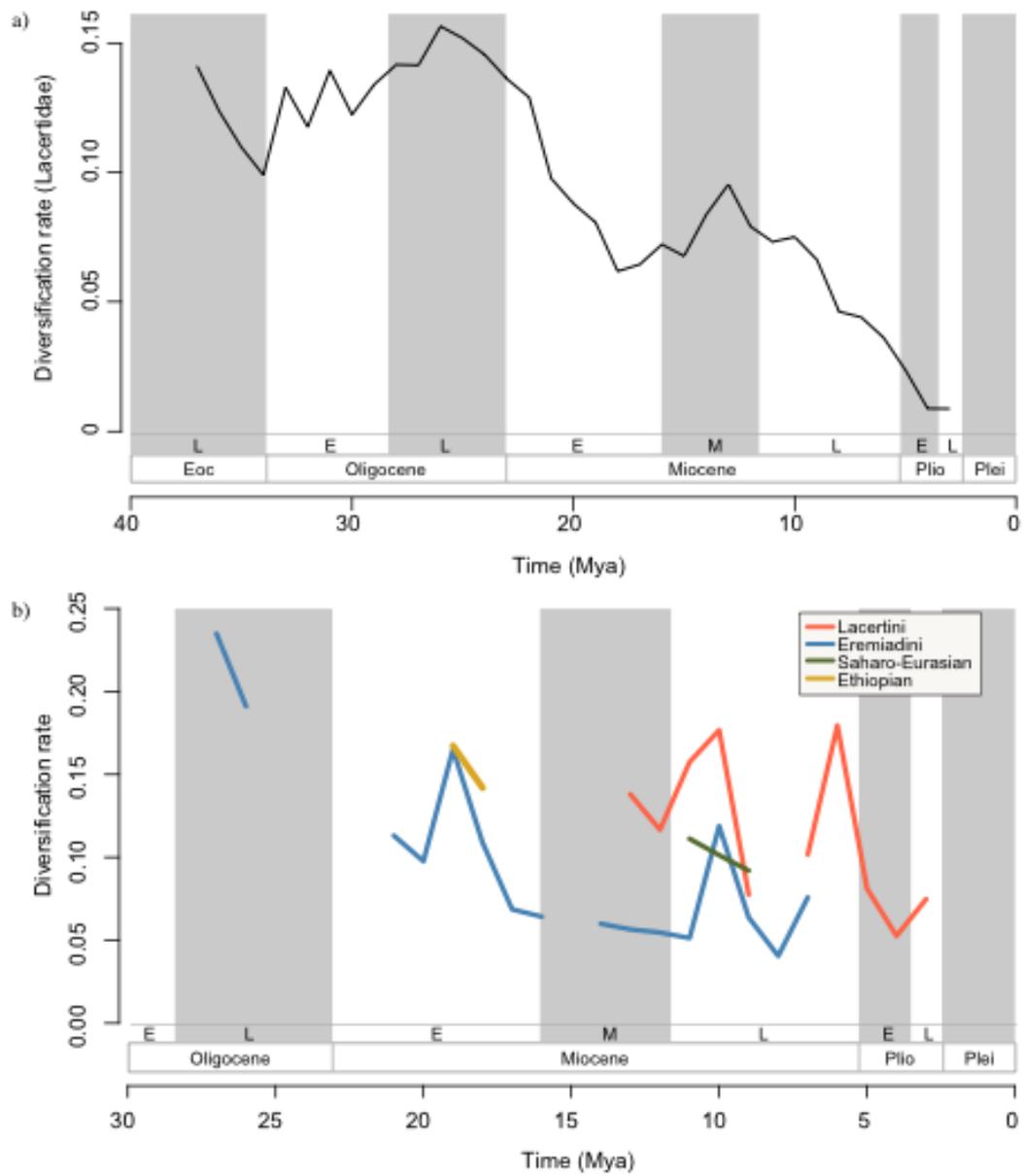
APPENDIX 1. Taxon sampling and catalogue numbers of museum specimens scored for osteological characters based on CT. ZMB=Museum für Naturkunde Berlin, Germany; ZFMK=Zoologisches Forschungsmuseum Alexander Koenig, Bonn, Germany; private=private collector or breeder.

Acanthodactylus boskianus ZMB 70859; *Acanthodactylus maculatus* ZMB 14877; *Acanthodactylus scutellatus* ZMB 13743, private; *Adolfus africanus* ZFMK 5804, ZFMK 41093, ZFMK 81207, ZFMK 88168; *Adolfus jacksoni* ZMB 48254, ZFMK 66637, ZFMK 71724, ZFMK 90516; *Algyroides fitzingeri* private; *Atlantolacerta andreanskyi* ZFMK 8751; *Australolacerta australis* private; *Australolacerta rupicola* private; *Congolacerta vauereselli* ZMB 26834, ZFMK 57597, ZFMK 58683; *Darevskia mixta* ZMB 44582, ZMB 44583; *Eremias arguta* ZMB 37830; *Eremias pleskei* ZMB 43016; *Gallotia galloti* ZMB 955; *Gastropholis prasina* ZMB 18087; *Gastropholis vittata* ZMB 74300; *Heliobolus lugubris* ZMB 7774; *Heliobolus spekii* ZMB 48327; *Holaspis guentheri* ZMB 11119, ZMB 13689; *Holaspis laevis* ZMB 19648, ZMB 22462; *Ichnotropis capensis* ZMB 15564, ZMB 25829; *Ichnotropis squamulosa* ZMB 6615, ZMB 53011; *Latastia longicaudata* ZMB 22443, ZMB 74545; *Meroles cuneirostris* ZMB 26757, ZMB 31319; *Meroles knoxii* ZMB 25512; *Meroles reticulatus* ZMB 25531; *Meroles suborbitalis* ZMB 25527, ZMB 6731; *Mesalina guttulata* ZMB 15306; *Mesalina rubropunctata* ZMB 18327, ZMB 77682; *Nucras lalandii* ZMB 23913; *Omanosaura cyanura* private, private; *Ophisops elegans* ZMB 38775; *Pedioplanis laticeps* ZMB 23443; *Pedioplanis undata* ZMB 18330; *Philochortus spinalis* ZMB 10270; *Podarcis muralis* ZMB 73919; *Poromera fordii* ZMB 15526; *Psammodromus algirus* ZMB 26522; *Psammodromus hispanicus* ZMB 6352; *Pseuderemias brenneri* ZMB 6443; *Takydromus amurensis* ZMB 9869; *Takydromus sexlineatus* ZMB 69327; *Tropidosaura cottrelli* private; *Tropidosaura essexi* private, private, private; *Tropidosaura gularis* private; *Tropidosaura montana* private

APPENDIX 2. Description of osteological characters listed in Table 2, based on morphological analyses of Arnold (1983, 1989a, b, 1991) and Arnold et al. (2007).

1. *Angle of snout*. Less than 45° (0); greater than 45° (1). As in indicator of the degree of dorsoventral flattening of the skull, the angle of the snout in lateral view from the ventral edge of the maxilla along the dorsal surface of the premaxilla and frontals was measured. Species with shovel or wedge-shaped snouts have a sharp angle (<45°), while those with rounded snouts have an angle far greater than 45°.

2. *Number of premaxillary teeth*. 7 (0); 9 or more (1). The premaxilla of adult lacertids typically bears seven to nine teeth with single cusps, occasionally reaching ten in some species. Tooth number usually increases with age and body size, so juveniles and smaller animals may have lower counts than large adults.

3. *Pterygoid teeth*. Absent (0); present (1). Additional teeth may be present on the pterygoid bones in some species.

4. *Dorsal skull surface*. Smooth (0); rugose (1). The layer of osteoderms covering the dorsal bones of the skull (crusta calcarea) may be thick and well developed in some species, or appear relatively thin and smooth in others.

5. *Anterior projection of septomaxilla*. Slight or absent (0); distinct (1). The septomaxilla may have a simple anterior shelf with at most a slight anterior projection or none at all, or have a distinct and often narrow and pointed anterior projection.

6. *Anterior descending process of frontal bone*. Reduced or absent (0); present and well developed (1). The frontals may be bifurcated anteriorly by the posterodorsal process of the maxilla, forming a narrow process in continuous contact with the prefrontal, or remain relatively straight medial to the maxilla and prefrontal with little to now descending process.

7. *Frontoparietal suture*. Simple (0); complex (1). In dorsal view, the anterior edge of the parietal bone may be relatively straight or slightly bow shaped with a small concavity near the midline and only weakly or not at all interdigitating with the frontal bones, or convex and strongly interdigitating with the frontals.

8. *Frontal bones*. Separate (0); fused (1). The frontals may be completely fused in adults or at least largely so in juveniles, or remain separate and pared throughout life.

9. *Postfrontal and postorbital bones*. Separate (0); fused (1). The postfrontal and postorbital bones are usually separate in hatchlings, but may become fused during life, or at least tightly joined and covered by a layer of osteoderms. The latter case was confirmed by cross section in CT.

10. *Pineal fontanelle*. Absent (0); present (1). A pineal fontanelle or window may be variable in presence and size in the parietal bone.

11. *Ossification of temporal scales*. Little or none (0); extensive (1). The temporal scales on the side of the head which cover the main adductor jaw muscles are typically unossifed but may contain osteoderms in some species.

12. *Supraocular osteoderms*. Medial fringe or fenestrated, reduced (0); complete (1). The series of four separate osteoderms in the skin above the eye (the supraocular osteoderms) frequently ossify completely by maturity, but can remain incomplete in the adult form, leaving a fenestra in which the skin remains flexible, or form only a slight fringe along the dorsal edge of the orbit.

13. *Quadratojugal process on jugal bone*. Absent (0); present (1). In lateral view, the jugal may bifurcate posteriorly and extend along the ventral margin in a posteriorly directed quadratojugal process, which can be distinct or very reduced or absent.

14. *Parietal and squamosal bones*. Not contacting (0); contacting (1). The squamosal may be separated posterolaterally from the supratemporal process of the parietal by the supratemporal bone, or be in contact with the parietal.

15. *Dorsoanterior portion of supraoccipital*. Visible in dorsal view (0); covered by parietal (1). The dorsoanterior portion of the supraoccipital may be visible in dorsal view, leaving a gap at the midline posterior to the parietal table, or the parietal bone may project backwards covering most or all of the supraoccipital.

16. *Nasal process of premaxilla*. Broad and short (0); slender and long (1). The nasal process of the premaxilla is typically long and slender, bifurcating the nasal bones up to half of their length, or be short and broad, reaching only a small portion (<1/3) of the nasal length.

17. *Nasal opening of skull*. Small, anteriorly exposed (0); large, dorsally exposed (1). The nasal openings may be small and exposed only anteriorly, or large and exposed predominantly on the dorsal surface of the skull.

18. *Parietal table*. Square shaped, or more wide than long (0); anteroposteriorly elongated, longer than wide (1). The parietal bone (excluding the supratemporal processes) of some species is shifted posteriorly, forming a table that is square or wider than long in dorsal view, or cover the majority of the postorbital surface of the skull, being more long than wide.

19. *Frontal bones*. Hourglass shaped in dorsal view, pinched between the orbits (0); lateral walls forming straight lines in dorsal view, not pinched between the orbits (1). The frontal bones of some species become extremely narrow between the orbits, forming an hourglass shape in dorsal view, or remain relatively straight along the lateral walls as they extend posteriorly across the orbits.

APPENDIX 3. Character distributions and habitat assignments used in ancestral state reconstructions of Lacertidae. Character numbering matches that in Table 2.

Taxon	1	2	3	4	5	6	7	8	9	10	11	12	13	14	15	16	17	18	19	Habitat
Acanthodactylus boskianus	0	0	0	0	1	1	0	1	0	1	0	0	0	0	0	1	1	0	0	arid
Acanthodactylus maculatus	0	0	0	0	1	1	0	1	0	1	0	0	0	0	0	1	1	0	0	arid
Acanthodactylus scutellatus	0	0	0	0	1	1	0	1	0	1	0	0	0	0	0	1	1	0	0	arid
Adolfus africanus	1	1	1	0	0	0	0	0	1	0	0	1	1	0	0	1	1	1	1	mesic
Adolfus jacksoni	1	1	0	1	0	0	1	0	0	0	1	1	1	0	1	1	0	1	1	mesic
Algyroides fitzingeri	0	1	0	0	0	0	0	0	0	1	0	0	1	0	0	1	0	1	1	mesic
Atlantolacerta andreanskyi	1	0	0	0	0	0	1	0	0	1	0	1	0	0	0	1	1	1	1	mesic
Australolacerta australis	0	0	0	0	0	1	0	0	0	1	0	0	1	0	0	1	1	1	1	mesic
Australolacerta rupicola	0	1	0	0	0	1	0	0	0	1	0	0	1	0	0	1	1	1	1	mesic
Congolacerta vaureselli	1	1	0	0	0	0	1	0	1	0	0	1	1	0	0	0	0	0	1	mesic
Darevskia mixta	1	0	0	0	0	1	1	0	0	1	0	0	1	0	0	1	1	1	1	mesic
Eremias arguta	0	0	1	0	0	1	1	1	1	1	0	0	1	0	0	1	1	0	0	arid
Eremias pleskei	1	0	0	0	0	1	0	1	1	1	0	0	1	0	0	1	1	0	0	arid
Gallotia galloti	1	0	1	0	1	1	0	0	1	1	0	1	1	0	1	1	1	1	1	mesic
Gastropholis prasina	1	1	1	1	0	1	1	0	1	0	1	1	1	1	1	1	0	1	1	mesic
Gastropholis vittata	1	1	1	1	0	1	1	0	1	0	1	1	1	1	1	1	0	1	1	mesic
Heliobolus lugubris	0	1	0	0	0	1	0	1	0	1	0	0	1	1	0	1	1	0	0	arid
Heliobolus spekii	0	1	0	0	0	1	0	1	0	1	0	0	1	1	0	1	1	0	0	arid
Holaspis guentheri	0	1	0	0	0	0	0	0	0	0	0	0	0	0	0	1	1	1	1	mesic
Holaspis laevis	0	1	0	0	0	0	0	0	0	0	0	0	0	0	0	1	1	1	1	mesic
Ichnotropis capensis	1	1	1	0	1	1	0	1	1	1	0	1	1	1	0	1	1	0	0	arid
Ichnotropis squamulosa	0	1	1	0	0	1	0	1	1	1	0	0	1	1	0	1	1	0	0	arid
Latastia longicaudata	1	1	0	0	1	1	1	1	0	1	1	1	1	1	0	1	1	1	1	arid
Meroles cuneirostris	0	1	1	0	0	1	0	1	1	1	0	1	1	1	0	1	1	0	0	arid
Meroles knoxii	0	0	0	0	1	1	0	1	1	1	0	1	1	1	0	1	1	0	0	arid
Meroles reticulatus	0	0	1	0	1	1	0	1	1	1	0	0	1	0	0	1	1	0	0	arid
Meroles suborbitalis	0	0	1	0	0	1	0	1	1	1	0	0	1	0	0	0	1	0	0	arid
Mesalina guttulata	0	0	0	0	1	1	0	1	0	1	0	0	0	0	0	1	1	0	0	arid
Mesalina rubropunctata	0	0	0	0	1	1	0	1	0	1	0	0	0	0	0	1	1	0	0	arid
Nucras lalandii	1	0	1	1	0	1	1	0	0	0	0	1	1	1	0	1	0	1	1	arid
Omanosaura cyanura	0	0	0	0	0	1	1	0	0	1	0	0	0	0	0	1	1	1	1	arid
Ophisops elegans	0	1	0	0	0	1	0	1	0	1	0	0	0	1	0	1	1	0	0	mesic
Pedioplanis laticeps	0	1	0	0	0	1	0	1	0	1	0	0	1	1	0	1	1	1	0	arid
Pedioplanis undata	0	1	0	0	0	1	0	1	0	1	0	0	1	1	0	1	1	0	0	arid
Philochortus spinalis	0	0	1	0	0	0	0	1	1	0	0	1	1	1	0	1	1	0	1	arid
Podarcis muralis	1	0	1	1	0	0	1	0	0	1	0	1	1	0	1	0	0	1	1	mesic
Poromera fordii	1	1	0	0	0	0	0	0	1	1	0	1	1	1	0	0	0	0	1	mesic

Psammodromus algirus	1	1	1	0	1	1	1	0	1	1	1	1	1	0	0	0	0	0	1	mesic
Psammodromus hispanicus	1	0	0	0	1	1	1	1	1	1	1	1	1	0	0	1	1	0	1	mesic
Pseuderemias brenneri	0	1	0	0	0	1	0	1	0	1	0	0	1	1	0	1	1	0	0	arid
Takydromus amurensis	1	1	0	0	0	0	0	0	1	1	0	1	1	1	0	0	0	1	1	mesic
Takydromus sexlineatus	1	1	0	0	0	1	1	0	1	1	0	1	1	0	0	0	0	1	1	mesic
Tropidosaura cottrelli	1	1	0	0	1	0	1	0	0	1	0	0	1	0	0	1	1	1	1	mesic
Tropidosaura essexi	1	1	0	0	1	0	1	0	0	1	0	0	1	0	0	0	0	0	1	mesic
Tropidosaura gularis	1	1	0	0	0	0	1	0	0	1	0	1	1	0	0	1	0	1	1	mesic
Tropidosaura montana	0	1	0	0	1	0	1	0	0	1	0	1	1	0	0	0	0	0	1	mesic

LITERATURE CITED

Aerts, P., D'Aout, K., Herrel, A. and R. Van Damme. 2002. Topics in Functional and Ecological Vertebrate Morphology. Shaker, Maastricht.

Ahmadzadeh, F., Carretero, M. A., Harris, D. J., Perera, A. and W. Böhme. 2012. A molecular phylogeny of the eastern group of ocellated lizard genus *Timon* (Sauria: Lacertidae) based on mitochondrial and nuclear DNA sequences. Amphibia-Reptilia 33:1-10.

Alfaro, M. E., Santini, F., Brock, C., Alamillo, H., Dornburg, A., Rabosky, D. L., Carnevale, G. and L. J. Harmon. 2009. Nine exceptional radiations plus high turnover explain species diversity in jawed vertebrates. Proceedings of the National Academy of Sciences USA 106:13410–13414.

Anderson, F. E. and D. L. Swofford. 2004. Should we be worried about long-branch attraction in real data sets? Investigations using metazoan 18S rDNA. Molecular Phylogenetics and Evolution 33:440-451.

Arnold, E. N. 1973. Relationships of the Palaearctic lizards assigned to the genera *Lacerta*, *Algyroides* and *Psammodromus* (Reptilia: Lacertidae). Bulletin of the British Museum (Natural History) Zoology 29:289-366.

Arnold, E. N. 1981. Competition, evolutionary change and montane distributions. Pp. 217-228 *in* P. L. Forey, ed. The Evolving Biosphere. British Museum (Natural History) and Cambridge University Press, London.

Arnold, E. N. 1983. Osteology, genitalia and the relationships of *Acanthodactylus* (Reptilia: Lacertidae). Bulletin of the British Museum (Natural History) 44:291-339.

Arnold, E. N. 1986. The hemipenis of lacertid lizards (Reptilia: Lacertidae): structure, variation and systematic implications. Journal of Natural History 20:1221-1257.

Arnold, E. N. 1989a. Towards a phylogeny and biogeography of the Lacertidae: relationships within an Old-world family of lizards derived from morphology. Bulletin of the British Museum, London (Zoology) 55:209–257.

Arnold, E. N. 1989b. Systematics and adaptive radiation of equatorial African lizards assigned to the genera *Adolfus*, *Bedriagaia*, *Gastropholis*, *Holaspis* and *Lacerta* (Reptilia: Lacertidae). Journal of Natural History 23:525-555.

Arnold, E. N. 1991. Relationships and evolution of the South African lacertids assigned to *Aporosaura*, *Meroles* and *Pedioplanis* (Reptilia: Lacertidae). Journal of Natural History 25:783–807

Arnold, E. N. 1995. Identifying the effects of history on adaptation: origins of different sand-diving techniques in lizards. Journal of Zoology (London) 235:351–388.

Arnold, E. N. 1987. Resource partitioning among lacertid lizards in southern Europe. Journal of Zoology (London) B 1:739-782.

Arnold, E. N. 2004. Overview of morphological evolution and radiation in the Lacertidae. Pp. 11-36 *in* V. Pérez-Mellado, N. Riera and A. Perera, eds. The biology of lacertid lizards. Evolutionary and ecological perspectives. Institut Menorquí d'Estudis, Recerca, Menorca.

Arnold, E. N., Arribas, O. and S. Carranza. 2007. Systematics of the Palaearctic and Oriental lizard tribe Lacertini (Squamata: Lacertidae: Lacertinae), with descriptions of eight new genera. Zootaxa 1430:1-86.

Atchley, W. R., C. T. Gaskins and D. Anderson. 1976. Statistical properties of ratios. I. Empirical results. Systematic Zoology 25:137–148.

Augé, M. 2003. La faune de Lacertilia (Reptilia, Squamata) de l'Éocène inférieur de Prémontré (Bassin de Paris, France). Geodiversitas 25:539-574.

Barahona, F. and L. J. Barbadillo. 1998. Inter- and intraspecific variation in the skull of some lacertid lizards. Journal of Zoology 245:393-405.

Barnosky, A. D., Hadly, E. A. and C. J. Bell. 2003. Mammalian response to global warming on varied temporal scales. Journal of Mammalogy 84:354–368.

Bauwens, D., Garland, T., Jr., Castilla, A. M. and R. Van Damme. 1995. Evolution of sprint speed in lacertid lizards: morphological, physiological, and behavioural covariation. Evolution 49:848-863.

Bauwens, D., Hertz, P. E. and A. M. Castilla. 1996. Thermoregulation in a lacertid lizard: the relative contributions of distinct behavioral mechanisms. Ecology 77:1818-1830.

Benton, M. J. and P. C. J. Donoghue. 2007. Paleontological evidence to date the Tree of Life. Molecular Biology and Evolution 24:26–53.

Benton, M. J., Donoghue, P. C. J. and R. J. Asher. 2009. Calibrating and constraining molecular clocks. Pp. 35-86 *in* S. B. Hedges and S. Kumar, eds. The Timetree of Life. Oxford University Press, Oxford.

Blackburn, T. M. and K. J. Gaston. 1998. Some methodological issues in macroecology. American Naturalist 151:68–83.

Blois, J. L. and E. A. Hadly. 2009. Mammalian response to Cenozoic climatic change. Annual Review of Earth and Planetary Sciences 37:181-208.

Bobe, R. 2006. The evolution of arid ecosystems in eastern Africa. Journal of Arid Environments 66:564-584.

Böhme, M. 2003. Miocene Climatic Optimum: evidence from Lower Vertebrates of Central Europe. Palaeogeography, Palaeoclimatology, Palaeoecology 195:389-401.

Böhme, M. U., Fritz, U., Kotenko, T., Džukić, G., Ljubisavljević, K., Tzankov, N. and T. U. Berendonk. 2006. Phylogeography and cryptic variation within the *Lacerta viridis* complex (Lacertidae, Reptilia). Zoologica Scripta 36:119-131.

Bonine, K. E. and T. Garland Jr. 1999. Sprint performance of phrynosomatid lizards, measured on a high-speed treadmill, correlates with hindlimb length. Journal of Zoology (London) 248:255–265.

Branch, B. R. 1998. Field Guide to Snakes and Other Reptiles of Southern Africa. Struik Publishers, Cape Town.

Broadley, D. G. 1972. A review of the *Nucras tessellata* group (Sauria: Lacertidae). Arnoldia 20:1-35.

Brock, C. D., Harmon, L. J. and M. E. Alfaro. 2011. Testing for temporal variation in diversification rates when sampling is incomplete and nonrandom. Systematic Biology 60:410-419.

Buckley, T. R., Attanayake, D. and S. Bradler. 2009. Extreme convergence in stick insect evolution: phylogenetic placement of the Lord Howe Island tree lobster. Proceedings of the Royal Society of London Series B Biological Sciences 276:1055–1062.

Butler, M. A. and J. B. Losos. 2002. Multivariate sexual dimorphism, sexual selection, and adaptation in Greater Antillean *Anolis* lizards. Ecological Monographs 72:541-559.

Carranza, S., Arnold, E. N. and F. Amat. 2004. DNA phylogeny of *Lacerta* (Iberolacerta) and other lacertine lizards (Reptilia: Lacertidae): did competition cause long-term mountain restriction. Systematics and Biodiversity 2:57-77.

Carroll, S. B. 2001. Chance and necessity: the evolution of morphological complexity and diversity. Nature 409:1102–1109.

Carsten, B. C. and L. L. Knowles. 2007. Shifting distributions and speciation: species divergence during rapid climate change. Molecular Ecology 16:619-627.

Čerňanský, A. 2010. Earliest world record of green lizards (Lacertilia, Lacertidae) from the Lower Miocene of Central Europe. Biologia 65:737-741.

Chadwick-Furman, N. E. 1996. Reef coral diversity and global change. Global Change Biology 2:559-568.

Chapple, D. G., Ritchie P. A. and C. H. Daugherty. 2009. Origin, diversification, and systematics of the New Zealand skink fauna. Molecular Phylogenetics and Evolution 52:470–487.

Clauzon, G. 1990. Restitution de l'évolution géodynamique néogène du bassin du Roussillon et de l'unité adjacente des Corbières d'après les données écostratigraphiques et paléogéographiques. Paléobiol. Cont. 17:125–155.

Collins, J. P., Zerba, K. E. and M. J. Sredl. 1993. Shaping intraspecific variation: development, ecology and the evolution of morphology and life history variation in tiger salamanders. Genetica 89:167-183.

Crame, J. A. 2000. Evolution of taxonomic diversity gradients in the marine realm: evidence from the composition of recent bivalve faunas. Paleobiology 26:188-214.

Currie, D. J. 1991. Energy and large-scale patterns of animal- and plant-species richness. American Naturalist 137:27-49.

Currie, D. J., Mittelbach, G. C., Cornell, H. V., Field, R., Guégan, J-F., Hawkins, B. A., Kaufman, D. M., Kerr, J. T., Oberdorff, T., O'Brien, E. M. and J. R. Turner. 2004. Predictions and tests of climate-based hypotheses of broad-scale variation in taxonomic richness. Ecology Letters 7:1121–1134.

Delsuc, F., Vizcaíno, S. F. and E. J. P. Douzery. 2004. Influence of Tertiary paleoenvironmental changes on the diversification of South American mammals: a relaxed molecular clock study within xenarthrans. BMC Evolutionary Biology 4:11.

de Menocal, P. B. 2004. African climate change and faunal evolution during the Pliocene-Pleistocene. Earth and Planetary Science Letters (Frontiers) 220:3-24.

Denoël, M., Joly, P. and H. H. Whiteman. 2005b. Evolutionary ecology of facultative paedomorphosis in newts and salamanders. Biological Reviews 80:663-671.

den Tex, R.-J., Thorington, R., Maldonado, J. E. and J. A. Leonard. 2010. Speciation dynamics in the SE Asian tropics: putting a time perspective on the phylogeny and biogeography of Sundaland tree squirrels, *Sundasciurus*. Molecular Phylogenetics and Evolution 55:711–720.

Depéret, C. 1890. Les animaux pliocènes du Roussillon. Mémoires de la Société Géologique de France, Paléontologie 3:1-194.

Donoghue, P. C. J. and M. J. Benton. 2007. Rocks and clocks: calibrating the Tree of Life using fossils and molecules. Trends in Ecology and Evolution 22:424–431.

Drummond, A. J., Ho, S. Y. W., Phillips, M. J. and A. Rambaut. 2006. Relaxed phylogenetics and dating with confidence. PLoS Biology 4:e88.

Drummond,, A. J., Ho, S. Y. W., Rawlence, N. and A. Rambaut,. 2007. A rough guide to BEAST 1.4. Available from: <http://beast.bio.ed.ac.uk/>.

Drummond, A. J., Suchard, M. A., Xie, D. and A. Rambaut. 2012. Bayesian phylogenetics with BEAUti and the BEAST 1.7. Molecular Biology and Evolution. doi: 10.1093/molbev/mss075.

Egan, A. N. and K. A. Crandall. 2008. Divergence and diversification in North American Psoraleeae (Fabaceae) due to climate change. BMC Biology 6:55.

Emerson, S. B. 1986. Heterochrony and frogs: the relationship of a life history trait to morphological form. American Naturalist 127:167-183.

ESRI 2011. ArcGIS Desktop: Release 10. Redlands, CA: Environmental Systems Research Institute.

Estes, R. 1983. Handbuch der Paläoherpetologie, Part 10: Sauria terrestria, Amphisbaenia. Gustav Fischer Verlag, Stuttgart.

Evans, S. E. 2003. At the feet of dinosaurs: the early evolutionary history and radiation of lizards. Biological Reviews 78:513-551.

Fejfar, O. and Z. Kvaček. 1993. Excursion Nr. 3 – Tertiary basins in Northwest Bohemia. Paläontologische Gesellschaft 63. Jahrestagung, 21–26, September 1993, 35 pp.

Felsenstein, J. 1985. Phylogenies and the comparative method. American Naturalist 125:1–15.

Flower, B. P. and J. P. Kennett. 1994. The middle Miocene climatic transition: East Antarctic ice sheet development, deep ocean circulation and global carbon cycling. Palaeogeography, Palaeoclimatology, Palaeoecology 108:537–555.

Folinsbee, K. E. and D. R. Brooks. 2007. Miocene hominoid biogeography: pulses of dispersal and differentiation. Journal of Biogeography 34:383-397.

Foote, M. 1997. The evolution of morphological diversity. Annual Review of Ecology and Systematics 28:129-152

Fordyce, J. A. 2010. Interpreting the gamma statistic in phylogenetic diversification rate studies: a rate decrease does not necessarily indicate an early burst. PLoSONE. 5:e11781

Fu, J. 2000. Toward the phylogeny of the family Lacertidae—Why 4708 base pairs of mtDNA sequences cannot draw the picture. Biological Journal of the Linnean Society 71:203–217.

Fuchs, J., Fjeldså, J., Bowie, R. C., Voelker, G. and E. Pasquet. 2006. The African warbler genus Hyliota as a lost lineage in the Oscine songbird tree: molecular support for an African origin of the Passerida. Molecular Phylogenetics and Evolution 39:186-97.

Gans, C. 2005. Checklist and bibliography of the amphisbaenia of the World. Bulletin of the American Museum of Natural History 280:1-30.

Garland, T., Jr and J. B. Losos. 1994. Ecological morphology of locomotor performance in squamate reptiles. Pp. 240-302 in Ecological Morphology. Integrative Organismal Biology. P. C. Wainwright and S. M. Reilly, eds. The University of Chicago Press, Chicago.

Garland, T., Jr., A. F. Bennett and E. L. Rezende. 2005. Phylogenetic approaches in comparative physiology. Journal of Experimental Biology 208:3015-3035.

Garland, T., Jr., Harvey, P. H. and A. R. Ives. 1992. Procedures for the analysis of comparative data using phylogenetically independent contrasts. Systematic Biology 41:18-32.

Garland Jr., T., Dickerman, A. W., Janis, C. M. and J. A. Jones. 1993. Phylogenetic

analysis of covariance by computer simulation. Systematic Biology 42:265–292.

Gaston, K. J. 2000. Global patterns in biodiversity. Nature 405:220-227.

Gibert, J. M. de and J. Martinell. 1998. El modelo de icnofácies, 30 años después. Revista Española de Paleontología 13:167-174.

Gibert, J. M. de, Domènech, R. and J. Martinell. 2007. Bioerosion in shell beds from the Pliocene Roussillon Basin, France: Implications for the (macro)bioerosion ichnofacies model. Acta Palaeontologica Polonica 52:783–798.

Godinho, R., Crespo, E. G., Ferrand, N. and D. J. Harris. 2005. Phylogeny and evolution of the green lizards, *Lacerta* spp. (Squamata: Lacertidae) based on mitochondrial and nuclear DNA sequences. Amphibia-Reptilia 26:271-285.

Goodman, B. A. Miles, D. B. and L. Schwarzkopf. 2008. Life on the rocks: habitat use drives morphological and performance evolution in lizards. Ecology 89:3462–3471.

Gouy, M. Guindon, S. and O. Gascuel. 2010. SeaView version 4: a multiplatform graphical user interface for sequence alignment and phylogenetic tree building. Molecular Biology and Evolution 27:221-224.

Grafen A. 1989. The phylogenetic regression. Philosophical Transactions of the Royal Society of London Series B 326:119-157.

Grechko, V. V., Bannikova, A. A., Kosushkin, S. A., Ryabinina, N. L., Milto, K. D., Darevsky, I. S. and D. A. Kramerov. 2007. Molecular genetic diversification of the lizard complex *Darevskia raddei* (Sauria: Lacertidae): early stages of speciation. Molecular Biology 41:764–775.

Guindon, S and O. Gascuel. 2003. A simple, fast, and accurate algorithm to estimate large phylogenies by maximum likelihood. Systematic Biology 52:696-704.

Harmon, L. J., Schulte, J. A., Larson, A. and J. B. Losos. 2003. Tempo and mode of evolutionary radiation in iguanian lizards. Science 301:961-964.

Harmon, L. J., Weir, J. T., Brock, C. D., Glor, R. E. and W. Challenger. 2008. GEIGER: investigating evolutionary radiations. Bioinformatics 24:129-131.

Harris, D. J., Arnold, E. N. and R. H. Thomas. 1998a. Relationships of lacertid lizards (Reptilia: Lacertidae) estimated from mitochondrial DNA sequences and morphology. Proceedings of the Royal Society of London Series B Biological Sciences 265:1939-1948.

Harris, D. J., Arnold, E. N. and R. H. Thomas. 1998b. Rapid speciation, morphological evolution, and adaptation to extreme environments in South African sand lizards (*Meroles*) as revealed by mitochondrial gene sequences. Molecular Phylogenetics and Evolution 10:37-48.

Harris, D. J. and E. N. Arnold. 2000. Elucidation of the relationships of spiny-footed lizards, *Acanthodactylus* ssp. (Reptilia: Lacertidae) using mitochondrial DNA

sequence, with comments of their biogeography and evolution. Journal of Zoology (London) 252:351-362

Harvey, P. H. and M. D. Pagel. 1991. The comparative method in evolutionary biology. Oxford University Press, Oxford.

Heads, M. 2011. Old taxa on young islands: a critique of the use of island age to date island-endemic clades and calibrate phylogenies. Systematic Biology 60:204-218.

Herrel, A., Spithoven, L., Van Damme, R. and F. De Vree. 1999. Sexual dimorphism of head size in *Gallotia galloti*; testing the niche divergence hypothesis by functional analyses. Functional Ecology 13:289–297.

Herrel, A., Van Damme, R. and F. De Vree. 1996. Sexual dimorphism of head size in *Podarcis hispanica atrata*: testing the dietary divergence hypothesis by bite force analysis. Netherlands Journal of Zoology 46:253–262.

Herrel, A., Meyers, J. J. and B. Vanhooydonck. 2002. Relations between microhabitat use and limb shape in phrynosomatid lizards. Biological Journal of the Linnean Society 77:149–163.

Hijmans, R. J., Cruz, M., Rojas, E. and L. Guarino. 2001. DIVA-GIS, Version 1.4. A geographic information system for the management and analysis of genetic resources data. Manual. International Potato Center, Lima, Peru.

Hijmans, R. J., Cameron, S. E., Parra, J. L., Jones, P. G. and A. Jarvis. 2005. Very high resolution interpolated climate surfaces for global land areas. International Journal of Climatology 25:1965-1978.

Hillebrand, H. 2004. On the generality of the latitudinal diversity gradient. American Naturalist 163:192-211.

Hipsley, C. A., Himmelmann, L., Metzler, D. and J. Müller. 2009. Integration of Bayesian molecular clock methods and fossil-based soft bounds reveals early Cenozoic colonization of African lacertid lizards. BMC Evolutionary Biology 9:1-13.

Ho, S. Y. W. and M. J. Phillips. 2009. Accounting for calibration uncertainty in phylogenetic estimation of evolutionary divergence times. Systematic Biology 58:367–380.

Huey, R. B. and E. R. Pianka. 1977. Seasonal variation in thermoregulatory behavior and body temperature of diurnal Kalahari lizards. Ecology 58:1066-1075.

Huey, R. B. and E. R. Pianka. 1981. Ecological consequences of foraging mode. Ecology 62:991–999.

Hugall, A. F., Foste, R. and M. S. Lee. 2007. Calibration choice, rate smoothing, and the pattern of tetrapod diversification according to the long nuclear gene RAG-1. Systematic Biology 56:543–563.

Irschick, D. J. and J. B. Losos. 1998. A comparative analysis of the ecological significance of locomotor performance in Caribbean *Anolis* lizards. Evolution 52: 219–226.

Irschick, D. J., Vitt, L. J., Zani, P. A. and J. B. Losos. 1997. A comparison of evolutionary radiations in mainland and West Indian *Anolis* lizards. Ecology 78:2191–2203.

Janis, C. M. 1993. Tertiary mammal evolution in the context of changing climates, vegetation, and tectonic events. Annual Review of Ecology, Evolution, and Systematics 24:467-500.

Kadereit, J. W, Griebeler, E. M and H. P. Comes. 2004. Quaternary diversification in European alpine plants: pattern and process. Philosophical Transactions of the Royal Society of London Series B, 359:265–274.

Kappelman, J., Rasmussen, D. T., Sanders, W. J., Feseha, M., Bown, T., Copeland, P., Crabaugh, J., Fleagle, J., Glantz, M., Gordon, A., Jacobs, B., Maga, M., Muldoon, K., Pan, A., Pyne, L., Richmond, B., Ryan, T., Seiffert, E. R., Sen, S., Todd, L., Wiemann, M. C. and A. Winkler. Oligocene mammals from Ethiopia and faunal exchange between Afro-Arabia and Eurasia. Nature 426:549–552.

Kearney, M. 2003. Systematics of the Amphisbaenia (Lepidosauria: Squamata) based on morphological evidence from recent and fossil forms. Herpetological Monographs 17:1-74.

Kearney, M., Shine, R. and W. P. Porter. 2009. The potential for behavioral thermoregulation to buffer ''cold-blooded'' animals against climate warming. Proceedings of the National Academy of Sciences 106:3835-3840.

Kendall, D. G. 1948. On the generalized "birth-and-death" process. Annals of Mathematical Statistics 19:1–15.

Klembara, J. 1979. Neue Funde der Gattungen *Ophisaurus* und *Anguis* (Squamata, Reptilia) aus dem Untermiozän Westböhmens (CSSR). Věst. Ústř. Úst Geol. 54:163-169.

Klingenberg, C. P. 1996. Multivariate allometry. Pp. 23–49 *in* L. F. Marcus, M. Corti, A. Loy, G. Naylor, and D. E. Slice, eds. Advances in Morphometrics. Plenum Press, New York.

Klingenberg, C. P. 1998. Heterochrony and allometry: the analysis of evolutionary change in ontogeny. Biological Reviews 73:79–123.

Lamb, T. and A. M. Bauer. 2003. *Meroles* revisited: complementary systematic inference from additional mitochondrial genes and complete taxon sampling of southern Africa's desert lizards. Molecular Phylogenetics and Evolution 29:360-364.

Lamb, T., Meeker, A. M., Bauer, A. M. and W. R. Branch. 2003. On the systematic status of the desert plated lizard (*Angolosaurus skoogi*): phylogenetic inference from DNA sequence analysis of the African Gerrhosauridae. Biological Journal of the Linnean Society 78:253-261.

Lear, C. H., Rosenthal, Y., Coxall, H. K. and P. A. Wilson. 2004. Late Eocene to early Miocene ice-sheet dynamics and the global carbon cycle. Paleoceanography 19:PA4015.

Lewis, P. O. 2001. A likelihood approach to estimating phylogeny from discrete morphological character data. Systematic Biology 50:913-925.

Lofgren, D. L., Lillegraven, J. A., Clemens, W. A., Gingerich, P. D. and T. E. Williamson. 2004. Paleocene biochronology of North America: the Puercan through Clarkforkian land mammal ages. Pp. 43-105 *in* M. O. Woodburne, ed. Late Cretaceous and Cenozoic mammals of North America: biostratigraphy and geochronology. Columbia University Press, New York.

Losos, J. B. 1990a. Ecomorphology, performance capability, and scaling of West-Indian lizards – an evolutionary analysis. Ecological Monographs 60:369-388.

Losos, J. B. 1990b. The evolution of form and function: morphology and locomotor performance in West Indian *Anolis* lizards. Evolution 44:1189-1203.

Losos, J. B. and D. B. Miles. 2002. Testing the hypothesis that a clade has adaptively radiated: iguanid lizard clades as a case study. American Naturalist 160:147-157.

Losos, J. B. 1992. The evolution of convergent community structure in Caribbean *Anolis* communities. Systematic Biology 41:403-420.

Losos, J. B. 2007. Detective work in the West Indies: integrating historical and experimental approaches to study island lizard evolution. Bioscience 57:585-597.

Losos, J. B., Jackman, T. R., Larson, A., de Queiroz, K. and L. Rodríguez-Schettino. 1998. Historical contingency and determinism in replicated adaptive radiations of island lizards. Science 279:2115-2118.

Luczkovich, J., Motta, P., Norton, S. and L. Liem. 1995. Ecological Morphology of Fishes. Kluwer Academic Publishers, The Netherlands.

Lunt, D. J., Ross, I., Hopley, P. J. and P. J Valdes. 2007. Modelling late Oligocene C4 grasses and climate. Palaeogeography, Palaeoclimatology, Palaeoecology 251:239–253.

Maddison, W. P. and D. R. Maddison. 2009. Mesquite: A modular system for evolutionary analysis. Version 2.7. http://mesquiteproject.org.

Magallón, S. 2010. Using fossils to break long branches in molecular dating: a comparison of relaxed clocks applied to the origin of angiosperms. Systematic Biology 59:384-399.

Magallón, S. and M. J. Sanderson. 2001. Absolute diversification rates in angiosperm clades. Evolution 55:762-1780.

Makokha, J. S., Bauer, A. M., Mayer, W. and C. A. Matthee. 2007. Nuclear and mtDNA-based phylogeny of southern African sand lizards, *Pedioplanis* (Sauria: Lacertidae).

Molecular Phylogenetics and Evolution 44:622-633.

Martins, E. P. and E. A. Housworth. 2002. Phylogeny shape and the phylogenetic comparative method. Systematic Biology 51:873-880.

Mawson, R. and M. A. J. Williams. 1984. A wetter climate in eastern Sudan 2,000 years ago? Nature 308:49-51.

Mayer, W. and G. Benyr. 1994. Albumin Evolution und Phylogenese in der Familie Lacertidae. Annalen des Naturhistorischen Museums in Wien 95B:621–648.

Mayer, W. and M. Pavlicev. 2007. The phylogeny of the family Lacertidae (Reptilia) based on nuclear DNA sequences: convergent adaptations to arid habitats within the subfamily Eremiainae. Molecular Phylogenetics and Evolution 44:1155-1163.

McBrayer, L. D. 2004. The relationship between skull morphology, biting performance and foraging mode in Kalahari lacertid lizards. Zoological Journal of the Linnean Society 140:403–416.

McBrayer, L.D. and J. E. Wylie. 2009. Concordance between locomotor morphology and foraging mode in lacertid lizards. Zoology 112:370-378.

McKinney, M. L. and K. J. McNamara. 1991. Heterochrony: the evolution of ontogeny. Plenum Press, New York.

McPeek, M. A. 2008. The ecological dynamics of clade diversication and community assembly. American Naturalist 172:E270-284.

Mein, P. 1990. Updating of MN zones. Pp. 73-90 *in* E. H. Lindsay, V. Fahlbusch and P. Mein, eds. European Neogene mammal chronology. Plenum Press, New York.

Melville, J. and R. Swain. 2000. Evolutionary relationships between morphology, performance and habitat openness in the lizards genus *Niveoscincus* (Scincidae: Lygosominae). Biological Journal of the Linnean Society 70:667–683.

Melville, J., Harmon, L. J. and J. B. Losos. 2006. Intercontinental community convergence of ecology and morphology in desert lizards. Proceedings of the Royal Society B: Biological Sciences 273:557–563.

Mercer, J. M. and V. L. Roth. 2003. The effects of Cenozoic global change on squirrel phylogeny. Science 299:1568-1572.

Miles, D. B. 1994. Covariation between morphology and locomotor performance in sceloporine lizards. Pp. 207-235 *in* Lizard Ecology: Historical and Experimental Perspectives. L. J. Vitt and E. R. Pianka, eds. Princeton University Press, Princeton.

Miles, D. B. and A. E. Dunham. 1993. Historical perspectives in ecology and evolutionary biology: the use of phylogenetic comparative analyses. Annual Review of Ecology and Systematics 24:587-619.

Mlynarski, M. 1956. Lizards from the Pliocene of Poland. Acta Palaeontologica Polonica 1:135-151.

Mosimann, J. 1970. Size allometry: size and shape variables with characterizations of the lognormal and generalized gamma distributions. Journal of the American Statistical Association 65:930-945.

Müller, J. and R. R. Reisz. 2005. Four well-constrained calibration points from the vertebrate fossil record for molecular clock estimates. BioEssays 27:1069-1075.

Müller, J., Hipsley, C. A., Head, J. J., Kardjilov, N., Hilger, A., Wuttke, M. and R. R. Reisz. 2011. Eocene lizard from Germany reveals amphisbaenian origins. Nature 473:364–367.

Naish, T. and L. Carter. 2003. Direct evidence of the Mi1 glaciation (C.24 Ma): Constraining its effect on Antarctic ice volume and deep ocean circulation. EGS – AGU - EUG Joint Assembly, Nice, France, 6-11 April 2003, Abstract #8214.

Near, T. J., Bolnick, D. I. and P. C. Wainwright. 2005. Fossil calibrations and molecular divergence time estimates in centrarchid fishes (Teleostei: Centrarchidae). Evolution 59:1768-1782.

Nee, S., May, R. M. and P. H. Harvey. 1994. The reconstructed evolutionary process. Philosophical Transactions of the Royal Society of London Series B Biological Sciences 344:305-311.

Nee, S. 2001. Inferring speciation rates from phylogenies. Evolution 55:661–668.

Nee, S., Mooers, A. O. and P. H. Harvey. 1992. Tempo and mode of evolution revealed from molecular phylogenies. Proceedings of the National Academy of Sciences USA 89:8322–8326.

Nydam, R. L. and R. L. Cifelli. 2002. Lizards from the Lower Cretaceous (Aptian-Albian) Antlers and Clovery formations. Journal of Vertebrate Paleontology 22:286-298.

Olson, D. M., Dinerstein, E., Wikramanayake, E. D., Burgess, N. D., Powell, G. V. N., Underwood, E. C., D'amico, J. A., Itoua, I., Strand, H. E., Morrison, J. C., Loucks, C. J., Allnutt, T. F., Ricketts, T. H., Kura, Y., Lamoreux, J. F., Wettengel, W. W., Hedao, P. and K. R. Kassem. 2001. Terrestrial ecoregions of the world: a new map of life on Earth. BioScience 51: 933-938.

Orriols, F. A. 2011. Preliminary analysis of correlated evolution of morphology and ecological diversification in lacertid lizards. Butll. Soc. Cat. Herp. 19:29-48.

Pagel, M. 1994. Detecting correlated evolution on phylogenies: a general method for the comparative analysis of discrete characters. Proceedings of the Royal Society of London Series B Biological Sciences 255:37-45.

Paradis, E., Claude, J. and K. Strimmer. 2004. APE: analyses of phylogenetics and evolution in R language. Bioinformatics 20:289–290.

Parham, J. F., Donoghue, P. C. J., Bell, C. J., Calway, T. D., Head, J. J, Holroyd, P. A., Inoue, J. G., Irmis, R. B., Joyce, W. G., Ksepka, D. T., Patané, J. S. L., Smith, N. D., Tarver, J. E., van Tuinen, M., Yang, Z., Angielczyk, K. D., Greenwood, J., Hipsley, C. A. , Jacobs, L., Makovicky, P. J., Müller, J. , Smith, K. T., Theodor, J. M., Warnock, R. C. and M. J. Benton. 2012. Best practices for justifying fossil calibrations. Systematic Biology 61:346–359.

Parmesan, C. 2006. Ecological and evolutionary responses to recent climate change. Annual Review of Ecology, Evolution, and Systematics 37:637–669.

Parmesan, C. and H. Galbraith. 2004. Observed impacts of climate change in the United States. Pew Center on Global Climate Change, Arlington, VA, 67pp.

Parmesan, C. and G. Yohe. 2003. A globally coherent fingerprint of climate change impacts across natural systems. Nature 421:37–42.

Pavlicev, M. and W. Mayer. 2009. Fast radiation of the subfamily Lacertinae (Reptilia: Lacertidae): history or methodical artefact? Molecular Phylogenetics and Evolution 52:727-734.

Pianka, E. R. 1969. Sympatry of desert lizards (*Ctenotus*) in western Australia. Ecology 50:1012–1030.

Pianka, E. R. 1986. Ecology and Natural History of Desert Lizards. Analyses of the Ecological Niche and Community Structure. Princeton University Press, Princeton, New Jersey.

Pianka, E. R. 2000. Evolutionary Ecology, 6th ed. Addison-Wesley-Longman, San Francisco.

Popov, S. V., Rögl, F., Rozanov, A. Y., Steininger, F. F., Shcherba, I. G. and M. Kovac. 2004. Lithological-Paleogeographic maps of the Paretethys. – 10 maps Late Eocene to Pliocene. Courier Forschungsinstitut Senckenberg 250:1-46.

Posada, D. 2008. jModelTest: Phylogenetic Model Averaging. Molecular Biology and Evolution 25:1253-1256.

Pough, F. H., Andrews, R. M., Cadle, J. E., Crump, M. L., Savitzky, A. H. and K. D. Wells. 2001. Herpetology. 2d ed. Prentice Hall, Upper Saddle River, N.J.

Prothero, D. R. and N. Shubin. 1989. The evolution of Oligocene horses. Pp. 142-175 *in* The Evolution of Perissodactyls. Clarendon Press, New York.

Prothero, D. R. 1993. Paradise Lost: The Eocene-Oligocene Transition. Columbia University Press, Columbia.

Pybus, O. G. and P. H. Harvey. 2000. Testing macro-evolutionary models using incomplete molecular phylogenies. Proceedings of the Royal Society of London Series B Biological Sciences 267:2267-2272.

R Development Core Team. 2008. R: a language and environment for statistical computing. R Foundation for Statistical Computing, Vienna, Austria.

Rabosky, D. L. 2006. LASER: A maximum likelihood toolkit for detecting temporal shifts in diversification rates from molecular phylogenies. Evolutionary Bioinformatics Online 2:247-250.

Rabosky, D. L., Donnellan, S. C., Talaba, A. L. and I. J. Lovette. 2007. Exceptional among-lineage variation in diversification rates during the radiation of Australia's most diverse vertebrate clade. Proceedings of the Royal Society B: Biological Sciences 274:2915-2923.

Rabosky, D. L. 2010. Extinction rates should not be estimated from molecular phylogenies. Evolution 6:1816-1824.

Rage, J.-C. 1976. Les squamates du Miocène de Béni Mellal, Maroc. Géologie Méditerranéenne 3:57–70.

Rambaut, A. and A. J. Drummond. 2008. Tracer v1.4: MCMC Trace Analysis Tool. Available from: <http://tree.bio.ed.ac.uk/software/tracer/>.

Rauscher, K. L. 1992. Die Echsen (Lacertilia, Reptilia) aus dem Plio-Pleistocän von Bad Deutsch-Altenburg, Niederösterreich. Beiträge zur Paläontologie Österreich-Ungarns und des Orients 17:81–177.

Reisz, R. R. and J. Müller. 2004. Molecular timescales and the fossil record: a paleontological perspective. Trends in Genetics 20:237–241.

Retallack, G. J. 1992. Middle Miocene fossil plants from Fort Ternan (Kenya) and evolution of African grasslands. Paleobiology 18:383-400.

Revell, L. J. 2012. Phytools: an R package for phylogenetic comparative biology (and other things). Methods in Ecology and Evolution 3:217-223.

Revell, L. J., Harmon, L. J., Langerhans, R. B. and J. J. Kolbe. 2007. A phylogenetic approach to determining the importance of constraint on phenotypic evolution in the Neotropical lizard *Anolis cristatellus*. Evolutionary Ecololgy Research 9:261–282.

Richardson J. E., Weitz, F. M., Fay, M. F., Cronk, Q. C. V., Linder, H. P., Reeves, G., and M. W. Chase. 2001. Rapid and recent origin of species richness in the Cape flora of South Africa. Nature 412:181-183.

Ricklefs, R. E. 2007. Estimating diversification rates from phylogenetic information. Trends in Ecology and Evolution 22:601-610.

Ricklefs, R. E., Losos, J. B. and T. M. Townsend. 2007. Evolutionary diversification of clades of squamate reptiles. Journal of Evolutionary Biology 20:1751-1762.

Roček, Z. 1984. Lizards (Reptilia: Sauria) from the Lower Miocene locality Dolnice (Bohemia, Czechoslovakia). Rozpr. Ropr. Ceskoslov. Akad. Ved. Rada Mat. Prir. Ved 94. 69 pp.

Roček, Z. 1995. Heterochrony: response of amphibia to cooling events, Geolines (Praha)

3:55–58.

Salvador, A. 1982. A revision of the lizards of the genus *Acanthodactylus* (Sauria: Lacertidae). Bonner Zoologische Monographien 16:1-167.

Salzmann, U., Haywood, A. M., and D. J. Lunt. 2009. The past is a guide to the future?, Comparing Middle Pliocene vegetation with predicted biome distributions for the twenty-first century, Philosophical Transactions of the Royal Society A: Mathematical, Physical, and Engineering Sciences 367:189–204.

Sandercock, B. K., Martin, K. and S. J. Hannon. 2005. Life history strategies in extreme environments: comparative demography of Arctic and Alpine Ptarmigan. Ecology 86:2176-2186.

Schluter, D. 1998. Ecological causes of speciation. Pp. 114-129 *in* Endless forms: species and speciation. D. Howard and S. Berlocher, eds. Oxford University Press, Oxford.

Schluter, D. 2000. The Ecology of Adaptive Radiations. Oxford University Press, New York.

Schulte, J. A. II, Losos, J. B., Cruz, F. B. and H. Núñez. 2004. The relationship between morphology, escape behaviour and microhabitat occupation in the lizard clade Liolaemus (Iguanidae: Tropidurinae: Liolaemini). Journal of Evolutionary Biology 17:408–420.

Schoener, T. W. 1971. Theory of feeding strategies. Annual Review of Ecology and Systematics 2:307–343.

Schuster, M., Duringer, P., Ghienne. J.-F. L., Vignaud, P., Mackaye, H. T., Likius, A. and M. Brunet. 2006. The age of the Sahara Desert. Science 311:821.

Sherbrooke, W. C., Scardino, A. J., de Nys, R. and L. Schwarzkopf. 2007. Functional morphology of scale hinges used to transport water: convergent drinking adaptations in desert lizards (*Moloch horridus* and *Phrynosoma cornutum*). Zoomorphology. 126:89-102.

Siesser, W. G. 1980. Late Miocene origin of the Benguela upwelling system off northern Namibia. Science 208:283-285.

Simmons, R. E., Griffin, M., Griffin, R. E., Marais, E. and H. Kolberg. 1998. Endemism in Namibia: patterns, processes, and predictions. Biodiversity and Conservation 7:513-530.

Simpson, G. G. 1951. Horses. Oxford University Press, Oxford.

Simpson, G. G. 1953. The Major Features of Evolution. Columbia University Press, New York.

Simpson, C., Kiessling, W., Mewis, H., Baron-Szabo, R. C. and J. Müller. 2011. Evolutionary diversification of reef corals: a comparison of the molecular and fossil records. Evolution. 65:3274–3284.

Sinervo, B., Méndez-de-la-Cruz, F., Miles, D. B., Heulin, B., Bastiaans, E., Villagrán-Santa Cruz, M., Lara-Resendiz, R., Martínez-Mendéz, N., Calderón-Espinosa, M. L., Meza-Lázaro, R. N., Gadsden, H., Avila, L. J., Morando, M., De la Riva, I. J., Sepulveda, P. V., Duarte Rocha, C. F., Ibargüengoytía, N., Puntriano, C. A., Massot, M., Lepetz, V., Oksanen, T. A., Chapple, D. G., Bauer, A. M., Branch, W. R., Clobert, J. and J. W. Sites Jr. 2010. Erosion of lizard diversity by climate change and altered thermal niches. Science 328:894-899.

Stanley. E. L., Bauer, A. M., Jackman, T. R. Branch, W. R. and P. Mouton. 2011. Between a rock and a hard polytomy: Rapid radiation in the rupicolous girdled lizards (Squamata: Cordylidae). Molecular Phylogenetics and Evolution 58:53-70.

Steckel, J., Penrith, M.-L., Henschel, J., Brandl, R. and J. Meyer. 2011. A preliminary molecular phylogeny of the Namib Desert darkling beetles (Tenebrionidae). African Zoology 45:107-114.

Steeman, M. E., Hebsgaard, M. B., Fordyce, R. E., Ho, S. Y. W., Rabosky, D. L., Nielsen, R., Rahbek, C., Glenner, H., Sørensen, M. V. and E. Willerslev. 2009. Radiation of extant cetaceans driven by restructuring of the oceans. Systematic Biology 58:573-585.

Stevens, R. D. 2006. Historical processes enhance patterns of diversity along latitudinal gradients. Proceedings of the Royal Society B 273:2283–2289.

Strömberg, C. A. E. 2011. Evolution of grasses and grassland ecosystems. Annual Review of Earth and Planetary Sciences 39:517-544.

Stokes, S., Thomas, D. S. G. and R. Washington. 1997. Multiple episodes of aridity in southern Africa since the last interglacial period. Nature 388:154-158.

Sullivan, R. M. 1985. A new middle Paleocene (Torrejonian) rhineurid amphisbaenian, *Plesiorhineura tsentasi* new genus, new species, from the San Juan basin, New Mexico. Journal of Paleontology 59:1481-1485.

Szczerbak, N. N. 1989. Catalogue of the African Sand Lizards (Reptilia: Sauria: Eremiainae: *Lampreremias, Pseuderemias, Taenieremias, Mesalina, Meroles*). Herpetozoa 1:119–132.

Tejedo, M., Marangoni, F., Pertoldi, C., Richter-Boix, A., Laurila, A., Orizaola, G., Nicieza, A. G., Álvarez, D. and I. Gomez-Mestre. 2010. Contrasting effects of environmental factors during larval stage on morphological plasticity in post-metamorphic frogs. Climate Research 43:31-39.

Tolley, K. A., Chase, B. M. and F. Forest. 2008. Speciation and radiations track climate transitions since the Miocene Climatic Optimum: a case study of southern African chameleons. Journal of Biogeography 35:1402-1414.

Townsend, T., Larson, A., Louis, E. and J. R. Macey. 2004. Molecular phylogenetics of Squamata: the position of snakes, amphisbaenians, and dibamids, and the root of the squamate tree. Systematic Biology 53:735-757.

Townsend, T. M., Alegre, E. R., Kelley, S. T., Wiens, J. J. and T. W. Reeder. 2008. Rapid development of multiple nuclear loci for phylogenetic analysis using genomic resources: an example from squamate reptiles. Molecular Phylogenetics and Evolution 47:129–142.

Vanhooydonck, B. and R. Van Damme. 2001. Evolutionary trade-offs in locomotor capacities in lacertid lizards: are splendid sprinters clumsy climbers? Journal of Evolutionary Biology 14:46-54.

Vanhooydonck, B., Herrel, A. and R. Van Damme. 2007. Interactions between habitat use, behavior, and the trophic niche of lacertid lizards. Pp. 427-449 in S. M. Reilly, L. D. McBrayer and D. B. Miles, eds. Lizard Ecology: The Evolutionary Consequences of Foraging Mode. Cambridge University Press, Cambridge.

Vanhooydonck, B., Meulepas, G., Herrel, A., Boistel, R., Tafforeau, P., Fernandez, V. and P. Aerts. 2009. Ecomorphological analysis of aerial performance in a non-specialized lacertid lizard, *Holaspis guentheri*. Journal of Experimental Biology 212:2475–92.

Vanhooydonck, B. and R. Van Damme. 1999. Evolutionary relationships between body shape and habitat use in lacertid lizards. Evolutionary Ecology Research 1:785-805.

Vanhooydonck, B., Van Damme, R. and P. Aerts. 2002. Variation in speed, gait characteristics, and microhabitat use in lacertid lizards. Journal of Experimental Biology 205:1037-1046.

Verwaijen, D. and R. Van Damme. 2007. Does foraging mode mould morphology in lacertid lizards? Journal of Evolutionary Biology 20:1950-1961.

Verwaijen D. and R. Van Damme. 2008. Foraging mode and locomotor capacities in Lacertidae. Amphibia-Reptilia 29:197-206.

Vidal, N. and S. B. Hedges. 2005. The phylogeny of squamate reptiles (lizards, snakes, and amphisbaenians) inferred from nine nuclear protein-coding genes. Comptes Rendus Biologies 328:1000–1008.

Wainwright, P. C. and S. M. Reilly (eds.). 1994. Ecological morphology: integrative organismal biology. University of Chicago Press, Chicago.

Wallace, A. R. 1876. The geographical distribution of animals: with a study of the relations of living and extinct faunas as elucidating the past changes of the earth's surface. Harper, New York.

Walther, G. R., Post, E., Convery, P., Menzel, A., Parmesan, C., Beebee, T. J. C., Fromentin, J. M., Hoegh-Guldberg, O. and F. Bairlein. 2002. Ecological responses to recent climate change. Nature 416:389–395.

Weir, J. T. and D. Schluter. 2004. Ice sheets promote speciation in boreal birds. Proceedings of the Royal Society B 271:1881–1887.

Wiedenhoeft, A. C., van Ee, B. and P. E. Berry. 2008. Comparative wood anatomy of Croton and tribe Crotoneae (Euphorbiaceae). Pp. 12-48 *in* Tracking the phylogeny of the Crotoneae with comparative wood anatomy. A. C. Wiedenhoeft, ed. University of Wisconsin, Madison, 2008.

Wiens, J. J., Brandley, M. C. and T. W. Reeder. 2006. Why does a trait evolve multiple times within a clade? Repeated evolution of snakelike body form in squamate reptiles. Evolution 60:123-141.

Williamson, T. E., Nichols, D. J. and A. Weil. 2008. Paleocene palynomorph assemblages from the Nacimiento Formation, San Juan Basin, New Mexico, and their biostratigraphic significance. New Mexico Geology 30:3-11.

Winkler, D. A., Murry, P. A. and L. L. Jacobs. 1990. Early Cretaceous (Comanchean) vertebrates of central Texas. Journal of Vertebrate Paleontology 10:95–116.

Yang, Z. and B. Rannala. 2006. Bayesian estimation of species divergence times under a molecular clock using multiple fossil calibrations with soft bounds. Molecular Biology and Evolution 23:212-226.

Zachos, J. C., Dickens, G. R. and R. E. Zeebe. 2008. An early Cenozoic perspective on greenhouse warming and carboncycle dynamics. Nature 451:279–283.

Zink, R. M. and J. B. Slowinski. 1995. Evidence from molecular systematics for decreased avian diversification in the Pleistocene epoch. Proceedings of the National Academy of Sciences USA 92:5832–5835.